DAVID W. TAYLOR NAVAL SHIP RESEARCH AND DEVELOPMENT CENTER

Bethesda, Md. 20084

THEORETICAL PREDICTION OF MOTIONS OF HIGH SPEED PLANING BOATS IN WAVES

SHIP PERFORMANCE DEPARTMENT
RESEARCH AND DEVELOPMENT REPORT

April 1976

Report 76-0069

THEORETICAL PREDICTION OF MOTIONS OF HIGH-SPEED PLANING BOATS IN WAVES Report 76-0069

MAJOR DTNSRDC ORGANIZATIONAL COMPONENTS

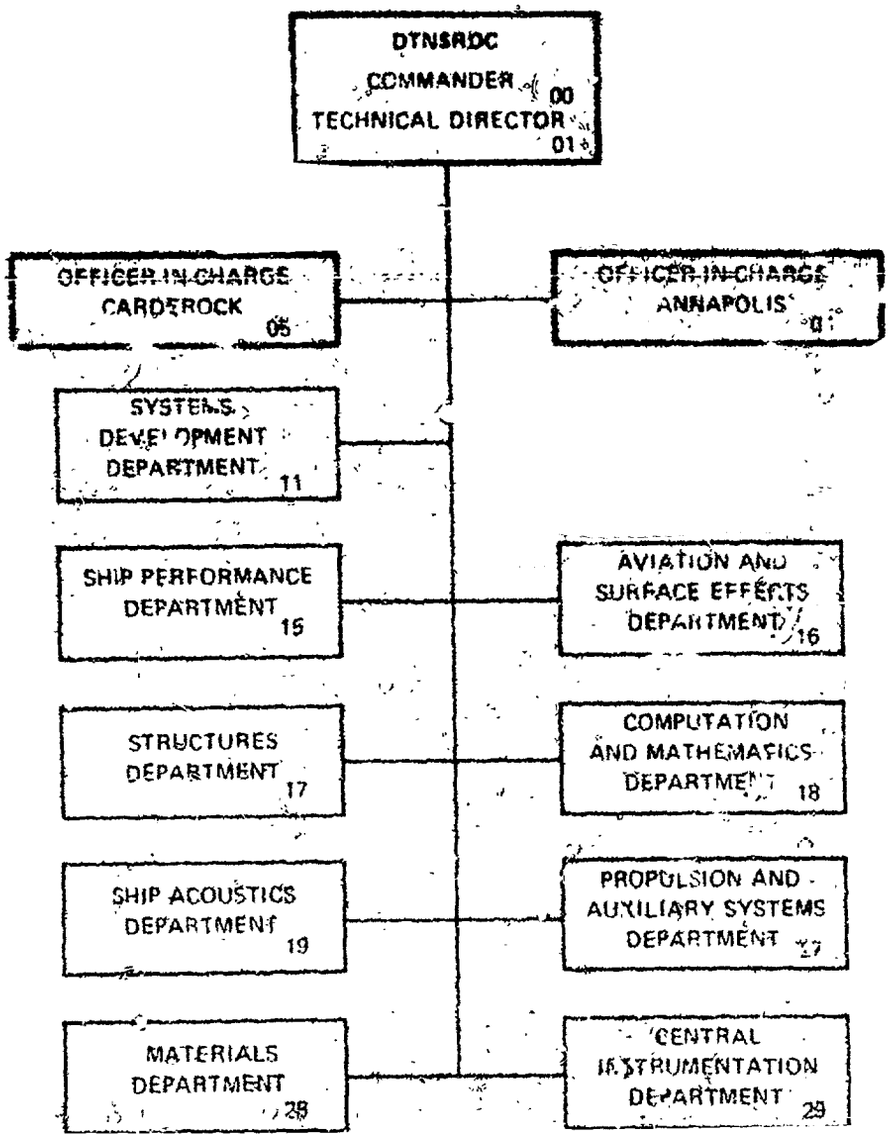

UNCLASSIFIED

SECURITY CLASSIFICATION OF THIS PAGE (When Data Entered)

REPORT DOCUMENTATION PAGE

READ INSTRUCTIONS BEFORE COMPLETING FORM

1. REPORT NUMBER: DTNSRDC [illegible]-76-0069
2. GOVT ACCESSION NO.
3. RECIPIENT'S CATALOG NUMBER
4. TITLE (and Subtitle): THEORETICAL PREDICTION OF MOTIONS OF HIGH-SPEED PLANING BOATS IN WAVES
5. TYPE OF REPORT & PERIOD COVERED
6. PERFORMING ORG. REPORT NUMBER
7. AUTHOR(s): Milton Martin
8. CONTRACT OR GRANT NUMBER(s)
9. PERFORMING ORGANIZATION NAME AND ADDRESS: David W. Taylor Naval Ship Research and Development Center, Bethesda, Maryland 20084
10. PROGRAM ELEMENT, PROJECT, TASK AREA & WORK UNIT NUMBERS: SR-023-0101, Work Unit 1-1562-002
11. CONTROLLING OFFICE NAME AND ADDRESS: Naval Sea Systems Command (SEA 035), Washington, D.C. 20362
12. REPORT DATE: April [illegible]76
13. NUMBER OF PAGES: 96 (94 pp.)
14. MONITORING AGENCY NAME & ADDRESS (if different from Controlling Office)
15. SECURITY CLASS. (of this report): UNCLASSIFIED
15a. DECLASSIFICATION/DOWNGRADING SCHEDULE

16. DISTRIBUTION STATEMENT (of this Report)

APPROVED FOR PUBLIC RELEASE: DISTRIBUTION UNLIMITED

17. DISTRIBUTION STATEMENT (of the abstract entered in Block 20, if different from Report)

18. SUPPLEMENTARY NOTES

19. KEY WORDS (Continue on reverse side if necessary and identify by block number)

Motions in Waves
Stability
Planing Boat Motions
Hydrodynamic Impact
Seakeeping
Marine Craft

20. ABSTRACT (Continue on reverse side if necessary and identify by block number)

A theoretical method is derived for predicting the linearized response characteristics of constant deadrise, high-speed planing boats in head and following waves. Comparisons of the theoretical predictions of the pitch and heave response-amplitude operators and phase angles with existing experimental data show reasonably good agreement for a wide variety of conditions of interest.

(Continued on reverse side)

DD FORM 1 JAN 73 1473 EDITION OF 1 NOV 65 IS OBSOLETE S/N 0102-014-6601

UNCLASSIFIED 387 682

SECURITY CLASSIFICATION OF THIS PAGE (When Data Entered)

bpg

(Block 20 continued)

It appears that nonlinear effects are more severe at a speed-to-length ratio of 6 than of, say, 4 or less, principally because of the reduction of the damping ratio of the boat with increasing speed, and the consequent increase in motions in the vicinity of the resonant encounter frequency. However, it is concluded that the linear theory in its present form can serve as a useful design tool, especially since it has already been shown that the effect of hull parameters on performance as obtained from data in the linear range is valid for operation in realistic seas.

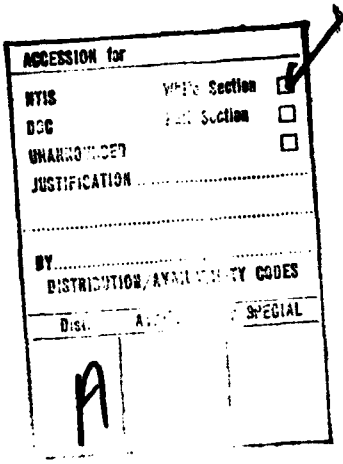

TABLE OF CONTENTS

	Page
ABSTRACT	1
ADMINISTRATIVE INFORMATION	1
INTRODUCTION	1
EQUATIONS OF MOTION	2
NATURAL FREQUENCIES AND DAMPING	5
STEADY STATE MOTION IN WAVES	7
COMPARISON WITH EXPERIMENT	11
CONCLUSIONS	19
ACKNOWLEDGMENTS	20
APPENDIX A - FORCE AND MOMENT DUE TO WAVES AND THE EQUATIONS OF MOTION	21
REFERENCES	82

LIST OF FIGURES

1 - Lines of Prismatic Models	47
2 - Heave and Pitch Responses ($V/\sqrt{\ell} = 4$) Configuration A	48
3 - Heave and Pitch Responses ($V/\sqrt{\ell} = 4$) Configuration E	50
4 - Heave and Pitch Responses ($V/\sqrt{\ell} = 4$) Configuration F	52
5 - Heave and Pitch Responses ($V/\sqrt{\ell} = 4$) Configuration I	54
6 - Heave and Pitch Responses ($V/\sqrt{\ell} = 4$) Configuration K	56
7 - Heave and Pitch Responses ($V/\sqrt{\ell} = 4$) Configuration N	58
8 - Heave and Pitch Responses ($V/\sqrt{\ell} = 4$) Configuration O	60
9 - Heave and Pitch Responses ($V/\sqrt{\ell} = 4$) Configuration P	62
10 - Heave and Pitch Responses ($V/\sqrt{\ell} = 6$) Configuration B	64

Page

11 - Heave and Pitch Responses ($V/\sqrt{\ell} = 6$) Configuration G 66

12 - Heave and Pitch Responses ($V/\sqrt{\ell} = 6$) Configuration M 68

13 - Heave and Pitch Responses ($V/\sqrt{\ell} = 6$) Configuration J 70

14 - Heave and Pitch Responses ($V/\sqrt{\ell} = 2$) Configuration C 72

15 - Heave and Pitch Responses ($V/\sqrt{\ell} = 2$) Configuration D 74

16 - Heave and Pitch Responses ($V/\sqrt{\ell} = 2$) Configuration H 76

17 - Heave and Pitch Responses ($V/\sqrt{\ell} = 2$) Configuration L 78

18 - Coordinate System and Symbol Illustrations 80

19 - Geometric Relationships in Steady State Planing 81

LIST OF TABLES

1 - Principal Characteristics of Configurations Investigated 13

2 - Cross Flow Drag Coefficient 30

NOTATION

a	Value of s at transverse plane through boat center of gravity
B	Bobyleff's function of deadrise
b	Beam of boat
$C_{D,c}$	Cross flow drag coefficient; see Table 2
C_f	Hydrodynamic friction coefficient
C_{Lb}	Boat lift coefficient nondimensionalized by the beam, $2C_\Delta/C_V^2$
C_V	Speed coefficient, $U/\sqrt{gb}$
C_Δ	Load coefficient, $\Delta/\rho gb^3$
C_λ	Modified version of nondimensional wave number; see Equation (32)
$C_{\lambda R}$	Value of C_λ at resonant encounter frequency
c	Wave celerity
F_{BS}	Steady state buoyancy force
F_D	Dynamic part of hydrodynamic normal force on hull
F_{DS}	Steady state part of F_D
$(F_h)_w$	Normal force due to wave elevation
$(F_P)_w$	Force on hull due to perturbation pressure from wave
$(F_1)_w$	Normal force due to slope of wave
$(F_2)_w$	Normal force due to orbital velocity
$(F_5)_w$	Normal force due to orbital acceleration
$f(\beta)$	Deadrise function of Wagner; see Equation (42)
g	Acceleration of gravity
H	Wave height, 2h
h	Amplitude of wave elevation, one-half wave height
I_y	Pitch moment of inertia about the boat center of gravity

k	Wave number, $2\pi/L_w$
k_0	Modified wave number; see Equation (81)
k_y	Radius of gyration of boat with respect to center of gravity
$\overline{LCG}$	Distance from transom to boat center of gravity, measured parallel to keel
L_w	Wavelength
l	Overall length of boat, in feet
l_g	Same as $\overline{LCG}$
l_k	Length of wetted portion of keel
l_m	Mean wetted length of hull
M	Hydrodynamic pitch moment relative to center of gravity
M_{BS}	Steady state pitch moment due to buoyancy
M_D	Dynamic part of hydrodynamic pitch moment on hull
M_{DS}	Steady state part of M_D
$(M_h)_w$	Pitching moment due to wave elevation
M_S	Total steady state pitch moment acting on hull
$M_z, M_{\dot{z}}, M_\theta$, etc.	Partial derivative of pitch moment with respect to motion variables z, $\dot{z}$, θ, etc., respectively
$(M_1)_w$	Pitching moment due to slope of wave
$(M_2)_w$	Pitching moment due to orbital velocity
$(M_5)_w$	Pitching moment due to orbital acceleration
RAO	Response amplitude operator (Equations 28 and 29)
s	Coordinate measured along keel from foremost immersed station of keel (see Figure 19)
s_{c1}	See Equation (40) and Figure 19
s_{c2}	See Equation (41) and Figure 19

t	Time
U	Steady reference speed of boat, in feet per second
u, $\dot{u}$	Perturbation surge velocity and acceleration
V_k	Steady reference speed of boat, in knots
W	Boat weight
X	Hydrodynamic force component in direction of positive x
X_D	Dynamic part of hydrodynamic X-force
X_S	Steady state part of X
$X_u, X_{\dot{u}}, X_{\ddot{z}}$, etc.	Partial derivative of X-force with respect to motion variables u, $\dot{u}$, $\ddot{z}$, etc., respectively
x	Horizontal coordinate in direction of U
x_b	Horizontal distance from center of gravity to foremost immersed point on keel, i.e., where s = 0
x_{cl}	$s_{cl}/\cos \tau$
x_d	See Equation (110)
Z	Hydrodynamic force component in direction of positive z
Z_D	Dynamic part of hydrodynamic Z-force
Z_S	Steady state part of Z
$Z_z, Z_{\dot{z}}, Z_\theta$, etc.	Partial derivative with respect to motion variables z, $\dot{z}$, θ, etc., respectively
z	Vertical coordinate, positive down
$\lvert z_0' \rvert$	Nondimensional amplitude of vertical displacement of center of gravity of boat from steady, calm water position
α_x, α_z, α_θ	Phase angle of surge, heave, and pitch motion, respectively, with respect to wave height
β	Deadrise angle; see Figure 19
β_h	Wave heading angle; see Figure 18
Δ	Weight of boat

$\dot{\zeta}$, $\ddot{\zeta}$	Components, normal to the keel, of the orbital velocity and acceleration, respectively
θ	Boat pitch angle perturbation, positive bow up
$\lvert\theta_0\rvert$	Amplitude of boat pitch angle perturbation from steady, calm water trim angle, radians
λ	Mean wetted length to beam ratio
λ_c	Length of wetted chine to beam ratio
λ_{c1}	Nondimensional value of s_{c1}, s_{c1}/b
λ_{c2}	Nondimensional value of s_{c2}, s_{c2}/b
λ_g	Nondimensional value of $\overline{LCG}$, $\overline{LCG}/b$
λ_k	Nondimensional value of l_k, l_k/b
μ	Total sectional added mass
μ_a	Contribution to sectional added mass
μ_s	Sectional added mass at transom
ν	Kinematic viscosity of water
ξ	Boat damping ratio
ρ	Mass density of water
σ	Stability root
σ_I	Imaginary part of σ
σ_R	Real part of σ
τ	Steady state trim angle measured from keel line to calm water free surface at reference speed U
τ_c	Calculated value of τ
τ_w	Average wave slope near bow; see Equation (69)
$\phi(\lambda)$	Three dimensional or aspect ratio correction
ψ	See Equation (80)
ψ_d	See Equation (110)

ω Circular frequency of wave

ω_e Circular encounter frequency with waves

The prime (') symbol is generally used to denote quantities in nondimensional form. Factors used for nondimensionalizing the previously described quantities are $\rho/2$, U, b. Typical examples are given as follows:

$F_{BS}' = F_{BS}/(1/2\ \rho U^2 b^2)$

$M_{BS}' = M_{BS}/(1/2\ \rho U^2 b^3)$

$M_{\ddot{\theta}}' = M_{\ddot{\theta}}/(1/2\ \rho b^5)$

$t' = tU/b$

$\lambda_{cl} = s_{cl}/b$

$\mu' = \mu/(1/2\ \rho b^2)$

$\sigma' = \sigma b/U$

Subscript:

w Refers to wave component

ABSTRACT

A theoretical method is derived for predicting the linearized response characteristics of constant deadrise, high-speed planing boats in head and following waves. Comparisons of the theoretical predictions of the pitch and heave response-amplitude operators and phase angles with existing experimental data show reasonably good agreement for a wide variety of conditions of interest.

It appears that nonlinear effects are more severe at a speed-to-length ratio of 6 than of, say, 4 or less, principally because of the reduction of the damping ratio of the boat with increasing speed, and the consequent increase in motions in the vicinity of the resonant encounter frequency. However, it is concluded that the linear theory in its present form can serve as a useful design tool, especially since it has already been shown that the effect of hull parameters on performance as obtained from data in the linear range is valid for operation in realistic seas.

ADMINISTRATIVE INFORMATION

This investigation was authorized and funded by the Naval Sea Systems Command (SEA 035) under the General Hydrodynamics Research Program, SR-023-0101, Work Unit 1-1562-002.

INTRODUCTION

The history of the development of planing hulls has depended almost exclusively in the past on acquisition and analysis of full-scale and model experimental data. This has been especially true in the area of seakeeping where until only a few years ago, practically no experimental data were available. Following a study by Savitsky,[1] in which he noted that the lack of such data led to continuous controversy among boat designers as to the makings of a good rough water boat, extensive experiments were carried out at the Davidson Laboratory. In 1969 Fridsma[2] carried out experiments on a series of constant-deadrise models in smooth water and regular head waves to define the effects of deadrise, trim, loading, speed, and length-to-beam ratio as well as wave proportions on added resistance, heave and pitch motions, and impact accelerations. Despite the fact that he

---

[1] Savitsky, D., "On the Seakeeping of Planing Hulls," Marine Technology (Apr 1968). A complete listing of references is given on page 82.

[2] Fridsma, G., "A Systematic Study of the Rough-Water Performance of Planing Boats," Davidson Laboratory, Stevens Institute of Technology Report R-1275 (Nov 1969).

observed a significant nonlinear dependence of the motions on wave height, he concluded that his findings, which were predominantly obtained from measurements in the linear range, were valid and extremely important. This was further confirmed by later experiments made with more realistic irregular head waves,[3] when he observed that the results generally correlated well with his regular wave findings.

The relative success of a recently developed theoretical method for predicting porpoising of planing hulls[4] gave encouragement to the belief that a reasonably good dynamic model for the planing hull was in hand for the first time. This consisted of a set of three linear equations in the surge, heave, and pitch motions of the boat in calm water. The solution of these homogeneous equations for the stability roots led to predictions of porpoising trim angles which were on the whole in good agreement with experimental data. Expressions for the linearized wave forces and moments due to regular waves were consequently derived in the present report and were used with the previously described equations for predicting motions in waves.

Although the theory is linear and has several approximations, it is felt that its basic structure is correct in view of the good overall agreement with the extensive model data obtained by Fridsma[2] in regular waves. Furthermore, as noted previously, since results obtained in the linear range are valid, concerning the effect of hull parameters on performance, it is felt that the theory will serve as a useful design tool in its present form.

EQUATIONS OF MOTION

The linearized equations for the longitudinal motions of surge, heave and pitch in regular head and following waves are derived in Appendix A. Although the derivation is for all three degrees of freedom, the numerical

---

[3]Fridsma, G., "A Systematic Study of the Rough-Water Performance of Planing Boats, Irregular Waves--Part 2," Davidson Laboratory, Stevens Institute of Technology Report R-1495 (Mar 1971).

[4]Martin, M., "Theoretical Prediction of Porpoising Instability of High-Speed Planing Boats," DTNSRDC Report 76-0068 (Apr 1976).

calculations in this report have been obtained from the solutions to the coupled pitch and heave equations only. This was felt to be justified on the basis of the experimental findings of Fridsma.[2,3] He found from visual observations and on examination of the time history record of model boat motions in regular head waves that little surging motion took place, particularly at speed-to-length ratios of 4 and 6. To verify this observation at a speed-to-length ratio of 2, comparative tests were made for both "constant speed" and "constant thrust" conditions. He found little difference in the pitch and heave motions. This result is not altogether surprising in view of the fact that, according to Equation (121) of Appendix A, the theoretical estimates of the surge component of the wave excitation force are essentially given by the product of the heave component with the tangent of the steady state, running-trim angle. Since the trim angles of his experiments were between 4 and 6 degrees, the wave excitation force in surge would be expected to be much less than in heave. Accordingly, the surge degree of freedom is omitted from the equations of motion given as follows. These equations, which are in nondimensional form, are for a planing boat moving with constant forward speed U and are written with respect to its body coordinate system at its steady calm water running trim; i.e., no motion except steady forward speed. The origin of the coordinate system is located at the boat center of gravity. The axes Ox, Oy, and Oz are, respectively, forward, starboard, and vertically down. From Equations (127) and (128) of Appendix A, we have

$$(m'-Z_{\ddot{z}}')\,\ddot{z}' - Z_{\dot{z}}'\dot{z}' - Z_z z' - Z_{\ddot{\theta}}'\ddot{\theta}' - Z_{\dot{\theta}}'\dot{\theta}' - Z_\theta'\theta = (Z)_w'\, e^{-i\omega_e' t'} \qquad (1)$$

$$-M_{\ddot{z}}'\ddot{z}' - M_{\dot{z}}'\dot{z}' - M_z'z' + (I_y'-M_{\ddot{\theta}}')\,\ddot{\theta}' - M_{\dot{\theta}}'\dot{\theta}' - M_\theta\theta = (M)_w'\, e^{-i\omega_e' t'} \qquad (2)$$

where the prime (') symbol indicates quantities nondimensionalized on the basis of U, b, and $\rho/2$, and

$\ddot{z}', \dot{z}', z'$ = vertical heave acceleration, velocity, and displacement, respectively, positive down

$\ddot{\theta}', \dot{\theta}', \theta$ = pitch angular acceleration, velocity, and displacement, respectively, positive bow up

m' = mass of the boat

I_y' = pitch moment of inertia of the boat about the y-axis through the center of gravity

ω_e' = wave encounter frequency $kb\left(1 \pm \frac{c}{U}\right)$

t' = time

$(Z)_w', (M)_w'$ = complex amplitudes of wave excitation force and wave excitation moment, respectively, about the center of gravity

b = boat beam

k = wave number, $2\pi/L_w$

c = wave celerity

L_w = wave length

U = steady reference boat speed.

The coefficients of the motion variables such as $Z_{\ddot{z}}', Z_{\dot{z}}'$, etc., are the stability derivatives of the boat. There are 12 of these in the previous equations and 24 when the surge degree of freedom is included. The equations for these coefficients were derived in Reference 4. The equations for the wave excitation force and moment are derived in Appendix A by treating the craft as a slender body with a correction factor for three-dimensional effects. These equations are conveniently written in terms of five components. From Equations (120) and (122) of Appendix A, they are

$$(Z)_w' \, e^{-i\omega_e' t'} = -\left[(F_1)_w' + (F_2)_w' + (F_5)_w' + (F_p)_w' + (F_h)_w'\right] \cos\tau \quad (3)$$

$$(M)_w' \, e^{-i\omega_e' t'} = (M_1)_w' + (M_2)_w' + (M_5)_w' + (M_p)_w' + (M_h)_w' \quad (4)$$

The definitions of the individual components are given as follows, and the appropriate equations for regular head and following waves are found in Appendix A.

$(F_1)_w', (M_1)_w'$ = integrated effect of the wave slope on the boat to chine immersion; see Equations (74) and (102)

$(F_2)_w', (M_2)_w'$ = integrated effect over the length of the boat of the wave orbital velocity; see Equations (82) and (103)

$(F_5)_w', (M_5)_w'$ = integrated effect over the length of the boat of the wave orbital acceleration; see Equations (87) and (104)

$(F_P)_w', (M_P)_w'$ = integrated effect over the length of the boat of the ambient perturbation pressure due to the waves; see Equations (111) and (115)

$(F_h)_w', (M_h)_w'$ = effect of change in boat wetted area due to wave elevation; see Equations (118) and (119).

All of the previously defined quantities are derived for the boat moving unperturbed at constant speed U in regular head or following waves. The effect of other wave headings is readily obtained as indicated in Appendix A. The hydrodynamic and inertial forces and moments resulting from the boat motions are given by the left-hand side of Equations (1) and (2).

NATURAL FREQUENCIES AND DAMPING

By setting the right-hand side of Equations (1) and (2) equal to zero and solving for the boat response to an initial perturbation, we obtain a solution which describes the dynamic characteristics of the boat in calm water.

$$z'(t) = z_1 e^{\sigma_1' t'} + z_2 e^{\sigma_2' t'} + \ldots\ldots \quad (5)$$

$$\theta(t) = \theta_1 e^{\sigma_1' t'} + \theta_2 e^{\sigma_2' t'} + \ldots\ldots \quad (6)$$

where $z_1, z_2, \ldots . \theta_1, \theta_2, \ldots$ are constants which depend on the initial conditions. The σ' terms determine the character of the time history response of the boat to any small disturbance. Four values of σ' are obtained from the roots of the resulting characteristic equation.

$$A\,\sigma'^4 + B\,\sigma'^3 + C\,\sigma'^2 + D\,\sigma' + E = 0 \quad (7)$$

where

$$A = (Z_{\ddot{z}}' - m')(M_{\ddot{\theta}}' - I_y') - M_{\ddot{z}}' Z_{\ddot{\theta}}'$$

$$B = Z_{\dot{z}}'(M_{\ddot{\theta}}' - I_y') + (Z_{\ddot{z}}' - m') M_{\dot{\theta}}' - M_{\ddot{z}}' Z_{\dot{\theta}}' - M_{\dot{z}}' Z_{\ddot{\theta}}'$$

$$C = Z_z'(M_{\ddot{\theta}}' - I_y') + Z_{\dot{z}}' M_{\dot{\theta}}' + (Z_{\ddot{z}}' - m') M_{\theta}' - M_{\ddot{z}}' Z_{\theta}' - M_{\dot{z}}' Z_{\dot{\theta}}' - M_z' Z_{\ddot{\theta}}' \quad (8)$$

$$D = Z_z' M_{\dot{\theta}}' + Z_{\dot{z}}' M_{\theta}' - M_{\dot{z}}' Z_{\theta}' - M_z' Z_{\dot{\theta}}'$$

$$E = Z_z' M_{\theta}' - M_z' Z_{\theta}'$$

The roots of these equations may be real or complex conjugate pairs. In either case it is seen from Equations (5) and (6) that if any root has a positive real part, the transient response increases without limit, and the boat is considered unstable in the linear sense.

In general a complex pair of roots represents an oscillatory mode; e.g., for the root pair $\sigma' = \sigma_R' \pm i\,\sigma_I'$, the z' response is

$$z' = e^{\sigma_R' t'} (c_1 \cos \sigma_I' t' + c_2 \sin \sigma_I' t') \quad (9)$$

where c_1 and c_2 are real constants which are determined by the initial conditions. The magnitude of the imaginary part of the root σ_I' is the nondimensional natural frequency of the modal motion. In dimensional form, the natural frequency and period are

$$\sigma_i = \sigma_I' \frac{U}{b} \text{ rad/sec} \quad (10)$$

$$T = \frac{2\pi}{\sigma_I} \text{ sec} \quad (11)$$

The effect of the real part of the root σ_R' may be illustrated by computing the time for a transient disturbance to either halve or double itself in magnitude. Thus, if σ_R' is negative, the envelope of the disturbance will be halved when

$$e^{\sigma_R' t'} = e^{\sigma_R t} = 1/2 \tag{12}$$

It follows that the time for the disturbance motion of each mode to halve or double itself is

$$t_{1/2} \text{ or } t_2 = 0.69/\sigma_R \text{ sec} \tag{13}$$

Another useful measure of damping of oscillatory modes is the damping ratio ξ, which is directly related to the rate of decay of disturbance oscillations. It is given by

$$\xi = -\frac{\sigma_R}{\sqrt{\sigma_R^2 + \sigma_I^2}} \tag{14}$$

In the vicinity of the resonant encounter frequency, in waves, the damping ratio is also inversely related to the amplification ratio of the boat response. Values of ξ between 0.6 and 1.0 are usually considered to give well-damped modes. Values less than about 0.4 are generally considered to produce underdamped modes. Although the foregoing may provide a rough indication of the vertical plane dynamic characteristics of the boat, a dynamic motions analysis is required for any detailed study.

STEADY STATE MOTION IN WAVES

The steady state solution of Equations (1) and (2) is a simple harmonic motion in heave and pitch and has the following form

$$z' = z_0' \, e^{-i\omega_e' t'} \tag{15}$$

$$\theta = \theta_0 \, e^{-i\omega_e' t'} \tag{16}$$

where z_0' and θ_0 are the complex amplitudes of the heave and pitch motion. Substituting these equations into Equations (1) and (2) leads to the following equations for z_0' and θ_0.

$$A_1 \, z_0' + A_2 \, \theta_0 = (Z)_w' \tag{17}$$

$$B_1 \, z_0' + B_2 \, \theta_0 = (M)_w' \tag{18}$$

where

$$A_1 = (Z_{\ddot{z}}' - m') \, \omega_e'^2 - Z_z' + i \, Z_z' \, \omega_e'$$

$$A_2 = Z_{\ddot{\theta}}' \, \omega_e'^2 - Z_\theta' + i \, Z_{\dot{\theta}}' \, \omega_e'$$

$$B_1 = M_{\ddot{z}}' \, \omega_e'^2 - M_z' + i \, M_{\dot{z}}' \, \omega_e'$$

$$B_2 = (M_{\ddot{\theta}}' - I_y') \, \omega_e'^2 - M_\theta' + i \, M_{\dot{\theta}}' \, \omega_e'$$

The solution to these equations is

$$z_0' = \frac{(Z)_w' \, B_2 - (M)_w' \, A_2}{A_1 \, B_2 - A_2 \, B_1} = z_R' + i \, z_I' \tag{19}$$

$$\theta_0 = \frac{(M)_w' \, A_1 - (Z)_w' \, B_1}{A_1 \, B_2 - A_2 \, B_1} = \theta_R + i \, \theta_I \tag{20}$$

Alternately, in terms of the amplitude and phase angle

$$z_0' = |z_0'| e^{i\alpha_z} \tag{21}$$

$$\theta_0 = |\theta_0| \, e^{i\alpha_\theta} \tag{22}$$

where

$$|z_0'| = (z_R'^2 + z_I'^2)^{1/2} \qquad \alpha_z = \tan^{-1}(z_I'/z_R')$$

$$|\theta_0| = (\theta_R^2 + \theta_I^2)^{1/2} \qquad \alpha_\theta = \tan^{-1}(\theta_I/\theta_R)$$

The denominator of Equations (19) and (20) is the characteristic quartic (Equation 7) where $i\omega_e'$ replaces σ'. This may be written in terms of the stability roots. When this is done, Equations (19) and (20) become

$$z_0' = \frac{(Z)_w' \, B_2 - (M)_w' \, A_2}{A \, Q} \tag{23}$$

$$\theta_0 = \frac{(M)_w' \, A_1 - (Z)_w' \, B_1}{A \, Q} \tag{24}$$

where A is given by Equation (8) and

$$Q = (i\omega_e' - \sigma_1')(i\omega_e' - \sigma_2')(i\omega_e' - \sigma_3')(i\omega_e' - \sigma_4')$$

For the planing hulls investigated there was always one dominant pair of complex conjugate stability roots. If the damping ratio of the mode is low, one may expect large motions when the wave encounter frequency is near the modal natural frequency. This is clear from the following form of the expression for modulus of Q in Equations (23) and (24).

$$|Q| = \omega_{UN}'^2 \, \sigma_3' \, \sigma_4' \left[\left(1 - \frac{\omega_e'^2}{\omega_{UN}'^2}\right) + 4 \frac{\omega_e'^2}{\omega_{UN}'^2} \xi_1^2\right]^{1/2} \times \left[\left(1 - \frac{\omega_e'^2}{\sigma_3' \, \sigma_4'}\right)^2 + 4 \frac{\omega_e'^2}{\sigma_3' \, \sigma_4'} \xi_2^2\right]^{1/2} \tag{25}$$

where $\omega_{UN}'^2 = \sigma_1' \sigma_2'$ is the square of the undamped natural frequency of the oscillatory mode, and $\xi_1 = -\dfrac{\sigma_1' + \sigma_2'}{2\sqrt{\sigma_1' \sigma_2'}}$ is the damping ratio of the oscillatory mode ($\xi_1 < 1$). Similar definitions apply to the σ_3', σ_4' modes, except in most cases $\xi_2 > 1$, so that the second mode is not oscillatory. It is seen that the first term can have a sharp minimum at the resonant value of ω_e', depending on how small ξ_1 is. If the remaining terms and the wave force vary slowly with frequency in the vicinity of this minimum, then the heave and pitch amplitude might be expected to have a well-defined resonance peak near this frequency. The encounter frequency at which this would occur is given by

$$\omega_R' = \omega_{UN}' \sqrt{1 - 2\xi_1^2} = \omega_{DN}' \left[\frac{1 - 2\xi_1^2}{1 - \xi_1^2}\right]^{1/2} \qquad (26)$$

$$\text{for } \xi_1 < 1/\sqrt{2}$$

where $\omega_{DN}' = \frac{1}{2}|\sigma_1' - \sigma_2'|$ is the damped natural frequency of the mode. It is seen that the value of this so-called resonance frequency is smaller than both the damped and undamped natural frequencies. If Equation (26) is substituted for ω_e' in Equation (25), the magnitude of $|Q|$ is approximately proportional to ξ_1 for small ξ_1, and the response z_0' and θ_0 at resonance is roughly inversely proportional to ξ_1. Thus, for the previously stated conditions

$$\left.\begin{aligned} z_0' &\sim 1/\xi_1 \\ \theta_0 &\sim 1/\xi_1 \end{aligned}\right\} \text{ near resonance for } \xi_1 \ll 1 \qquad (27)$$

COMPARISON WITH EXPERIMENT

Since the only systematic experimental data available about motions of prismatic planing hulls (Figure 1) in regular waves are those obtained by Fridsma,[2] the theory will be compared with these data only. This is not particularly restrictive since experiments have been performed with 16 configurations built around a rather large series of constant deadrise models (Figure 1), and, as stated earlier, measurements were obtained for effects of deadrise, trim, loading, length-to-beam ratio and speed on the pitch-and-heave amplitude and the phase angle in regular head waves. To facilitate comparisons of the theory with these measurements, the amplitudes of the heave and pitch motion are nondimensionalized by the amplitudes of the wave height and wave slope, respectively. These so-called response-amplitude operators (RAO) are then

$$\frac{|z_0|}{h} = |z_0'| \frac{b}{h} = \text{heave RAO} \tag{28}$$

$$\frac{|\theta_0|}{kh} = \text{pitch RAO} \tag{29}$$

Since the sense of positive boat displacement was assumed opposite to that for wave surface elevation in the equations of motion (Appendix A), the phase lag ε_z, when both displacements are taken in the same sense, is

$$\varepsilon_z = \alpha_z - \pi \tag{30}$$

The phase lead in pitch is given by

$$\varepsilon_\theta = 2\pi - \alpha_\theta \tag{31}$$

The previously described quantities, Equations (28) to (31), are plotted against a modified version of the nondimensional wave number

$$C_\lambda = \frac{b}{L_w}\left(C_\Delta \frac{\ell}{b}\right)^{1/3} \tag{32}$$

The factor $\left(C_\Delta \frac{\ell}{b}\right)^{1/3}$ was determined empirically[2] so as to minimize the effect of the boat length-to-beam ratio, ℓ/b (or rather the radius-of-gyration--to--beam ratio) and the load factor C_Δ (or the mass) on the value of C_λ at the resonant encounter frequency.

The principal geometric characteristics of each of the 16 configurations investigated are given in Table 1. The values of the non-dimensional longitudinal position of the center of gravity from the transom $(\overline{LCG}/b)_1$ shown in the table were obtained from interpolations of cross plots of $\overline{LCG}$ versus trim angle curves obtained from smooth water experiments. These were estimated by Fridsma[2] to give the running trim angles τ_E shown in the table.

For the theoretical predictions, it was necessary to calculate the running trim. This was determined for all configurations from the previously mentioned values of $(\overline{LCG}/b)_1$. Although most of the calculated trim angles τ_c were within approximately one-half degree of the desired τ_E values, a few were about 1 degree lower. Since the trim angle plays the major role in determining the dynamic characteristics of the boat, it has been necessary, in these cases, to make calculations for a second $\overline{LCG}$ position selected to give a calculated trim angle closer to the desired value. The resulting determinations are shown in Table 1B and designated by subscript 2.

For each configuration theoretical calculations were made of the pitch and heave RAO's and the corresponding phase angles as defined by Equations (28) to (31) for wavelengths ranging between 1 and 60 boat lengths. In addition the stability roots for each configuration were also determined. It was found that for speed-to-length ratios of 4 and 6 there was only one pair of complex conjugate roots in virtually every case. For a speed-to-length ratio of 2, however, there were two pairs

TABLE 1 - PRINCIPAL CHARACTERISTICS OF CONFIGURATIONS INVESTIGATED

TABLE 1A											TABLE 1B		
Configuration	β deg	C_Δ	k_y/b	$\frac{1}{b}$	$\frac{V_k}{\sqrt{\ell}}$	$\left(\frac{LCG}{b}\right)_1$	τ_E	τ_C	ζ	$C_{\lambda R}$	$\left(\frac{LCG}{b}\right)_2$	τ_c	ξ
A	20	0.608	1.255	5	4	2.00	4.0	4.0	0.47	0.084	—	—	—
B			1.275		6	1.90	4.0	2.9	0.40	0.085	1.50	3.5	0.21
C			1.265		2	1.93	4.0	3.8	0.56	0.118	—	—	—
D			1.325		2	1.63	6.0	5.7	0.35	0.112	1.50	6.7	0.35
E			1.310		4	1.73	6.0	4.8	0.39	0.094	1.50	5.8	0.29
F		0.912	1.020		4	2.10	6.0	5.4	0.52	0.075	1.90	6.2	0.48
G		0.912	1.020		6	2.10	5.0	4.1	0.43	0.084	1.70	4.8	0.27
H	10	0.608	1.280		2	1.90	4.0	4.3	0.40	0.093	2.00	3.8	0.39
I			1.250		4	2.03	4.0	4.1	0.53	0.072	1.65	5.3	0.39
J			1.310		6	1.60	4.0	3.4	0.21	0.105	1.30	3.8	0.06
K	30		1.235		4	1.95	4.0	3.6	0.40	0.096	1.75	4.3	0.38
L			1.245		2	1.88	4.0	3.8	0.28	0.147	1.60	5.4	0.30
M			1.240		6	1.98	4.0	2.7	0.40	0.080	1.50	3.6	0.24
N	20		1.488	6	4	2.13	4.0	3.3	0.46	0.086	1.85	4.0	0.39
O		0.912	1.200	6	4	2.40	4.0	4.1	0.52	0.075	2.00	5.5	0.44
P		0.631	0.948	4	4	1.90	4.0*	4.5	0.52	0.073	1.65	5.6	0.48

*Running trim of 4.0 degrees was reported in Reference 2 for this configuration; however, a check of calm water trim data suggests that angle was actually closer to 5 degrees.

of complex conjugate roots in every case. This presumably was due to the importance of buoyancy forces at these lower speeds. Calculations were also made of the value of $C_{\lambda R}$. This is the value of C_λ for which the encounter frequency is equal to the so-called resonance frequency ω_R' as determined from Equation (26). This occurs for head waves when L_w/b in Equation (32) is given by the following equation

$$\frac{L_w}{b} = 2\pi \left[\frac{1 + \sqrt{1 + 4\,\omega_R'\,C_V^2}}{2\,\omega_R'\,C_V} \right]^{1/2} \tag{33}$$

where $C_V = \dfrac{U}{\sqrt{g\,b}}$ is the speed coefficient.

These, together with the estimated damping ratios, are shown in Table 1. It is seen that the values of $C_{\lambda R}$ for nearly all cases lie between 0.075 and 0.10. The effect of increased trim angle, decreased load coefficient, and increased speed are seen to decrease the damping ratios. The effect of length-to-beam ratio does not appear to be significant. The effect of deadrise appears to be small at a speed-to-length ratio of 4; however, at a speed-to-length ratio of 6, the damping ratio decreases with decreasing deadrise angle for similar running-trim angles. The 10-degree-deadrise configuration J, having an estimated damping ratio of 0.06 at a trim angle just under 4 degrees, is seen to have the lowest damping ratio by far. It will be seen that this condition resulted in the most violent motion of all.

The results of the theoretically determined RAO's and phase angles are plotted in Figures 2 through 17. The figures for each speed-to-length ratio are discussed separately.

SPEED-TO-LENGTH RATIO EQUALS 4

Most of the parametric study has been performed at the speed-to-length ratio of 4 because this speed is more typical in planing craft operation than speed-to-length ratios of 2 and 6. Figures 2 to 9 show comparisons of the measured and computed values of the pitch and heave RAO and phase angle as a function of the modified nondimensional wave number parameter C_λ.

Also shown on the abscissa is a scale of wavelength-to-beam ratio. The solid curves represent RAO's and phase angles as calculated on the basis of the model $(\overline{LCG}/b)_1$ values shown in Table 1A. In some cases broken curves are also shown. These represent the effect of a small change in the $\overline{LCG}$ position and trim angle as listed in Table 1B. The data points are indicated by the symbols shown. The experimental wave height-to-beam ratio was 0.111 for all configurations, except the one shown in Figures 2a and 2b, where the effect of wave height was also investigated. It may be seen from this latter figure that the effect of wave height does not appear to be large, except perhaps at $C_\lambda = 0.15$. However, it will be seen later that this is not necessarily true for all configurations.

Examinations of Figures 2 through 9 shows that the motions reach their maximum amplitudes very close to the predicted resonant encounter frequency, corresponding to the value of $C_{\lambda R}$ given in Table 1A. It is also seen that the slope of the phase angle curve tends to be a maximum near this value of C_λ, as one might expect. The overall agreement between the calculated and measured RAO's and phase angles is seen to be quite good even for the cases in which the conditions of the experiment were not simulated by the theory in all respects. For example, the running-trim angle for Configuration E was estimated to be 4.8 degrees, while the model value was reported to be 6.0 degrees. A recalculation using an $\overline{LCG}$ position of 1.50 beams instead of the original 1.73 beams gave a calculated running-trim angle of 5.8 degrees and better agreement with the data, as shown by the broken curves in Figures 3a and 3b. Although the assumed $\overline{LCG}$ position was further aft than on the model, this discrepancy had much less influence on the boat dynamics than the running-trim angle. It is of interest to note from Table 1B that the increased trim angle resulted in a decrease in the damping ratio from 0.39 to 0.29, thus accounting for the sharper peak response. It is also worth noting that the phase angles in Figures 3a and 3b were unaffected by the trim angle change to a value of C_λ of 0.15. However, for larger values there is a larger phase lag, though the motion amplitudes are not greatly affected. Fridsma[2] made the same observations

on the basis of comparing the data from Configurations A with those from E; see Figures 2 and 3. These configurations have estimated damping ratios of 0.47 and 0.29, respectively. However, when a boat is in a more stable configuration due, for example, to increased loading or smaller running trim angle, the damping ratio is higher, and the effect of a small increase in trim angle is significantly smaller. This is shown in Figures 4, 7, and 9.

In a few cases, where part of the bow was estimated to be in water, the agreement with theory is better than one might expect, since the present theory does not include this effect. This was especially true for Configurations K and P; see Figures 6 and 9. The former had a 30-degree-deadrise angle and the latter a length-to-beam ratio of 4.

SPEED-TO-LENGTH RATIO EQUALS 6

At a speed-to-length ratio of 6, the planing craft becomes less stable and the motions more severe. According to Table 1B, the damping ratios at this speed are the lowest. It is seen that the damping ratios of Configurations B, J, and M decrease with a decrease in deadrise for running-trim angles slightly under 4.0 degrees. On the other hand, Configuration G, because of its higher loading has the highest damping ratio even though the trim angle is close to 5.0 degrees.

The effect of wave height was investigated with Configuration B (Figure 10) only. It is seen from this figure that the nonlinear effects are more pronounced than at the lower speed. This is especially true near the resonant encounter frequency and may, in part at least, account for the measured peak RAO's being lower than the theoretical ones. Reasonably good agreement was obtained between the computed and measured RAO's for the more highly loaded 20-degree-deadrise boat; see Figure 11. The predictions for the 30-degree-deadrise boat (Figure 12) were not as good, particularly for the pitch RAO. This may, in part, be due to the fact that a portion of the model bow was in the water. The poorest agreement with the predictions of RAO were for the 10-degree-deadrise boat; see Figure 13. The possible reasons for this will be discussed later.

For every data point, except one, by using the theory the variation of phase angle with encounter frequency is predicted quite well. This is especially evident from the solid phase angle curves shown in Figures 10 through 13, which were computed from the original $\overline{LCG}$ position. The reason for the discrepancy at $C_\lambda = 0.10$ in Figure 13 is not apparent. Calculations for the more aft position of $\overline{LCG}$ generally show an increase in the phase lag at $C_\lambda > 0.15$ which is larger than that at a speed-to-length ratio of 4. This indicates that the boat response is more sensitive at this speed than at the lower speed to the shift in $\overline{LCG}$ position required to correct the estimated running trim. It appears that an improved method of estimating running-trim angles, within the context of the present theory, would be desirable and would contribute toward removal of this type of discrepancy, not only in the phase angle but also in RAO predictions.

As noted earlier, poorest agreement between theory and data was obtained for RAO's of Configuration J; see Figure 13. According to Table 1B this boat had an estimated damping ratio of approximately 0.06 and was therefore not far from a porpoising condition. This is indicated also by the sharply tuned peak in measured RAO's and the steep slope in the phase angle data curve. Although the theoretical phase angle curve is shifted to the right, it is apparent that it exhibits a variation with C_λ in the vicinity of resonance similar to the data. This suggests that the theoretical prediction of the damping ratio is reasonable. Since the peak RAO is roughly inversely proportional to the damping ratio (Equation (27)) a small error in damping ratio, when this quantity is less than 0.1, can lead to large discrepancies in RAO. It also becomes more difficult to find the resonant peak experimentally. One would expect to find it close to the region of maximum slope in the phase angle curve. Since there was no recorded data point in the interval of wavelengths between 15 and 20 beam widths, where the phase angle changed by more than 100 degrees, it is possible that the resonant condition was not measured. It is, therefore, also possible that peak RAO's are actually higher than those

shown by data points in the figures. Even if this were so it would be expected that nonlinear effects would limit the response to something less than predicted.

It is also seen in Figure 13 that a second peak in RAO's occurred for a wavelength of approximately 7.5 boat widths. According to Reference 2 the model was reported to rebound from a wave crest, completely "fly over" a second wave crest, and land on the third. It thus had an actual excitation frequency of one-half that normally expected. This is very close to the resonant frequency of the craft, which presumably occurs at a wavelength between 15 and 20 beam widths. Although the phenomenon is undoubtedly due to nonlinear effects, it is doubtful that it would have occurred if the boat were not in a highly tuned condition due to the fact that it was not far from a porpoising condition. It should be remarked, however, that it is somewhat surprising that the resonant frequency of the boat seems to have been altered very little, although the change in the flow condition on the boat is apparently very large.

SPEED-TO-LENGTH RATIO EQUALS 2

The speed-to-length ratio of 2 represents the prehump condition where buoyancy forces are predominant, and significant side wetting above the chines occurs. Furthermore, at this speed the hydrodynamic coefficients may be Froude number and frequency dependent. Since the theoretical predictions of the hydrodynamic forces assume no side wetting or Froude number dependence, it should be expected that the motion predictions would suffer somewhat because of this. Furthermore, it was estimated that most of the bow of each of the boat models tested at this speed was in the water. As noted earlier, the present theory does not include the effect of bow immersion. Despite these shortcomings, the theory was exercised, and comparisons were made with the experimental data for all of the configurations tested.

As mentioned before, all of these configurations had two pairs of complex conjugate roots, representing two natural frequencies. However, one of them was a low-frequency, highly damped mode. The values of $C_{\lambda R}$ and ξ for the other mode are shown in Table 1. It is seen that all of the configurations (C, D, H, and L) are predicted to have a fair amount of damping. Comparisons of the theoretical predictions of RAO and phase angle with the experimental data for the 10- and 20-degree-deadrise boats; i.e., Configurations C, D, and H, shown in Figures 14 through 16, are better than might have been expected. The predictions for the 30-degree-deadrise model appear to be worse than the others. This is probably due to the fact that this boat ran with the greatest amount of bow immersion.

CONCLUSIONS

The theoretical method proposed in the present report appears to provide reasonably good predictions of the linear response characteristics of high-speed planing boats in waves. Accuracy of the predictions of RAO's and phase angles is best around a speed-to-length ratio of 4. This is fortunate since this is the most typical speed for planing craft operation. Although the predictions of the phase angles at a speed-to-length ratio of 6 are good, there is a tendency to overestimate resonant RAO's in most cases. This problem appears to be most severe when the boat is operating near its porpoising condition. Part of the reason for overestimation may be due to the fact that nonlinear effects are not accounted for in the theory. In addition it is felt that a more precise method for estimating the running-trim angle, in the context of the present theory, would lead to a further improvement in these predictions.

Since the present theory was derived for prismatic planing hulls, it does not take into account detailed variations in hull geometry. Furthermore, it is a linear theory, and a number of simplifications and approximations have been incorporated in it. It is anticipated that further development to eliminate these shortcomings will take place. Nevertheless it is considered to be a useful design tool in its present

form, especially since it has been shown that the effect of hull parameters on performance, as obtained from data in the linear range, is valid for operation in realistic seas.

ACKNOWLEDGMENTS

I wish to express my deep gratitude to Mr. Jaques B. Hadler, under whose supervision the present work was started, and to Mr. Grant R. Hagen, Head--Ship Dynamics Division, for their continuing encouragement and interest in the present effort. My appreciation is also extended to Dr. William E. Cummins, Head--Ship Performance Department, and to Mr. Vincent J. Monacella for their valuable assistance and support. Furthermore, special thanks are due to Ms. Nadine Hubble, who developed the computer program and carried out all of the calculations with her characteristic skill and efficiency.

APPENDIX A

FORCE AND MOMENT DUE TO WAVES AND THE EQUATIONS OF MOTION

FORCE AND MOMENT DUE TO WAVES

It is assumed that the craft is proceeding in straight-line motion at constant speed U and arbitrary heading angle β_h through regular waves. Perturbations from the straight-line motion are assumed to be zero and only the force and pitch moment excitation in the vertical plane, due to waves, are to be determined in this section. Since the theory is concerned mainly with the high-speed, low-aspect ratio condition, it is assumed that the craft may be treated as a slender body with a three-dimensional flow, or aspect-ratio correction, and that unsteady effects are small.

The total hydrodynamic force on the craft is taken as the sum of the time rate of change of the transverse momentum in the vertical plane imparted to the water by the presence of the moving craft and the ambient perturbation pressure due to the waves. Determination of the first of these, the dynamic part of the force, initially follows the lines used by the author in deriving the equations for porpoising planing craft.[4]

This type of analysis was originally suggested in 1924 by Munk[5] and Jones[6] in connection with the analysis of airships and slender wings and has more recently been generalized by Bryson[7] for slender finned missiles.

---

[5]Munk, M.M., "The Aerodynamic Forces on Airship Hulls," National Advisory Committee for Aeronautics Report 184 (1924).

[6]Jones, R.T., "Properties of Low-Aspect-Ratio Wings at Speeds Below and Above the Speed of Sound," National Advisory Committee for Aeronautics Report 835 (1946).

[7]Bryson, A.E., Jr., "Stability Derivatives for a Slender Missile with Application to Wing-Body-Vertical Tail Configuration," Journal of Aeronautical Sciences, Vol. 20, No. 5, pp. 297-308 (1953).

It has been applied to the problem of the translational impact of seaplanes on water by Mayo[8] and others.[9,10]

The equations for the wave force and moment are described with respect to orthogonal axes Ox, Oy, and Oz with origin fixed at the center of gravity of the boat. The axis Ox is in the fixed direction of the forward reference speed U of the boat. The axis Oy is starboard, and Oz is vertically down; see Figures 18 and 19.

The flow over the hull is assumed to occur in transverse planes which are fixed in space and oriented normal to the keel. The momentum of each layer of water transverse to the keel is $\mu\dot{\zeta}\ ds$, where μ is the two-dimensional added mass of the section of the hull at point s, interacting with the wave motion in the section of flow plane of length ds, and $\dot{\zeta}$ is the component of the orbital velocity* normal to the keel at that section. The coordinate s is measured aft from the foremost immersed station along the keel. The dynamic part of the normal force on the section ds of the hull is the time rate of change of the momentum imposed on the layer of water ds by the presence of the hull

$$dF = \frac{d}{dt}(\mu\dot{\zeta})\ ds \tag{34}$$

Both μ and $\dot{\zeta}$ will in general be functions of the longitudinal position coordinate x of the hull section and time t. Since the time derivative is in the fixed transverse plane, it must reflect the changing coordinate x of the transverse plane with time. Thus

---

[8]Mayo, W.L., "Analysis and Modification of Theory for Impact of Seaplanes on Water," National Advisory Committee for Aeronautics Report 810 (1945).

[9]Milwitzky, B., "A Generalized Theoretical and Experimental Investigation of the Motions and Hydrodynamic Loads Experienced by V-Bottom Seaplanes During Step-Landing Impacts," National Advisory Committee for Aeronautics TN 1516 (1948).

[10]Schnitzer, E., "Theory and Procedure for Determining Loads and Motions in Chine--Immersed Hydrodynamic Impacts of Prismatic Bodies," National Advisory Committee for Aeronautics Report 1152 (1953).

*This is reasonably constant over the depth of planing craft.

$$\frac{d}{dt} = \frac{\partial}{\partial t} - U \frac{\partial}{\partial x} \tag{35}$$

The normal force on the entire hull due to the orbital motion is obtained by integrating Equation (34) along the wetted length of the hull l_k and multiplying by a correction factor $\phi(\lambda)$ to account for the three-dimensionality of the flow.

$$F_D = \phi(\lambda) \left[\int_0^{\ell_k} \dot{\zeta} \frac{d\mu}{dt} \, ds + \int_0^{\ell_k} \mu \frac{d\dot{\zeta}}{dt} \, ds \right] \tag{36}$$

The sectional added mass at any transverse section depends on the sectional geometry of the boat and the magnitude of ζ. According to Reference 4 the transverse sectional added mass distribution for a prismatic hull form may be estimated from the following equations for the separate contributions μ_a

$$\mu_a = \begin{cases} \frac{\rho\pi}{2} f(\beta)^2 \zeta^2 & 0 < s \leq s_{c1} \quad (37) \\ \frac{\rho \pi b^2}{4} (1 - \sin \beta) & s_{c1} < s \leq \ell_k \quad (38) \\ \frac{\rho}{2} Bb (\zeta - \zeta_{c2}) & s_{c2} \leq s \leq \ell_k \quad (39) \end{cases}$$

where ℓ_k = wetted length along keel; see Figure 19

$s_{c2} = l_k - l_m$

ℓ_m = mean wetted length of hull

$$s_{c1} = \frac{\sqrt{2}}{\pi} \frac{\tan \beta}{\tan \tau} b \quad \text{in calm water} \tag{40}$$

$$s_{c2} = (0.5\ (0.57 + 0.001\beta)\ (\tan \beta/(2 \tan \tau) - 0.006\beta) - 0.03)b \quad (41)$$

$$f(\beta) = \frac{90}{\beta} - 1 \quad (42)$$

β = deadrise angle, degrees

ζ_{c2} = ζ at $s = s_{c2}$

b = boat beam

The quantity s_{c1} is the value of s at which the chine becomes "effectively" immersed. The term B, which is Bobyleff's function, is a function of deadrise angle. The sectional added mass μ at any section is the sum of the contributions μ_a at that section. It follows from Equations (37) through (39) that we may put

$$\frac{d\mu}{dt} = \dot{\zeta} \frac{\partial \mu}{\partial \zeta} = \dot{\zeta} \frac{\partial \mu}{\partial s} \cot \tau \quad (43)$$

so that Equation (36) becomes

$$F_D = \phi(\lambda) \left[\int_0^{\ell_k} \dot{\zeta}^2 \frac{\partial \mu}{\partial \zeta}\, ds + \int_0^{\ell_k} \mu \frac{d\dot{\zeta}}{dt}\, ds \right] \quad (44)$$

where

$$\frac{\partial \mu}{\partial \zeta} = \begin{cases} \rho\, \pi\, \zeta\, f(\beta)^2 & 0 < s \leq s_{c1} \\ \\ \frac{\rho}{2} B\, b & s_{c2} \leq s \leq \ell_k \end{cases} \quad (45)$$

The corresponding moment is obtained by integrating the product of the stripwise force and the moment arm from the center of gravity (a-s).

$$M_D = \phi(\lambda) \left[\int_0^{\ell_k} (a-s)\, \dot{\zeta}^2 \frac{\partial \mu}{\partial \zeta}\, ds + \int_0^{\ell_k} (a-s)\, \mu \ddot{\zeta}\, ds \right] \quad (46)$$

where a is the value of s at the transverse flow plane through the center of gravity; i.e., $a = l_k - \overline{LCG}$, and $\overline{LCG}$ is the distance from transom to center of gravity; see Figure 18.

Determination of ζ, $\dot{\zeta}$ and $\ddot{\zeta}$

For the condition of the boat moving with constant speed and trim angle τ through waves, we may write

$$\zeta = s \tan \tau + \zeta_w \tag{47}$$

where the first term is the calm water value, and ζ_w is the contribution from the waves. With the aid of Equation (35) we have

$$\dot{\zeta} = U \sin \tau + \dot{\zeta}_w \tag{48}$$

since, according to Figure 19 we see that

$$\frac{\partial s}{\partial x} = - \cos \tau$$

Also since U sin τ is a constant

$$\ddot{\zeta} = \ddot{\zeta}_w \tag{49}$$

The values of ζ_w, $\dot{\zeta}_w$ and $\ddot{\zeta}_w$ are next determined from the velocity potential ϕ_w for the wave motion. This may be written with respect to the moving boat axes as follows, where x, y, and z are measured from a point directly above the center of gravity, and the real part is to be taken.

$$\phi_w = ihc\, e^{-kz}\, e^{ik\,[x \cos \beta_h + y \sin \beta_h + (U \cos \beta_h - c)\, t]} \tag{50}$$

where β_h = angle of wave crests from boat x-axis; β_h = 0 and π for following and head seas respectively; see Figure 18

h = wave amplitude, 1/2 wave height

c = wave celerity

k = $2\pi/L_w$ = wave number

L_w = wavelength

t = time

In the following we will consider only the head and following sea cases. We then have

$$\phi_w = ihc\, e^{-kz}\, e^{\mp ik[x + (U \pm c)\, t]} \tag{51}$$

In Equation (51) and the following, the upper sign refers to head seas; the lower sign, to following seas. The encounter frequency ω_e is given by

$$\omega_e = k\,(U \pm c) \tag{52}$$

The wave elevation is

$$\eta(x,t) = \frac{1}{g}\left(\frac{d\,\phi_w}{dt}\right)_{z=0} = h\, e^{\mp i(kx + \omega_e\, t)} \tag{53}$$

since $c^2 = g/k$. The horizontal and vertical components of the orbital velocity are given, respectively, by

$$v_w = -\frac{\partial\,\phi_w}{\partial x} = \mp\,\omega h\, e^{-kz}\, e^{\mp i(kx + \omega_e\, t)} \tag{54}$$

$$w_w = -\frac{\partial\,\phi_w}{\partial z} = i\omega h\, e^{-kz}\, e^{\mp i(kx + \omega_e\, t)} \tag{55}$$

where the circular frequency of the orbital motion is given by

$$\omega = kc$$

The expression for $\dot{\zeta}_w$ may be obtained as the sum of the components of the orbital velocity normal to the keel.

$$\dot{\zeta}_w = - v_w \sin \tau - w_w \cos \tau \tag{56}$$

Inserting Equations (54) and (55) leads to

$$\dot{\zeta}_w = - i\omega h \, e^{-kz} \, e^{\mp i(kx - \tau + \omega_e t)} \tag{57}$$

The expression for ζ_w is readily found from this equation and Equation (53) as

$$\zeta_w = \eta \, e^{\mp i\tau} \tag{58}$$

By operating on Equation (57) with Equation (35), we obtain the expression for the acceleration term, Equation (49).

$$\ddot{\zeta} = \ddot{\zeta}_w = - \omega^2 h \, e^{-kz} \, e^{\mp i(kx - \tau + \omega_e t)} \tag{59}$$

Evaluation of F_D

If we substitute Equations (45) and (47) through (49) into Equation (44) we obtain, on discarding second order terms in the wave disturbance,

$$F_D = F_1 + F_2 + F_3 + F_4 + F_5 \tag{60}$$

where

$$F_1 = \phi(\lambda) \, \rho \, \pi \, f(\beta)^2 \, U^2 \sin^2 \tau \int_0^{s_{cl}} (s \tan \tau + \zeta_w) \, ds \tag{61}$$

$$F_2 = 2 \, \phi(\lambda) \, \rho \, \pi \, f(\beta)^2 \, U \sin \tau \tan \tau \int_0^{s_{cl}} s \, \dot{\zeta}_w \, ds \tag{62}$$

$$F_3 = \phi(\lambda)\ B\ \rho\ U \sin\tau\ b \int_{s_{c2}}^{\ell_k} \dot{\zeta}_w\ ds \tag{63}$$

$$F_4 = \phi(\lambda)\ B\ \frac{\rho}{2}\ U^2 \sin^2\tau\ b \int_{s_{c2}}^{\ell_k} ds \tag{64}$$

$$F_5 = \phi(\lambda) \int_0^{\ell_k} \mu\ \ddot{\zeta}_w\ ds \tag{65}$$

The first term represents the effect of the variation in added mass to the point of effective chine immersion for constant normal speed component U sin τ. The next two terms give the effect of the orbital velocity. The fourth term is the calm water normal force contribution over that portion of the hull from s_{c2} to the transom. The last term gives the force due to wave orbital acceleration.

In Reference 4 the quantity s_{c1}, which is the value of s at which the chine just becomes effectively immersed, is evaluated on the basis of Wagner's[11] wave rise theory and an empirical correction by Shuford[12] for the calm water case. In that derivation, the value of ζ is s tan τ and s_{c1} is defined by the following equation

$$(f(\beta)\ s_{c1} \tan\tau)^2 = \frac{b^2}{2}(1 - \sin\beta) \tag{66}$$

To make use of this result, the expression for ζ_w in Equations (58) and (61) is approximated by the following equation in the range s = 0 to s = s_{c1}.

---

[11] Wagner, H., "The Phenomena of Impact and Planing on Water," National Advisory Committee for Aeronautics Translation 1366, ZAMM Bd 12, Heft 4, pp. 193-215 (Aug 1932).

[12] Shuford, C.L., Jr., "A Theoretical and Experimental Study of Planing Surfaces Including Effects of Cross Section and Plan Form," National Advisory Committee for Aeronautics Report 1355 (1957).

$$\zeta_w = s\left[\frac{\zeta_w(s_{c1}) - \zeta_w(0)}{s_{c1}}\right] + \zeta_w(0) \tag{67}$$

Making use of Equation (58) in Equation (67) and substituting this for ζ_w in Equation (61), we obtain

$$s \tan \tau + \zeta_w = s \tan (\tau + \tau_w) + \zeta_w(0) \tag{68}$$

where

$$\tau_w = \frac{h\, e^{\mp i(kx_b - \tau)}}{x_{c1}/\cos \tau}\left[e^{\mp ikx_{c1}} - 1\right] e^{\mp i\omega_e t} \tag{69}$$

x_b = horizontal distance from center of gravity to foremost immersed station on keel

$x_{c1} = s_{c1}/\cos \tau$

The first term on the right-hand side of Equation (68) represents the combined effect of trim angle and wave slope on the force in the interval $s = 0$ to $s = s_{c1}$. The second term is the effect of wave elevation on the force. This effect will be evaluated later. On substituting the first term on the right side of Equation (68) into Equation (61) and making use of Equation (66) with τ replaced by $\tau + \tau_w$, we obtain to the first order in the wave term

$$F_1 = \phi(\lambda)\, \rho\, \pi\, \frac{b^2}{4}\, (1 - \sin \beta)\, U^2\, (\sin \tau \cos \tau - \tau_w) \tag{70}$$

The first term in this equation is the calm water normal force contribution. When this is added to F_4 we obtain the total dynamic part of the steady state normal force F_{DS} on the hull. We nondimensionalize by dividing through by $1/2\, \rho\, U^2\, b^2$ and obtain

$$F_{DS}' = \frac{\lambda}{1+\lambda}\frac{\pi}{2}(1 - \sin\beta)\sin\tau\cos\tau + C_{D,c}\sin^2\tau\cos^2\tau\,\lambda\cos\beta \quad (71)$$

where we have made the following substitutions from Reference 4.

$$\phi(\lambda) = \frac{\lambda}{1+\lambda} \quad (72)$$

$$\phi(\lambda)\, B = C_{D,c}\cos^2\tau\cos\beta \quad (73)$$

$C_{D,c}$ = cross flow drag coefficient; see Table 2

λ = mean wetted length-to-beam ratio

TABLE 2 - CROSS FLOW DRAG COEFFICIENT*

Section Shape.....$C_{D,c}$
V-Bottom, constant deadrise.....1.33
V-Bottom, horizontal chine flare.....1.33 + 0.0147 β^o
V-Bottom, vertical chine strips.....1.60 + 0.0147 β^o

*Reference 12.

If we nondimensionalize the wave term in Equation (70) we obtain

$$(F_1)_w' = -\frac{\lambda}{1+\lambda} G\,\tau_w \quad (74)$$

where

$$G = \frac{\pi}{2}(1 - \sin\beta) \quad (75)$$

Equations (62), (63), and (65) are expressed in terms of the orbital motion at some depth z_a. For planing boats there is generally very little difference whether we take z_a at the keel or at the free surface.

Nevertheless we approximate it by the equation

$$z_a = \gamma\, s \sin \tau \tag{76}$$

where γ is taken as the fraction of the depth to the keel at which the orbital motion is considered to act. Since integrations are to be carried out from the foremost wetted portion of the keel aft, we substitute for x in Equations (57) and (59) the following

$$x = x_b - \frac{s}{\cos \tau} \tag{77}$$

Substituting Equations (76) and (77) into Equations (57) and (59) gives

$$\dot{\zeta}_w = - i\omega h\, e^{\mp i(\psi - k_0 s)} \tag{78}$$

$$\ddot{\zeta}_w = - \omega^2 h\, e^{\mp i(\psi - k_0 s)} \tag{79}$$

where

$$\psi = k\, x_b - \tau + \omega_e\, t \tag{80}$$

$$k_0 = (k/\cos \tau)\ (1 \mp i\, \gamma \sin \tau \cos \tau) \tag{81}$$

On substituting Equation (78) into Equations (62) and (63), carrying out the integration, and nondimensionalizing, we obtain with the aid of Equations (66), (72), (73), and (75) the following expression for the normal force due to orbital velocity.

$$(F_2)_w' = F_2' + F_3' = - i\, 4\, \frac{\omega b}{U} \left(\frac{h}{b}\right) e^{\mp i\psi} (H_1 \cos \tau + H_2 \sin \tau) \tag{82}$$

where

$$H_1 = \begin{cases} \dfrac{\lambda}{1+\lambda}\dfrac{G}{(k_0 s_{c1})^2}\left[e^{\mp i k_0 s_{c1}}(1 \mp i k_0 s_{c1}) - 1\right] & \text{for } \beta > 2^\circ \quad (83) \\ \\ \dfrac{\lambda}{1+\lambda}\dfrac{\pi}{4} & \text{for } \beta < 2^\circ \quad (84) \end{cases}$$

$$H_2 = \mp i \frac{C_{D,c}}{2 k_0 b} \cos^2 \tau \cos \beta \left(e^{\mp i k_0 s_{c2}} - e^{\mp i k_0 \ell_k}\right) \quad (85)$$

The selection of a 2-degree-deadrise angle in Equations (83) through (84) was to avoid the computational problem of a near zero in the term $(k_0 s_{c1})^2$ at a deadrise angle close to zero. It is assumed that Equation (84), which is strictly for zero deadrise angle, is suitable for angles to at least 2 degrees.

The force due to orbital acceleration is obtained by substituting Equations (37), (38), (39), and (79) into Equation (65). Thus

$$F_5 = -\phi(\lambda)\,\omega^2 h\, e^{\mp i\psi}\left[\frac{\rho\pi}{2} f(\beta)^2 \tan^2\tau \int_0^{s_{c1}} s^2 e^{\mp i k_0 s}\, ds + \frac{\rho\pi b^2}{4}(1-\sin\beta)\int_{s_{c1}}^{\ell_k} e^{\mp i k_0 s}\, ds + \frac{\rho B b \tan\tau}{2}\int_{s_{c2}}^{\ell_k}(s-s_{c2})\, e^{\mp i k_0 s}\, ds\right] \quad (86)$$

If we carry out the integrations, make the substitutions indicated by Equations (66), (72), and (73) and nondimensionalize, we obtain finally

$$(F_5)_w' = -2\left(\frac{\omega b}{U}\right)^2\left(\frac{h}{b}\right) e^{\mp i\psi}\left[\mp\frac{i H_3}{2} + H_4 + \tan\tau\,(H_5 - H_2 \lambda_{c2})\right] \quad (87)$$

where

$$H_3 = \begin{cases} \frac{\lambda}{1+\lambda} \frac{G\,\lambda_{c1}}{(k_0 s_{c1})^3} \left\{ e^{\mp i k_0 s_{c1}} \left[2 - (k_0 s_{c1})^2 \mp i2(k_0 s_{c1}) \right] - 2 \right\} & \text{for } \beta > 2^\circ \\ 0 & \text{for } \beta < 2^\circ \end{cases} \tag{88}$$

$$H_4 = \mp i \frac{\lambda}{1+\lambda} \frac{G}{2 k_0 b} \left(e^{\mp i k_0 s_{c1}} - e^{\mp i k_0 \ell_k} \right) \tag{89}$$

$$H_5 = \frac{C_{D,c} \cos^2 \tau \cos \beta}{2(k_0 b)^2} \left[e^{\mp i k_0 \ell_k} (1 \mp i k_0 \ell_k) - e^{\mp i k_0 s_{c2}} (1 \mp i k_0 s_{c2}) \right] \tag{90}$$

$$\lambda_{c2} = s_{c2}/b$$

In summary the dynamic part of the nondimensional force on the boat moving with constant speed and trim through regular head or following waves is given by

$$(F_D)' = F_{DS}' + (F_1)_w' + (F_2)_w' + (F_5)_w' \tag{91}$$

The effect of the ambient pressure and increased wetted area due to the waves will be determined later.

Evaluation of M_D

The dynamic part of the moment about the boat center of gravity is obtained, according to Equation (46), by multiplying each integrand in Equations (61) through (65) by the moment arm (a - s). The corresponding moment equation becomes

$$M_D = M_1 + M_2 + M_3 + M_4 + M_5 \tag{92}$$

where

$$M_1 = \phi(\lambda)\ \rho\pi\ f(\beta)^2\ U^2\ \sin^2\tau\ \tan(\tau + \tau_w) \int_0^{s_{c1}} (as - s^2)\ ds \qquad (93)$$

$$M_2 = 2\ \phi(\lambda)\ \rho\pi\ f(\beta)^2\ U\ \sin\tau\ \tan\tau \int_0^{s_{c1}} (as - s^2)\ \dot{\zeta}_w\ ds \qquad (94)$$

$$M_3 = \phi(\lambda)\ B\ \rho\ U\ \sin\tau\ b \int_{s_{c2}}^{\ell_k} (a - s)\ \dot{\zeta}_w\ ds \qquad (95)$$

$$M_4 = \phi(\lambda)\ B\ \frac{\rho}{2}\ U^2\ \sin^2\tau\ b \int_{s_{c2}}^{\ell_k} (a - s)\ ds \qquad (96)$$

$$M_5 = \phi(\lambda) \int_0^{\ell_k} (a - s)\ \mu\ \ddot{\zeta}_w\ ds \qquad (97)$$

On carrying out the integration in Equation (93) and using the result of Equation (70) one readily obtains

$$M_1 = \phi(\lambda)\ \frac{\rho\pi\ b^2}{4}\ (1 - \sin\beta)\ U^2\ (\sin\tau\cos\tau - \tau_w) \left(\ell_k - \overline{LCG} - \frac{2}{3}\ s_{c1}\right) \qquad (98)$$

The last term in parentheses is the moment arm of F_1 from the center of gravity. It is readily evaluated with the aid of Equations (40) and (41) where τ is replaced by $\tau + \tau_w$. Thus

$$\ell_k - \overline{LCG} - \frac{2}{3}\ s_{c1} = \ell_m - \overline{LCG} - \left(0.157 - \frac{0.001\beta}{4}\right) \frac{\tan\beta}{\tan(\tau + \tau_w)}\ b + b\ R(\beta) \qquad (99)$$

where $R(\beta) = -0.003\beta\ (0.57 + 0.001\beta) - 0.03$

Combining this with Equation (98) and discarding terms of higher order than one in the wave components yields

$$M_1 = \phi(\lambda) \frac{\rho\pi b^2}{4} (1-\sin\beta)\, U^2 b \left[\sin\tau \cos\tau \left(\lambda_k - \lambda_g - \frac{2}{3}\lambda_{c1} \right) \right.$$
$$\left. - \left(\lambda - 2\left(0.157 - \frac{0.001\beta}{4} \right) \frac{\tan\beta}{\tan\tau} - \lambda_g - R(\beta) \right) \tau_w \right] \tag{100}$$

where λ_{c1} is s_{c1}/b for calm water. The first term in the brackets is the calm water moment contribution. When this is added to M_4 we obtain the total dynamic part of the steady state moment. We nondimensionalize this by dividing by $1/2\ \rho\ U^2 b^3$ and obtain

$$M_{DS}' = \frac{\lambda}{1+\lambda} G \sin\tau \cos\tau \left(\lambda_k - \lambda_g - \frac{2}{3}\lambda_{c1} \right)$$
$$+ C_{D,c} \sin^2\tau \cos^2\tau \cos\beta\, \lambda \left(\frac{\lambda}{2} - \lambda_g \right) \tag{101}$$

where Equations (72), (73), and (75) have been made use of. If we nondimensionalize the term in Equation (100) due to the wave slope we obtain

$$(M_1)_w' = -\frac{\lambda}{1+\lambda} G \left[\lambda - 2\,(0.157)\,\frac{\tan\beta}{\tan\tau} - \lambda_g \right] \tau_w \tag{102}$$

where the terms in β were dropped since they were found to have very little effect on the accuracy of the calculations.

The part of the moment $(M_2 + M_3)$ due to the wave orbital velocity is seen to be expressible as the sum of the moment of the force $(F_2)_w$ acting at $s = 0$ and the contribution obtained from the integration of the second term in the integrands of Equations (94) and (95). On carrying out this operation, making the appropriate substitutions from Equations (66), (72), (73), and (75) and nondimensionalizing, one obtains

$$(M_2)_w' = M_2' + M_3' = (F_2)_w' \ (\lambda_k - \lambda_g) + 4\left(\frac{\omega b}{U}\right)\left(\frac{h}{b}\right) \sin\tau \ e^{\mp i\psi}\left(iH_5 - \frac{H_3}{\tan\tau}\right) \tag{103}$$

That part of the moment M_5, due to the acceleration, is expressible as the sum of three integrals analogous to that given in Equation (86) for F_5. On carrying out the integrations indicated in Equation (97), making the appropriate substitutions as before, and nondimensionalizing one obtains

$$(M_5)_w' = (F_5)_w' \ (\lambda_k - \lambda_g) + 2\left(\frac{\omega b}{U}\right)^2\left(\frac{h}{b}\right) e^{\mp i\psi} \ (M_{51} + M_{52} + M_{53}) \tag{104}$$

where

$$M_{51} = \begin{cases} \dfrac{G}{2}\dfrac{\lambda}{1+\lambda}\dfrac{\lambda_{c1}^2}{(k_0 s_{c1})^4}\left\{e^{\mp i k_0 s_{c1}}\left[3(k_0 s_{c1})^2 - 6 + \right.\right. \\ \left.\left. \mp i\left(6 k_0 s_{c1} - (k_0 s_{c1})^3\right)\right] + 6\right\} & \text{for } \beta > 2^\circ \\ 0 & \text{for } \beta < 2^\circ \end{cases}$$

$$M_{52} = \frac{G}{2}\frac{\lambda}{1+\lambda}\frac{1}{(k_0 b)^2}\left[e^{\mp i k_0 \ell_k}(1 \mp i k_0 \ell_k) - e^{\mp i k_0 s_{c1}}(1 \mp i k_0 s_{c1})\right]$$

$$M_{53} = -\tan\tau\left[\lambda_{c2} H_5 \mp \frac{C_{D,c}\cos^2\tau\cos\beta}{2(k_0 b)^3} i H_6\right]$$

$$H_6 = e^{\mp i k_0 \ell_k}\left[2 - (k_0 \ell_k)^2 \mp i 2(k_0 \ell_k)\right]$$

$$- e^{\mp i k_0 s_{c2}}\left[2 - (k_0 s_{c2})^2 \mp i 2(k_0 s_{c2})\right]$$

In summary the dynamic part of the nondimensional moment on the boat moving with constant speed and trim through regular head or following waves is given by

$$(M_D)' = M_{DS}' + (M_1)_w' + (M_2)_w' + (M_5)_w' \tag{105}$$

Normal Force and Moment Due to Ambient Pressure

The force due to local pressure effects F_P is obtained by integrating the ambient pressure over the bottom of the hull. Thus

$$F_P = \int_0^{\ell_k} \rho \left[gz + \frac{d\,\phi_w}{dt} \right] dS \tag{106}$$

where the second term is the effect of the wave perturbation

$$\frac{d\,\phi_w}{dt} = g\,h\,e^{-kz}\,e^{\mp i(kx + \omega_e t)} \tag{107}$$

and the first term represents the static buoyancy force. We will consider only cases for speed coefficient C_V at more than 0.5, where the water breaks clear of the transom, thus ventilating the backside of the boat to the atmosphere and removing the component of force parallel to the keel. For this case the force due to ambient pressure may be assumed to act normal to the keel. The following expression for the static buoyancy force was found to fit existing data reasonably well.[13,14]

$$F_{BS} = \kappa \frac{1}{2} \rho\, g\, b^3\, \lambda^2 \sin \tau \tag{108a}$$

---

[13] Hsu, C.C., "On the Motions of High Speed Planing Craft," Hydronautics Report 603-1 (May 1967).

[14] Brown, P.W., "An Experimental and Theoretical Study of Planing Surfaces with Trim Flaps," Davidson Laboratory, Stevens Institute of Technology Report 1463 (Apr 1971).

This is equivalent to $\kappa \rho g b \int_{s_{c2}}^{\ell_k} (s - s_{c2}) \sin \tau \, ds$

where κ is an empirical correction factor, which accounts for the ventilation effects. A value of 0.624, obtained from data on prismatic hulls,[14] has been used in the present calculations and in Reference 4. Thus Equation (108a) becomes, in nondimensional form

$$F_{BS}' = \frac{0.624}{C_V^2} \lambda^2 \sin \tau \tag{108b}$$

For the sake of consistency with the above result, the same value for κ and the same integration limits were used also in evaluating the force due to the wave perturbation pressure $(F_p)_w$. Thus the second term in Equation (106) becomes

$$(F_p)_w = 0.624 \, \rho g b h \, e^{\mp i \psi_d} \int_{s_{c2}}^{\ell_k} e^{-(\sin \tau \mp i \cos \tau) k(s - s_{c2})} \, ds \tag{109}$$

where the following substitutions have been made in Equations (106) and (107)

$$\begin{aligned} dS &= b \, ds \\ z &= (s - s_{c2}) \sin \tau \\ \psi_d &= k x_d + \omega_e t \\ x_d &= x_b - s_{c2} \cos \tau \\ x &= x_d - (s - s_{c2}) \cos \tau \end{aligned} \tag{110}$$

On carrying out the integration, we obtain in nondimensional form

$$(F_P)_w' = \pm \frac{2(0.624)}{C_V^2} \frac{h}{b} \frac{i\, e^{\mp i(\psi_d + \tau)}}{kb} \left(1 - e^{-k\lambda b(\sin\tau \mp i\cos\tau)}\right) \quad (111)$$

where $C_V = U/\sqrt{gb}$

Thus the total normal force due to the ambient pressure is

$$F_P' = F_{BS}' + (F_P)_w' \quad (112)$$

According to Reference 14 the assumption that the buoyancy force acts one-third of the mean wetted length forward of the stern gives good agreement with data. Accordingly, the nondimensional moment about the center of gravity, due to the buoyancy force, is

$$M_{BS}' = \frac{0.624}{C_V^2} (\lambda^2 \sin\tau) \left(\frac{\lambda}{3} - \lambda_g\right) \quad (113)$$

The moment due to the wave perturbation pressure is, with the aid of Equation (109)

$$(M_P)_w = 0.624\, \rho\, gbh\, e^{\mp i\psi_d} \int_{s_{c2}}^{\ell_k} (s_d - s)\, e^{-(\sin\tau \mp i\cos\tau)\, k(s-s_{c2})}\, ds \quad (114)$$

where $s_d = (\lambda - \lambda_g)b$

Carrying out the integration, we obtain in nondimensional form

$$(M_P)_w' = (F_P)_w' (\lambda - \lambda_g) + \frac{2(0.624)}{C_V^2} \frac{h}{b} \frac{e^{\mp i(\psi_d + 2\tau)}}{k\, b^2} (1 - H_7) \quad (115)$$

where

$$H_7 = [1 + k\,\lambda\, b(\sin\tau \mp i\cos\tau)]\, e^{-k\,\lambda\, b(\sin\tau \mp i\cos\tau)}$$

Thus the total moment about the center of gravity due to the ambient pressure is

$$(M_p)' = M_{BS}' + (M_p)_w' \tag{116}$$

Normal Force and Moment Due to Change in Wetted Length

It is recalled that only part of the force and moment contributions arising from the effect of wave elevation has so far been accounted for. These are given by Equations (74) and (102) respectively, and represent the effect of the mean wave slope τ_w in Equations (67 through 69). The wave elevation term $\zeta_w(0)$ of Equation (67), which must also be included, has the effect of increasing the wetted length of the boat. The effect of this on the force may be determined with the aid of Equations (71) and (101), which express the effect of the mean wetted length λ and trim angle τ on the steady normal force and moment due to forward speed alone. The change in mean wetted length due to wave elevation will be approximated from the free surface elevation at the point $x = x_d$.

$$\Delta\lambda \approx \frac{h\, e^{\mp i(k\, x_d + \omega_e\, t)}}{b\sin\tau} \tag{117}$$

The position x_d, rather than $\left(x_b - \frac{\tau}{k}\right)$, has been used since λb is measured from the transom to the point $s = s_{c2}$, which, we have seen from Equation (110), is directly below the point $x = x_d$ on the free surface. With the aid of Equations (71), (75), and (117) we may estimate the non-dimensional normal force $(F_h)_w'$, due to wave elevation, from the

following expression

$$(F_h)_w' = \frac{\partial F_{DS}'}{\partial \lambda} \Delta \lambda$$

which, on making the appropriate substitutions, yields

$$(F_h)_w' = \left[\frac{G \sin \tau \cos \tau}{(1 + \lambda)^2} + C_{D,c} \cos \beta \sin^2 \tau \cos^2 \tau \right] \frac{h\, e^{\mp i(k x_d + \omega_e t)}}{b \sin \tau} \tag{118}$$

The nondimensional moment about the center of gravity due to wave elevation is obtained in an analogous manner with the aid of Equation (101). Thus

$$(M_h)_w' = \frac{\partial M_{DS}'}{\partial \lambda} \Delta \lambda$$

or

$$(M_h)_w' = \left\{ G \sin \tau \cos \tau \left[\frac{1}{(1 + \lambda)^2} \left(\lambda_k - \lambda_g - \frac{2}{3} \lambda_{cl} \right) + \frac{\lambda}{1 + \lambda} \right] + C_{D,c} \cos \beta \sin^2 \tau \cos^2 \tau \, (\lambda - \lambda_g) \right\} \frac{h\, e^{\mp i(k x_d + \omega_e t)}}{b \sin \tau} \tag{119}$$

The next step is to incorporate all of the foregoing results for wave excitation into equations of motion of the boat.

EQUATIONS OF MOTION

The equations of motion of planing craft in the longitudinal degrees of freedom are most conveniently expressed in terms of heave, surge, and pitch motions. Accordingly the normal force due to the waves are resolved into the vertical and horizontal components. We employ the convention that the nondimensional surge force and displacement are denoted by X' and x', respectively, and are positive in the direction of the calm water speed;

the nondimensional vertical force and displacement are denoted by Z' and z', respectively, and are positive in the downward direction normal to the calm water free surface. The nondimensional pitching moment and displacement angle are M' and θ and are positive for the bow-up direction of rotation; see Figure 18.

Since the motions due to waves will be determined relative to the steady state attitude and draft of the boat, the steady state hydrodynamic force and moment make no contribution, in the linear sense, to the boat motions. This is discussed further in Reference 4, where the complete steady state equilibrium equations are derived. The vertical component of the linearized wave force is therefore obtained by adding the contributions from Equations (91), (112), and (118) and by omitting F_{DS}' and F_{BS}'.

$$(Z)_w' \, e^{\mp i \omega_e' t'} = - [(F_1)_w' + (F_2)_w' + (F_5)_w' + (F_P)_w' + (F_h)_w'] \cos \tau \quad (120)$$

The horizontal component of the wave force is

$$(X)_w' \, e^{\mp i \omega_e' t'} = (Z)_w' \tan \tau \, e^{\mp i \omega_e' t'} \quad (121)$$

The moment due to the waves is obtained by summing Equations (105), (116), and (119) and by omitting M_{DS}' and M_{BS}'. Thus

$$(M)_w' \, e^{\mp i \omega_e' t'} = (M_1)_w' + (M_2)_w' + (M_5)_w' + (M_P)_w' + (M_h)_w' \quad (122)$$

In the previous equations $(X)_w'$, $(Z)_w'$, and $(M)_w'$ are of course complex constants.

Equations for estimating the linearized hydrodynamic forces on the boat due to perturbations from steady state motion in surge, heave, and pitch have been derived in Reference 4 for use in the theoretical prediction of calm water porpoising. The same equations are of course applicable for calculating the linearized hydrodynamic force and moment on the boat

arising from its motion response to waves. If we express the two nondimensional force components and the nondimensional moment due to the boat motions, as linear functions of the nondimensional perturbations in surge, heave and pitch, we have[4]

$$(X')_{BM} = X_{\dot{u}}\,\dot{u} + X_u\,u + X_{\ddot{z}}\,\ddot{z} + X_{\dot{z}}\,\dot{z} + X_z\,z + X_{\ddot{\theta}}\,\ddot{\theta} + X_{\dot{\theta}}\,\dot{\theta} + X_\theta\,\theta \quad (123)$$

$$(Z')_{BM} = Z_{\dot{u}}\,\dot{u} + Z_u\,u + Z_{\ddot{z}}\,\ddot{z} + Z_{\dot{z}}\,\dot{z} + Z_z\,z + Z_{\ddot{\theta}}\,\ddot{\theta} + Z_{\dot{\theta}}\,\dot{\theta} + Z_\theta\,\theta \quad (124)$$

$$(M')_{BM} = M_{\dot{u}}\,\dot{u} + M_u\,u + M_{\ddot{z}}\,\ddot{z} + M_{\dot{z}}\,\dot{z} + M_z\,z + M_{\ddot{\theta}}\,\ddot{\theta} + M_{\dot{\theta}}\,\dot{\theta} + M_\theta\,\theta \quad (125)$$

where $u = \dot{x}'$, and $\dot{u} = \ddot{x}'$. The primes used to denote nondimensional values have been omitted on the right-hand side of the equations for convenience. The coefficients $X_{\dot{u}}$, X_u, etc., in the previous equations, are the (stability) derivatives of the force and moment with respect to the motion perturbations $\dot{u}$, u, etc. The dot above the symbols represent derivative with respect to time. Theoretical estimates for all of the stability derivatives in the previous equations are derived in Reference 4.

The equations of motion in waves may now be written in terms of Equations (120 through 125) as

$$m'\dot{u}' - (X')_{BM} = (X)_w'\, e^{\mp i\,\omega_e' t'} \qquad \text{(surge equation)} \quad (126)$$

$$m'\ddot{z}' - (Z')_{BM} = (Z)_w'\, e^{\mp i\,\omega_e' t'} \qquad \text{(heave equation)} \quad (127)$$

$$I_y'\ddot{\theta}' - (M')_{BM} = (M)_w'\, e^{\mp i\,\omega_e' t'} \qquad \text{(pitch equation)} \quad (128)$$

where $m' = \dfrac{m}{\frac{1}{2}\rho b^3}$ is the nondimensional boat mass, and $I_y' = \dfrac{I_y}{\frac{1}{2}\rho b^5}$ is the nondimensional pitch moment of inertia of the boat about the y-axis through the center of gravity.

Equations (126 through 128), with the wave force and moment terms set equal to zero, are the equations for porpoising stability.[4] The steady state solution of Equations (126 through 128) is a simple harmonic motion in the perturbations. Thus

$$x' = x_0' \, e^{\mp i \omega_e' t'} \tag{129}$$

$$z' = z_0' \, e^{\mp i \omega_e' t'} \tag{130}$$

$$\theta = \theta_0 \, e^{\mp i \omega_e' t'} \tag{131}$$

where x_0', z_0', θ_0 are the complex amplitudes of the displacement and pitch angle perturbations. If we substitute Equations (129 through 131) into Equations (126 through 128) we obtain the equations for the amplitudes and phase angles of the motions.

$$\left[(X_{\dot{u}} - m)\,\omega_e^2 \mp i\, X_u\, \omega_e\right]' x_0' + \left[X_{\ddot{z}}\,\omega_e^2 - X_z \mp i\, X_{\dot{z}}\,\omega_e\right]' z_0' + \left[X_{\ddot{\theta}}\,\omega_e^2 - X_\theta \mp i\, X_{\dot{\theta}}\,\omega_e\right]' \theta_0 = (X)_w' \tag{132}$$

$$\left[Z_{\dot{u}}\,\omega_e^2 \mp i\, Z_u\,\omega_e\right]' x_0' + \left[(Z_{\ddot{z}} - m)\,\omega_e^2 - Z_z \mp i\, Z_{\dot{z}}\,\omega_e\right]' z_0' + \left[Z_{\ddot{\theta}}\,\omega_e^2 - Z_\theta \mp i\, Z_{\dot{\theta}}\,\omega_e\right]' \theta_0 = (Z)_w' \tag{133}$$

$$\left[M_{\dot{u}}\,\omega_e^2 \mp i\, M_u\,\omega_e\right]' x_0' + \left[M_{\ddot{z}}\,\omega_e^2 - M_z \mp i\, M_{\dot{z}}\,\omega_e\right]' z_0' + \left[(M_{\ddot{\theta}} - I_y)\,\omega_e^2 - M_\theta \mp i\, M_{\dot{\theta}}\,\omega_e\right]' \theta_0 = (M)_w' \tag{134}$$

The prime on the brackets indicates that each term is primed. The solution to these equations give the complex amplitude of the boat motions

$$x_0' = x_R' + i\, x_I' = |x_0'|\, e^{i\,\alpha_x} \tag{135}$$

$$z_0' = z_R' + i\, z_I' = |z_0'|\, e^{i\,\alpha_z} \tag{136}$$

$$\theta_0 = \theta_R + i\, \theta_I = |\theta_0|\, e^{i\,\alpha_\theta} \tag{137}$$

where the subscripts R and I refer to the real and imaginary component. The displacement amplitudes and phase angles are given by the following equations

$$|x_0'| = \sqrt{x_R'^2 + x_I'^2} \qquad \alpha_x = \tan^{-1}(x_I'/x_R')$$

$$|z_0'| = \sqrt{z_R'^2 + z_I'^2} \qquad \alpha_z = \tan^{-1}(z_I'/z_R')$$

$$|\theta_0| = \sqrt{\theta_R^2 + \theta_I^2} \qquad \alpha_\theta = \tan^{-1}(\theta_I/\theta_R)$$

Since the convention for heave displacement is positive down while the convention used for the change in free-surface elevation due to waves is positive up, it is necessary to shift the phase angle for the heave motion by 180 degrees if we wish to determine the phase angle of the heave motion with respect to the free-surface displacement, positive up in both cases. On this basis, we readily find that the phase lag of the heave displacement with respect to the free-surface elevation η at the boat center of gravity is

$$\begin{aligned} \varepsilon_z &= \alpha_z - \pi \qquad \text{head waves} \\ \varepsilon_z &= \pi - \alpha_z \qquad \text{following waves} \end{aligned} \tag{138}$$

The phase leads of the surge amplitude and pitch angle with respect to η at the same point are, respectively

$$\varepsilon_x = 2\pi - \alpha_x \qquad \text{head waves}$$

$$\varepsilon_x = \alpha_x \qquad \text{following waves} \tag{139}$$

$$\varepsilon_\theta = 2\pi - \alpha_\theta \qquad \text{head waves}$$

$$\varepsilon_\theta = \alpha_\theta \qquad \text{following waves} \tag{140}$$

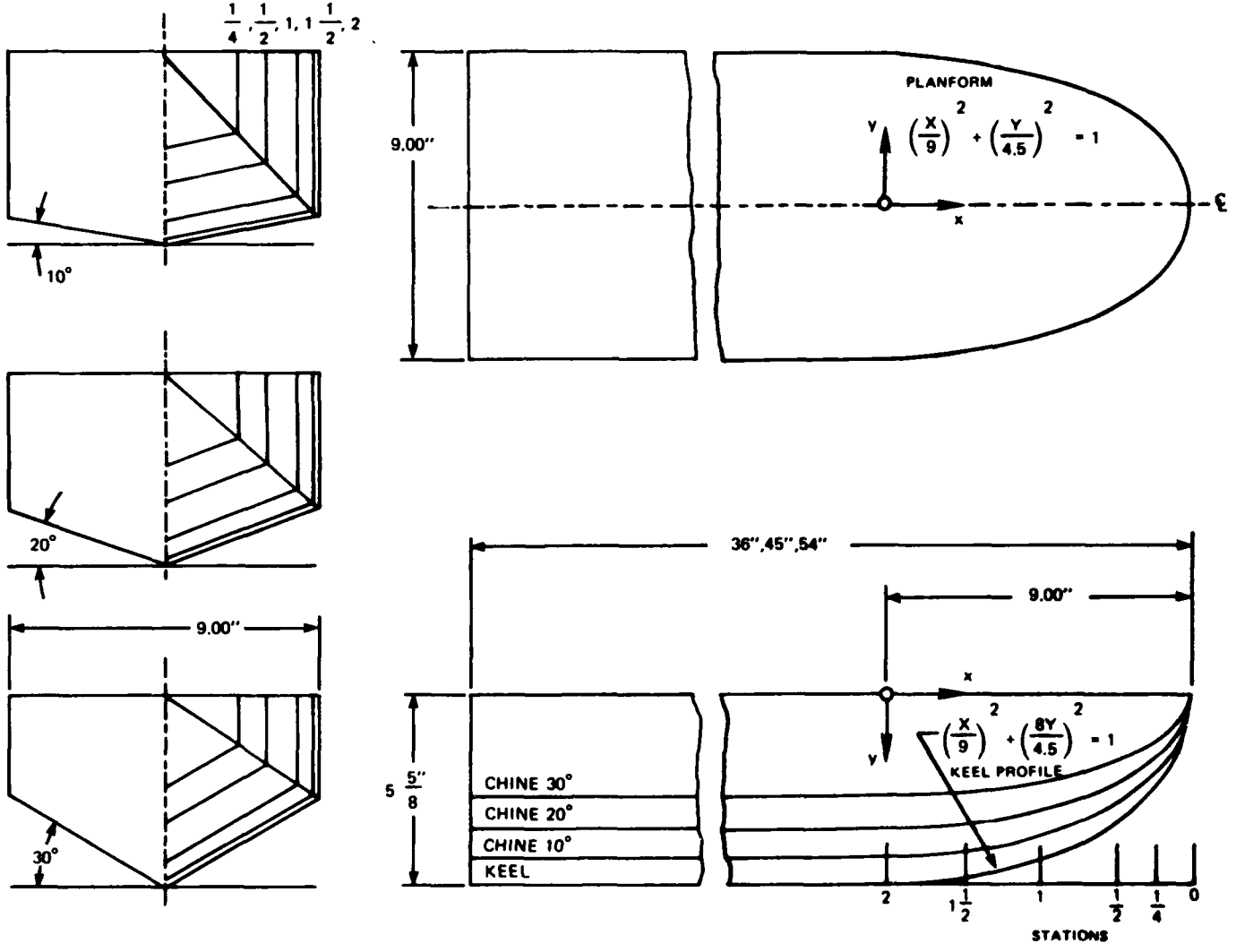

Figure 1 - Lines of Prismatic Models
(From Reference 2)

Figure 2 - Heave and Pitch Responses ($V/\sqrt{\ell} = 4$) Configuration A

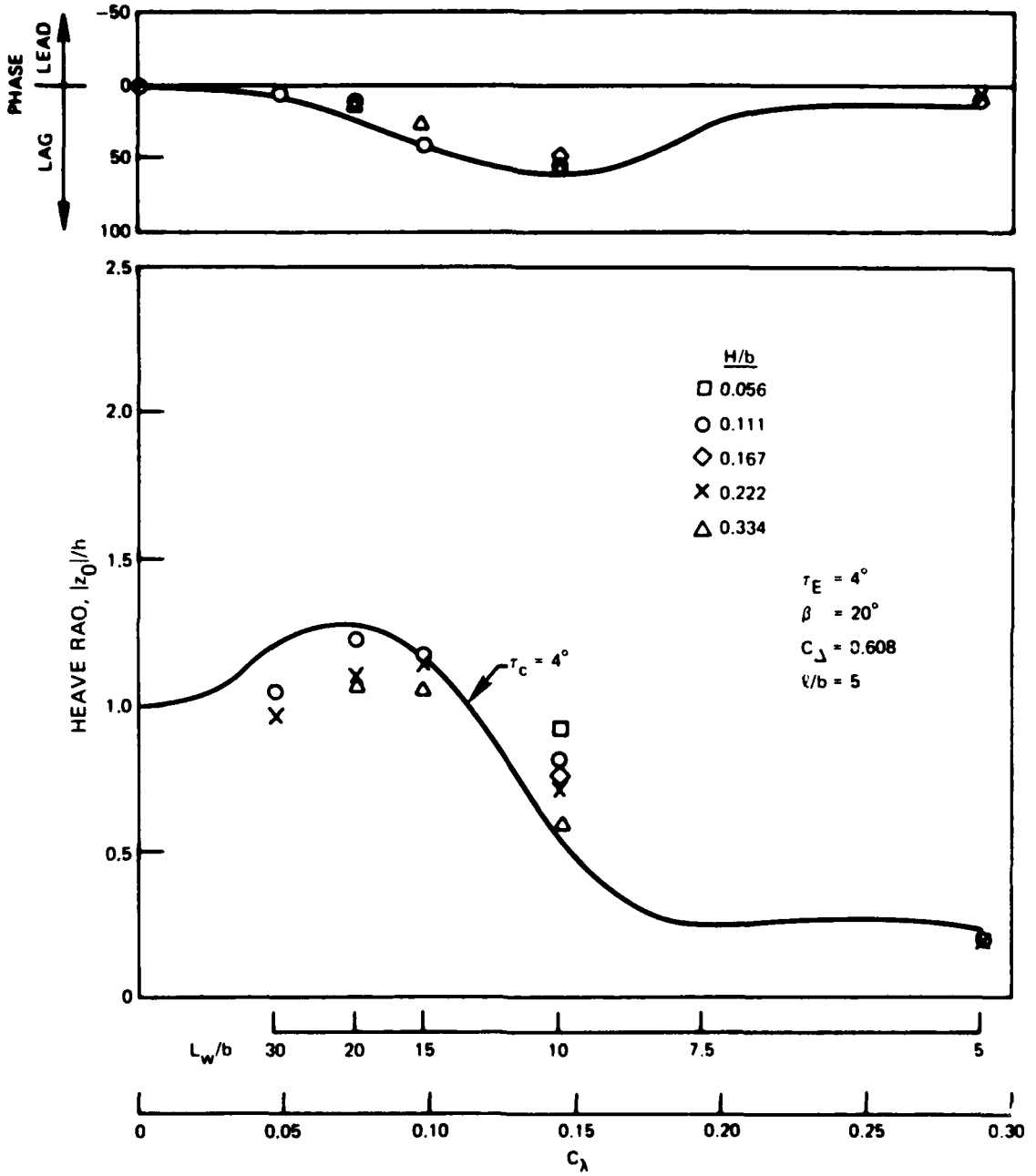

Figure 2a - Heave Response, Speed-to-Length Ratio of 4

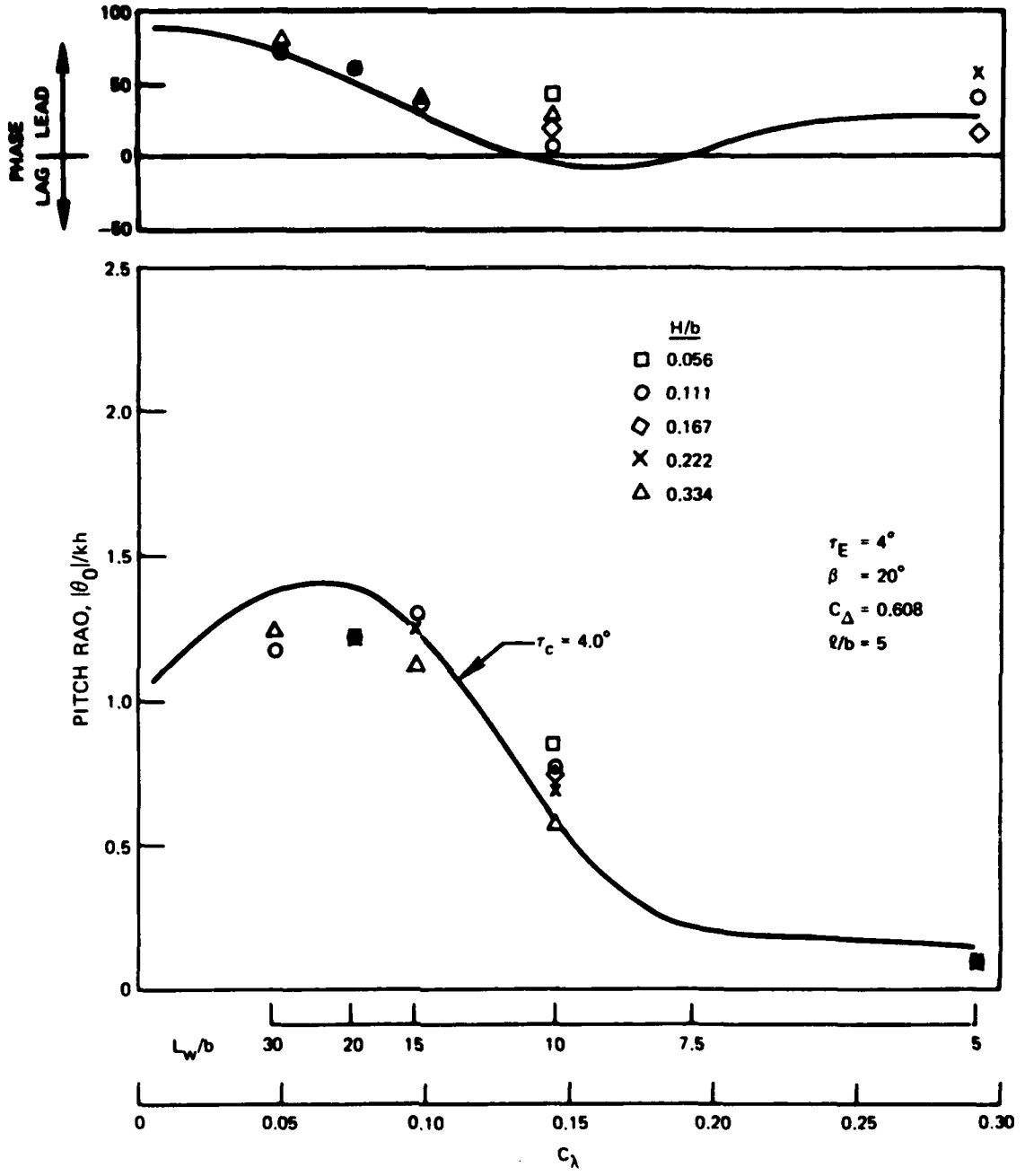

Figure 2b - Pitch Response, Speed-to-Length Ratio of 4

Figure 3 - Heave and Pitch Responses ($V/\sqrt{\ell} = 4$) Configuration E

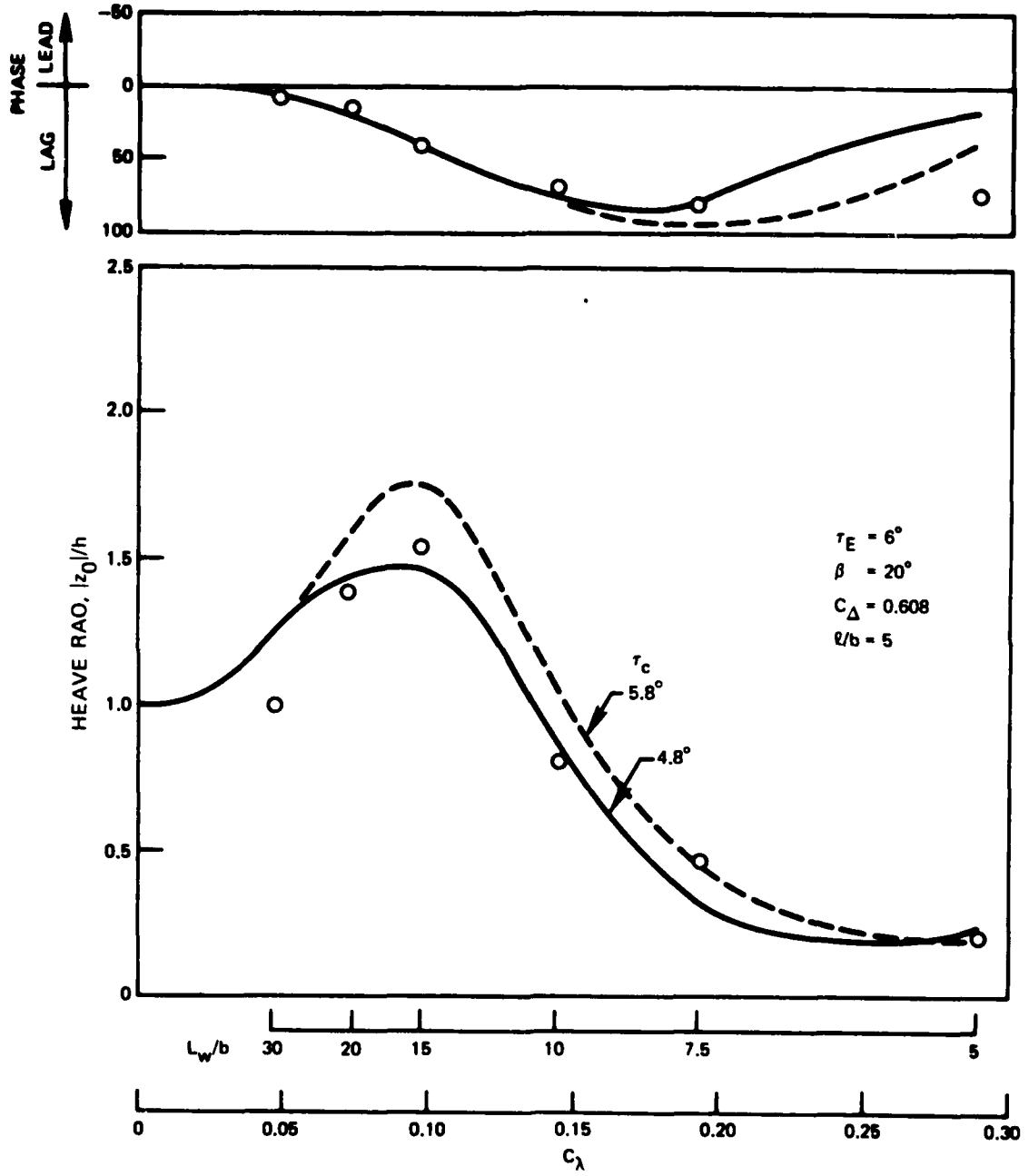

Figure 3a - Heave Response, Speed-to-Length Ratio of 4

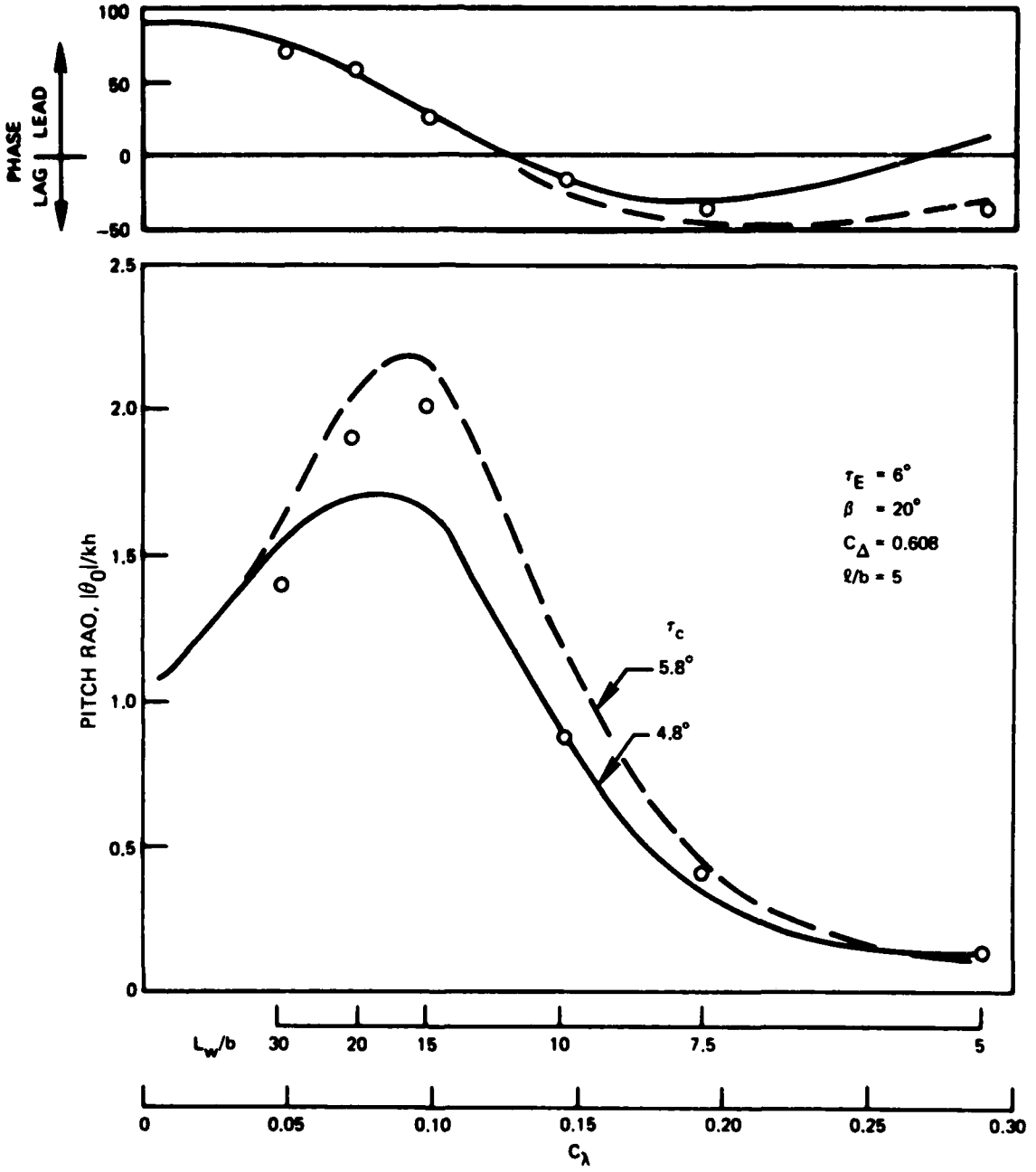

Figure 3b - Pitch Response, Speed-to-Length Ratio of 4

Figure 4 - Heave and Pitch Responses ($V/\sqrt{\ell} = 4$) Configuration F

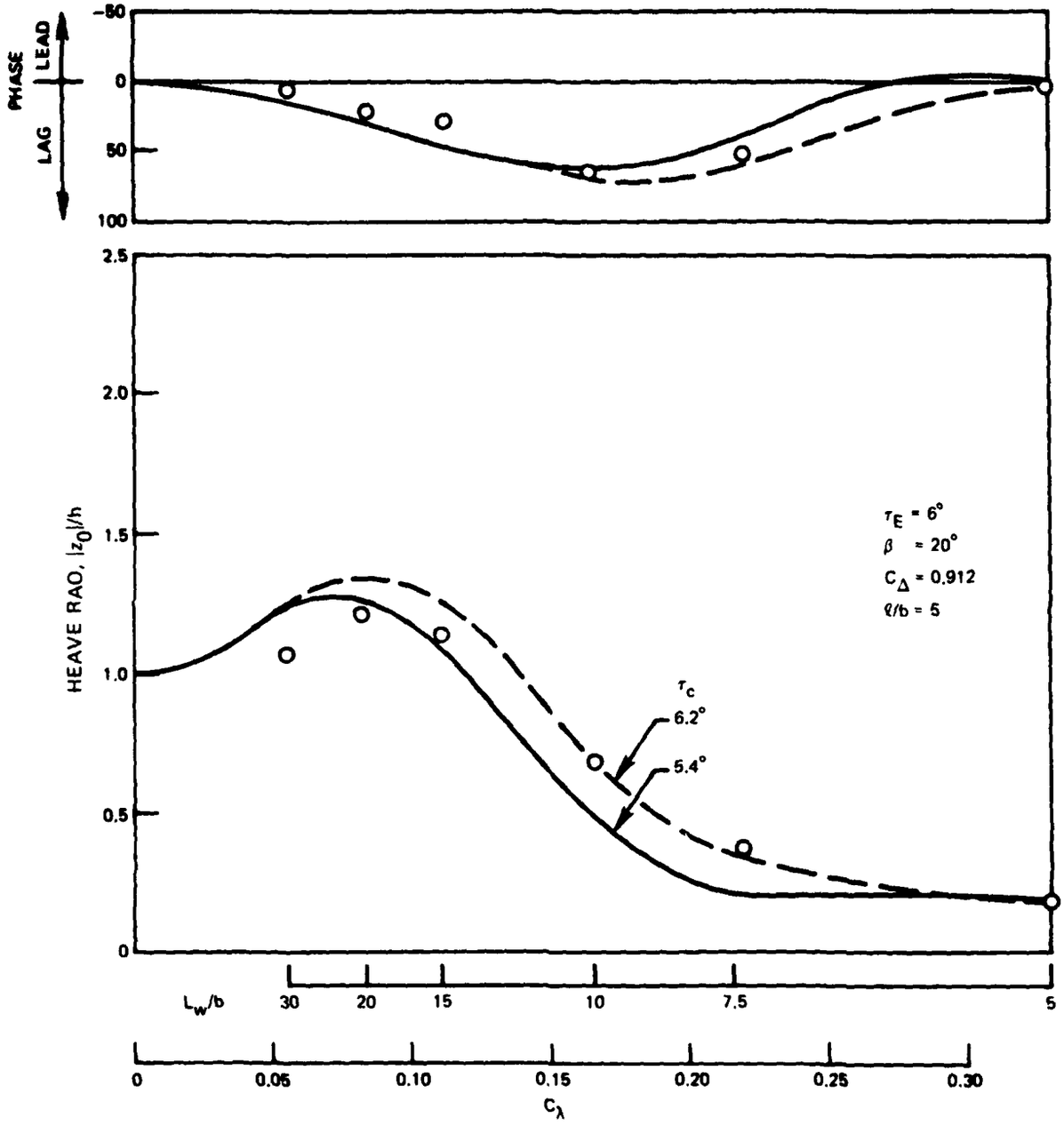

Figure 4a - Heave Response, Speed-to-Length Ratio of 4

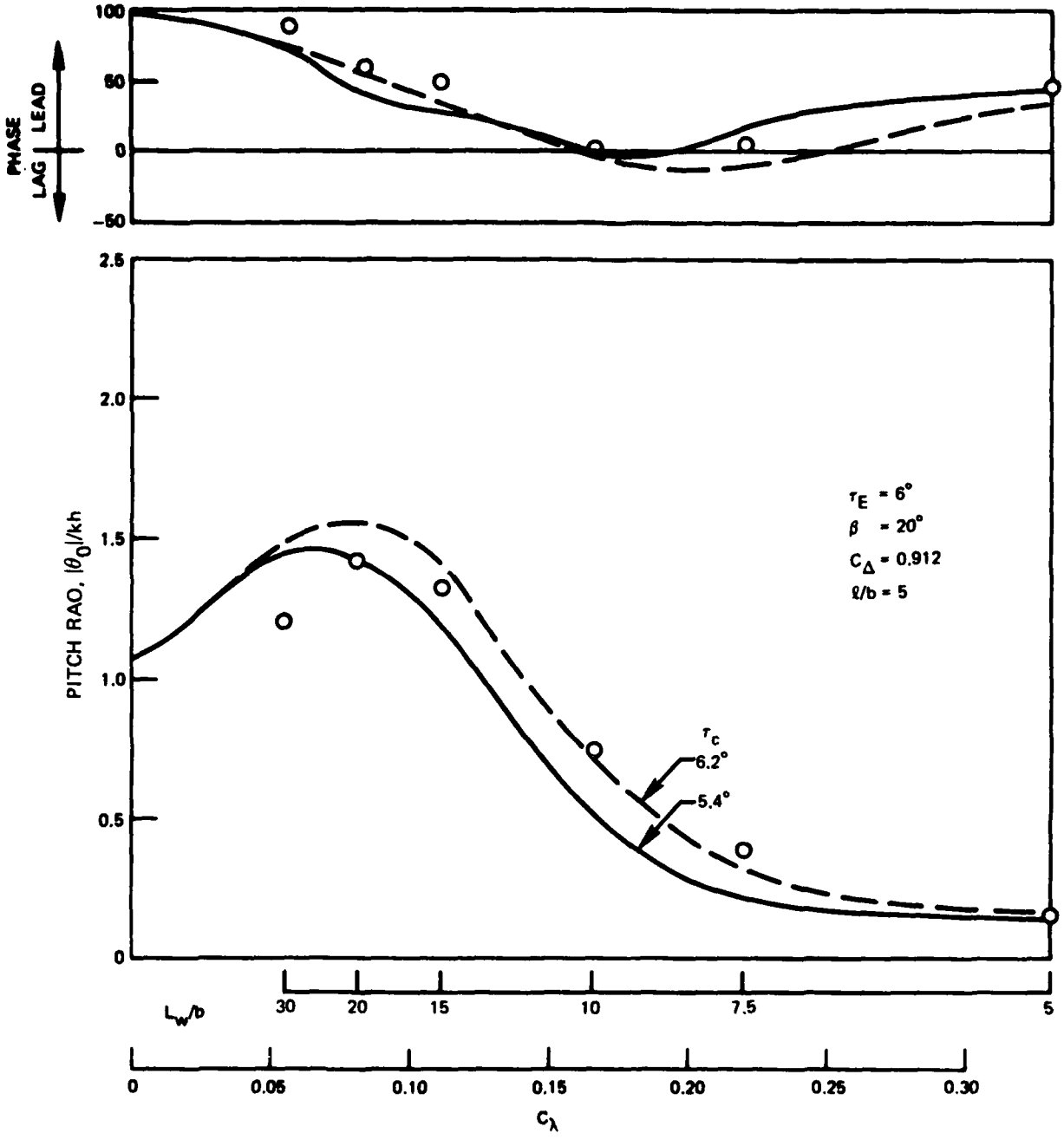

Figure 4b - Pitch Response, Speed-to-Length Ratio of 4

Figure 5 - Heave and Pitch Responses ($V/\sqrt{\ell} = 4$) Configuration I

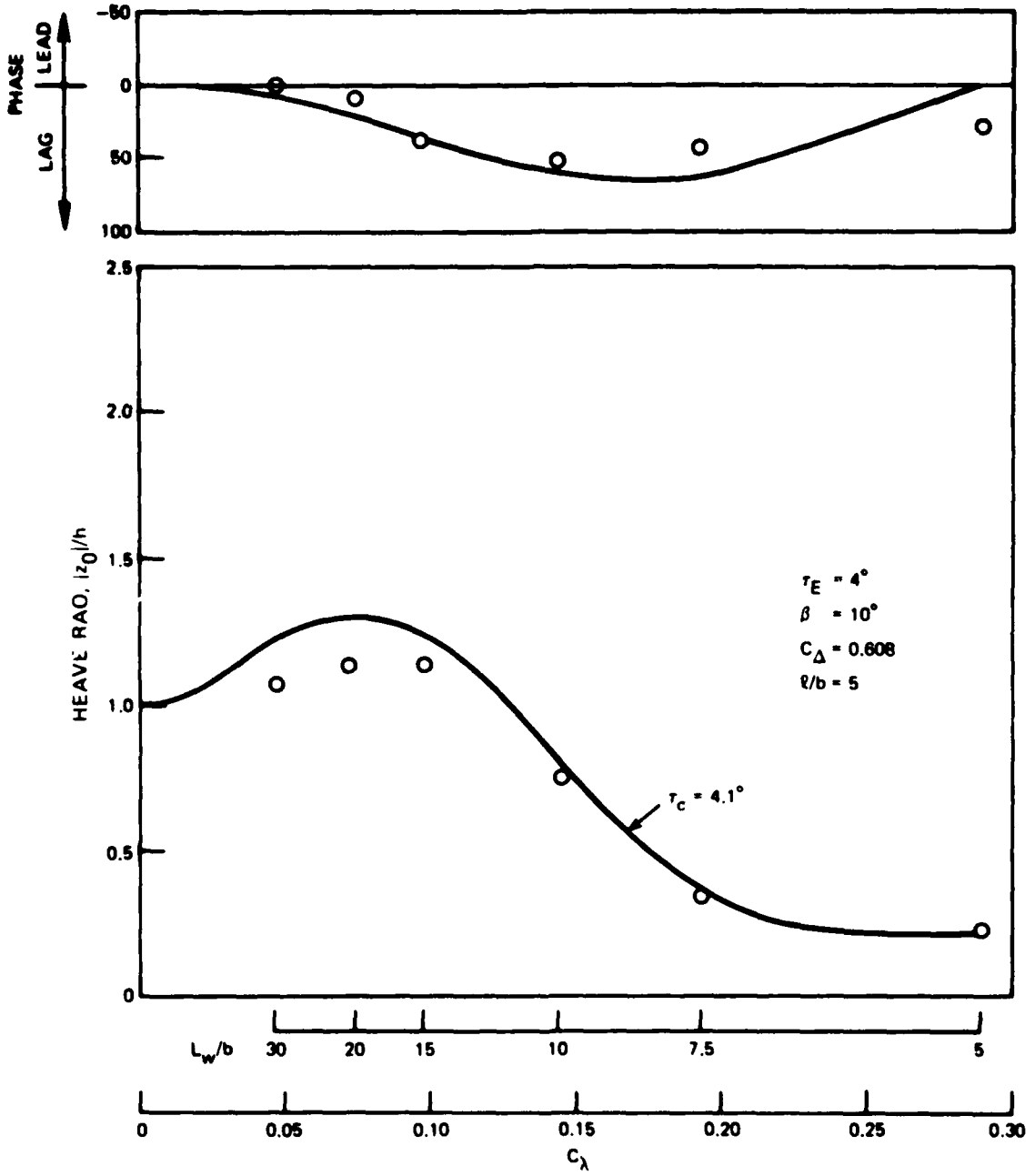

Figure 5a - Heave Response, Speed-to-Length Ratio of 4

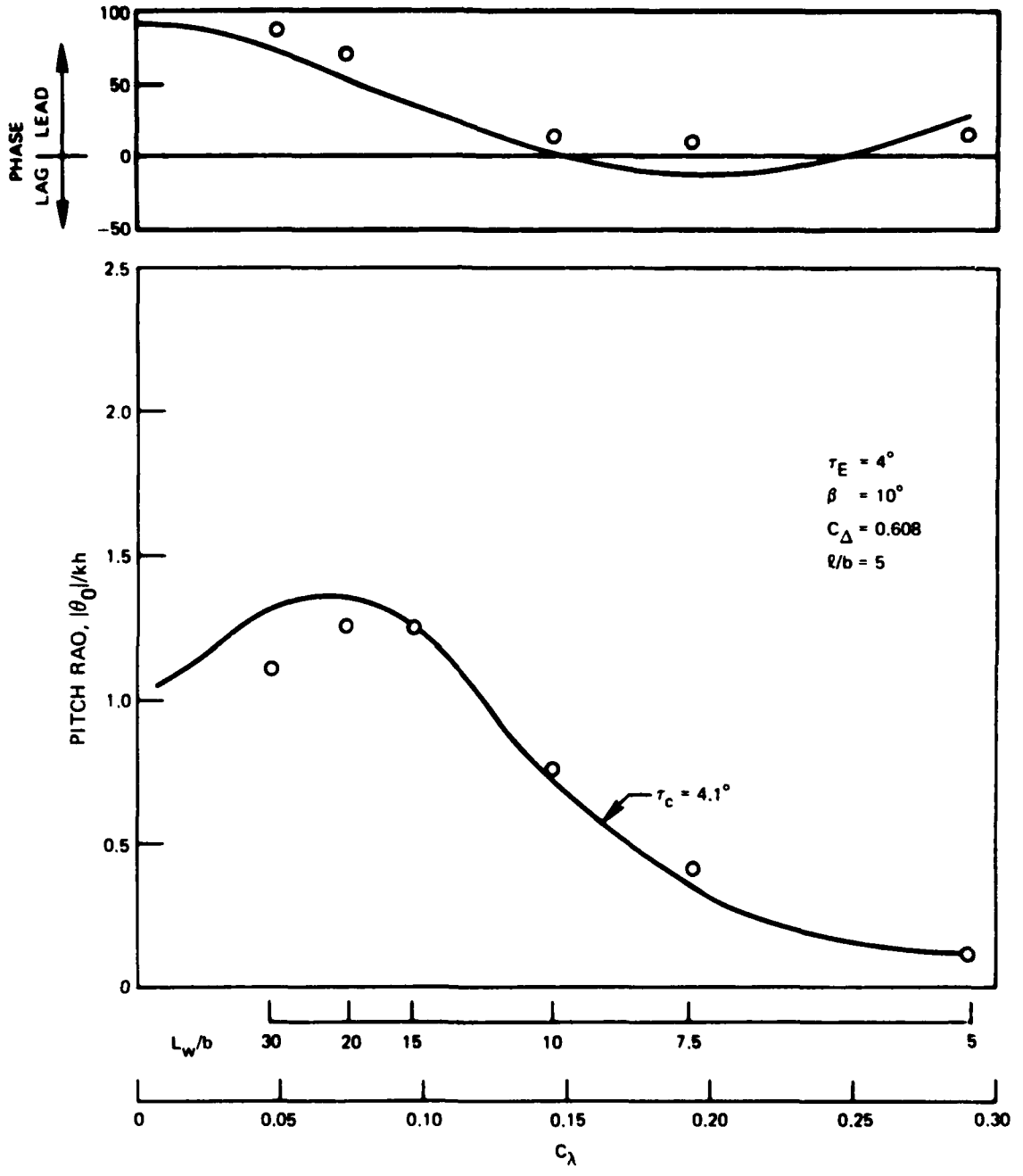

Figure 5b - Pitch Response, Speed-to-Length Ratio of 4

Figure 6 - Heave and Pitch Responses ($V/\sqrt{\ell} = 4$) Configuration K

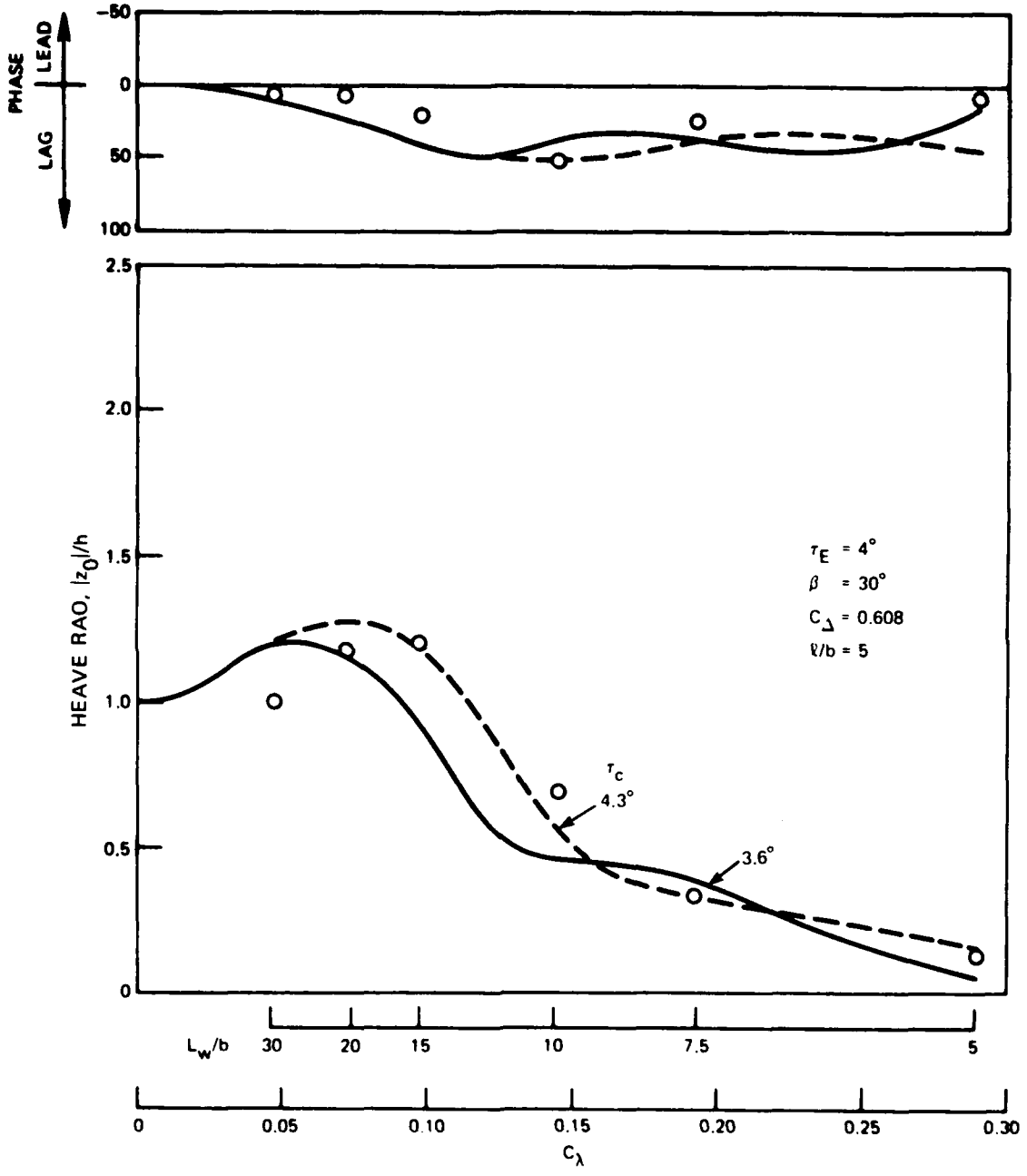

Figure 6a - Heave Response, Speed-to-Length Ratio of 4

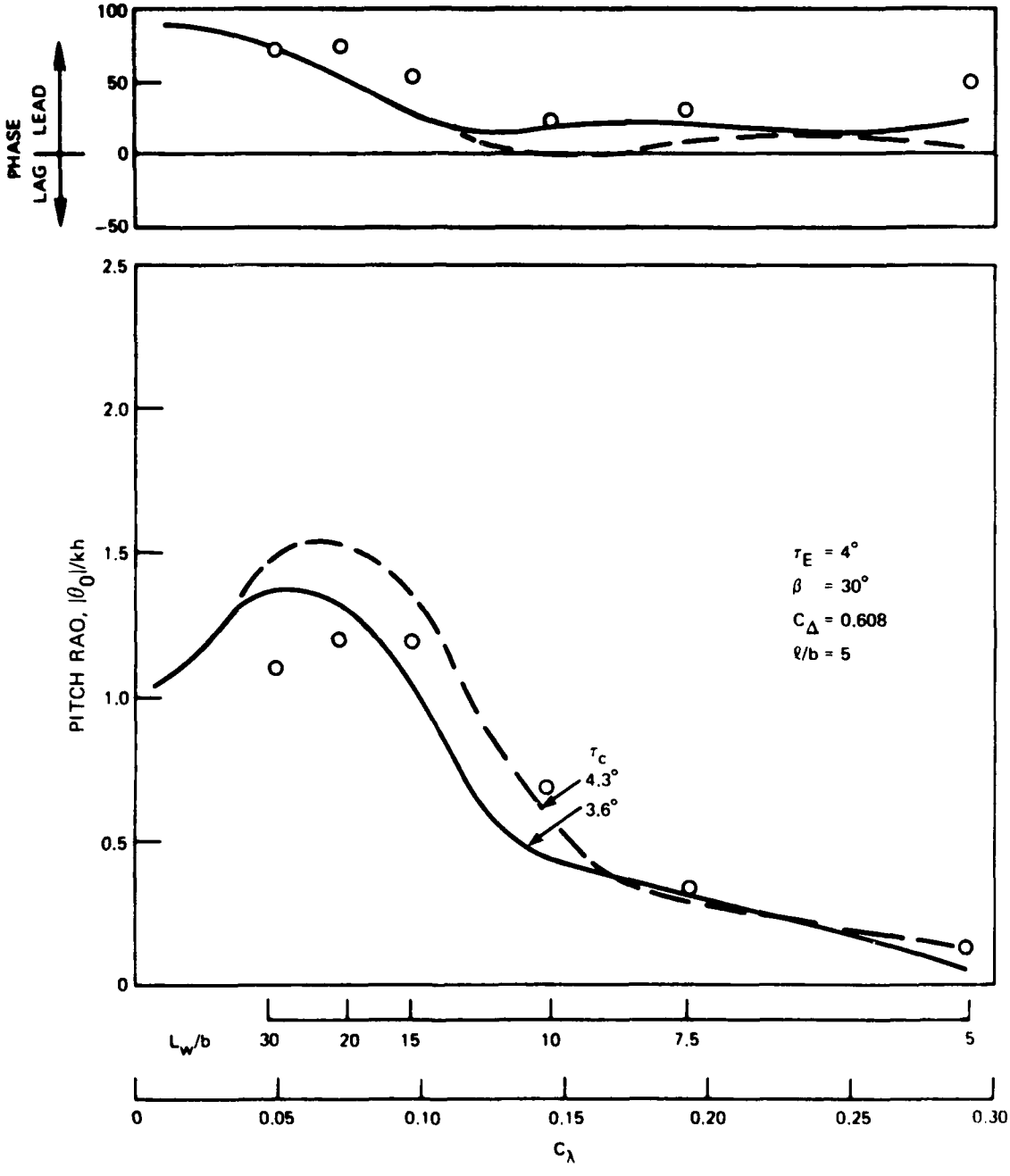

Figure 6b - Pitch Response, Speed-to-Length Ratio of 4

Figure 7 - Heave and Pitch Responses ($V/\sqrt{\ell} = 4$) Configuration N

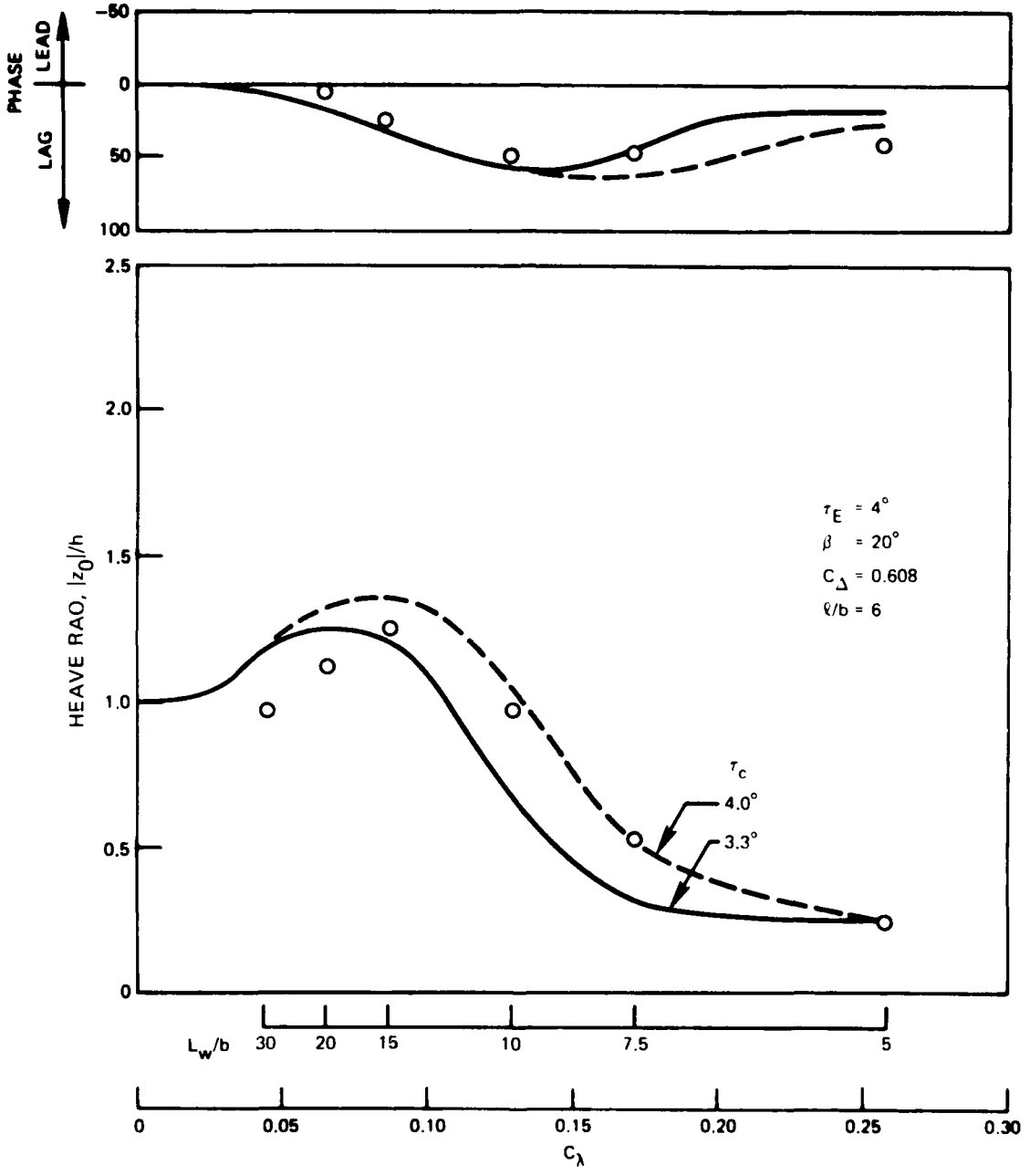

Figure 7a - Heave Response, Speed-to-Length Ratio of 4

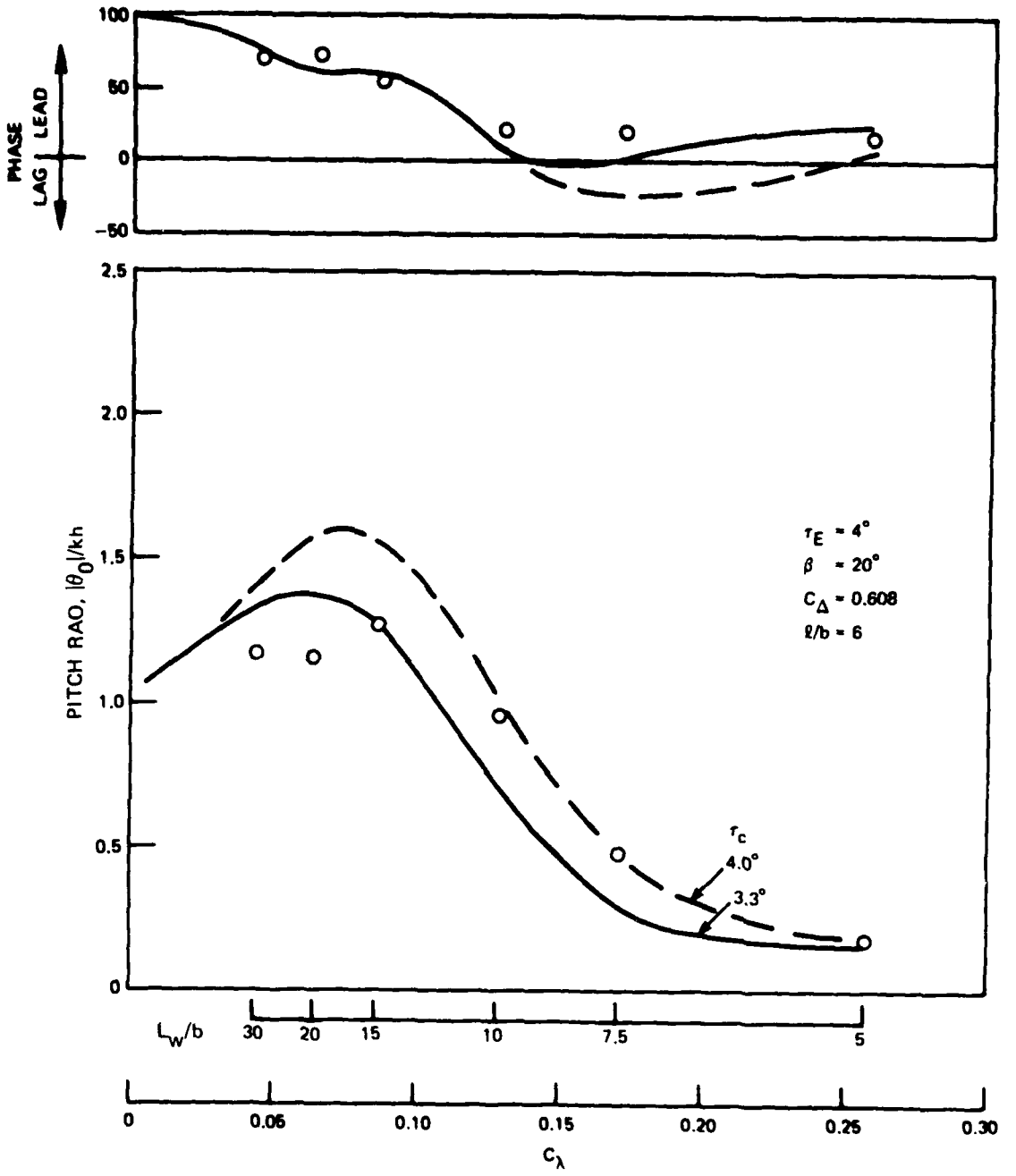

Figure 7b - Pitch Response, Speed-to-Length Ratio of 4

Figure 8 - Heave and Pitch Responses ($V/\sqrt{\ell} = 4$) Configuration 0

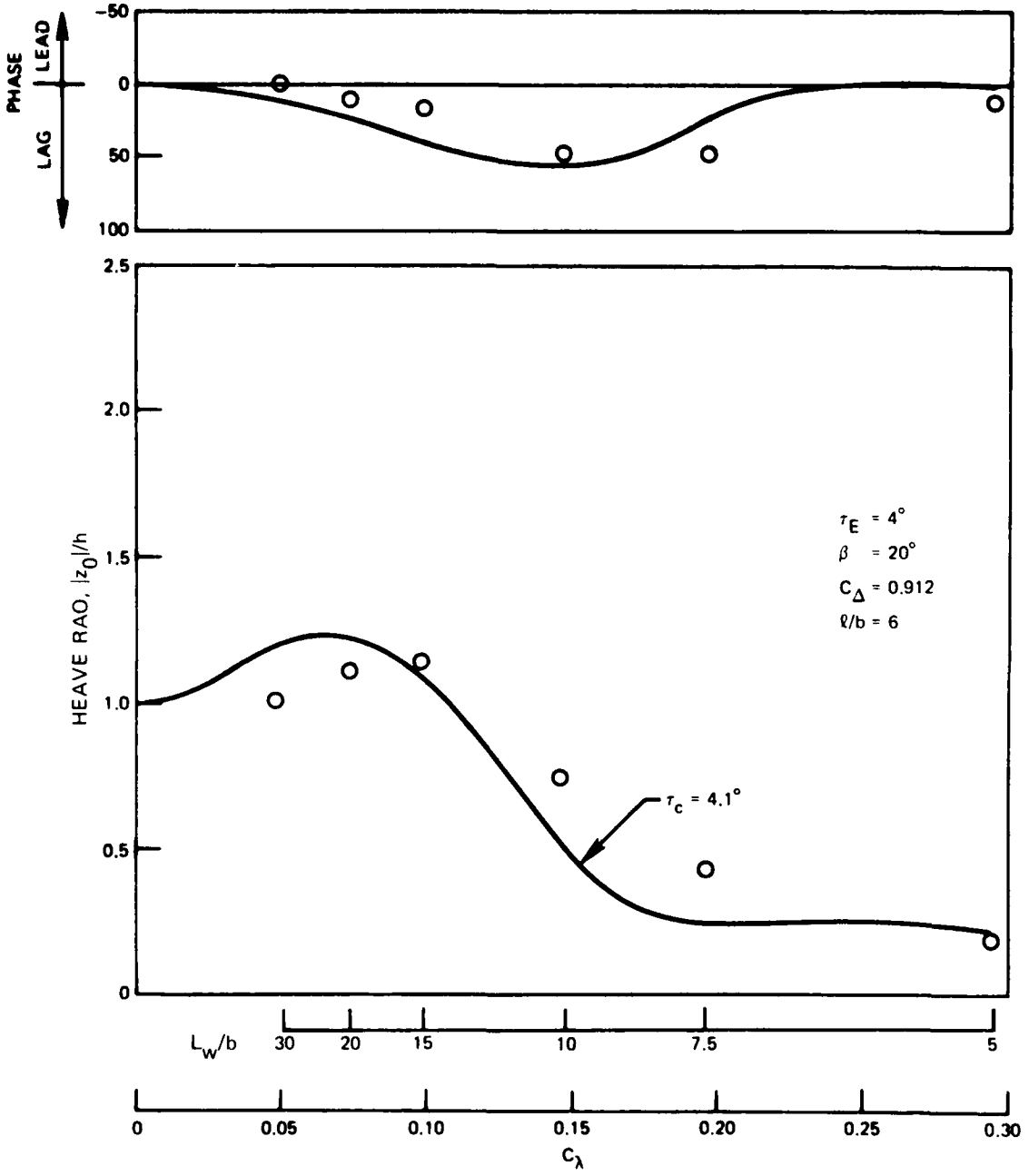

Figure 8a - Heave Response, Speed-to-Length Ratio of 4

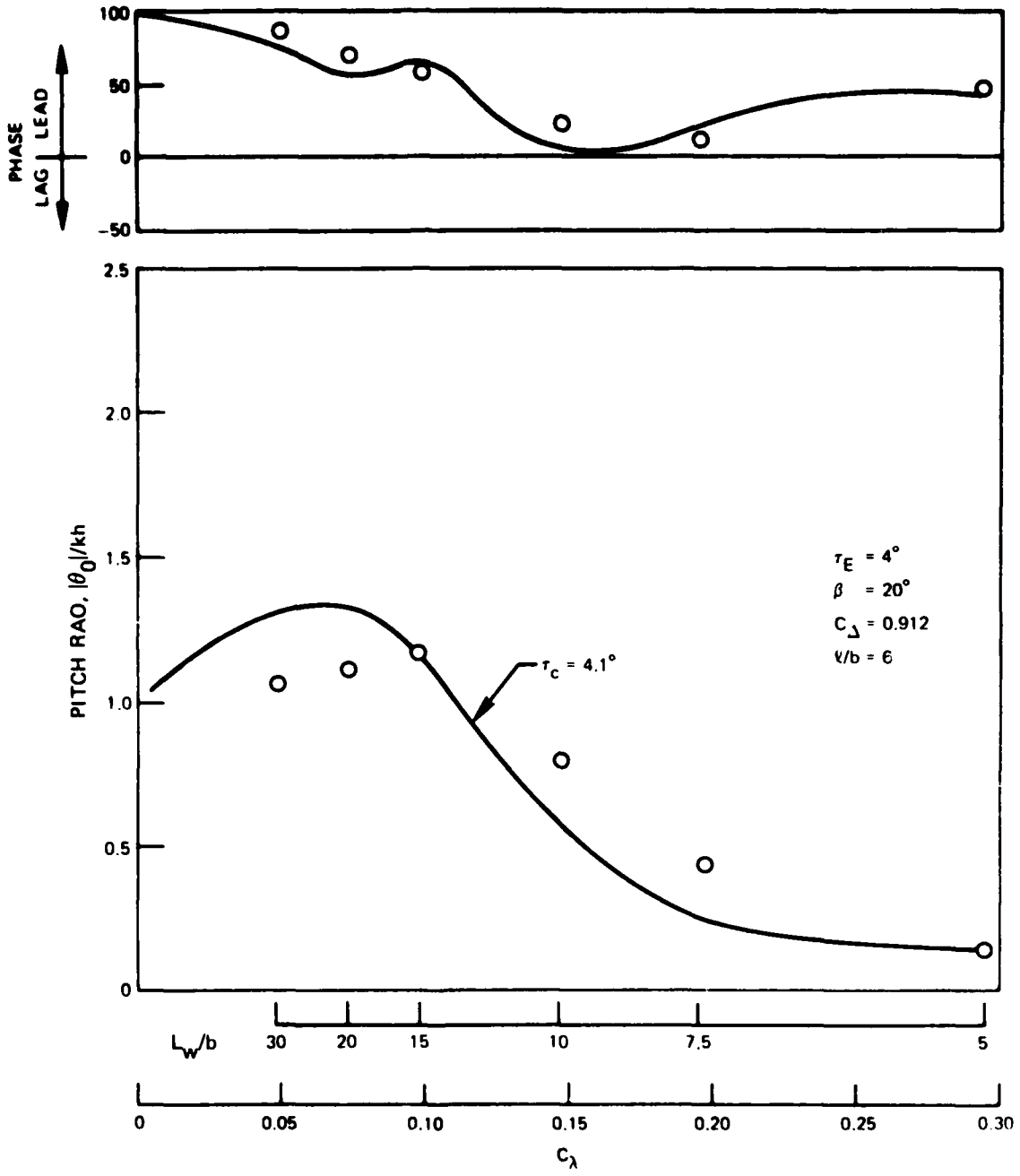

Figure 8b - Pitch Response, Speed-to-Length Ratio of 4

Figure 9 - Heave and Pitch Responses ($V/\sqrt{\ell} = 4$) Configuration P

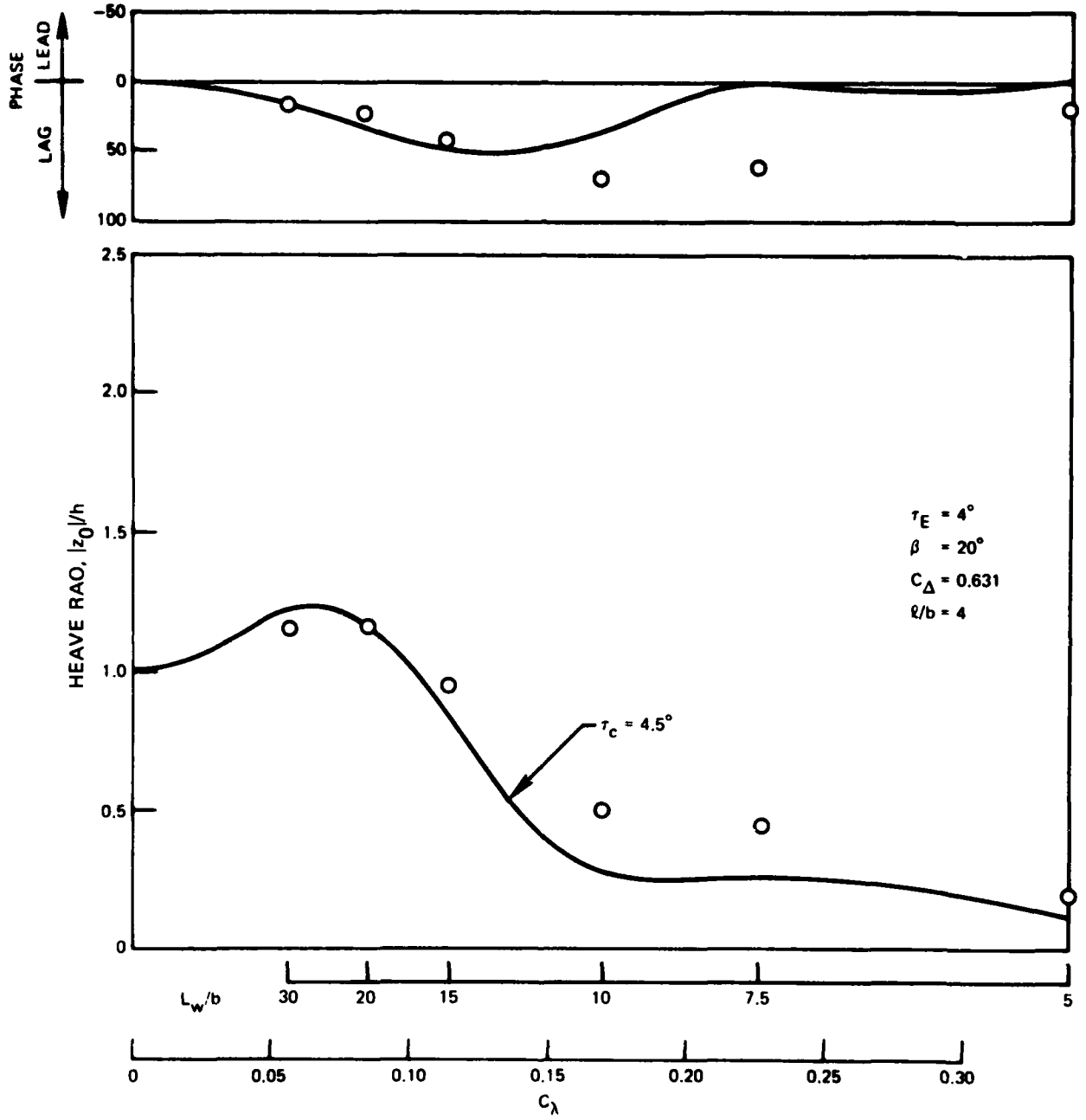

Figure 9a - Heave Response, Speed-to-Length Ratio of 4

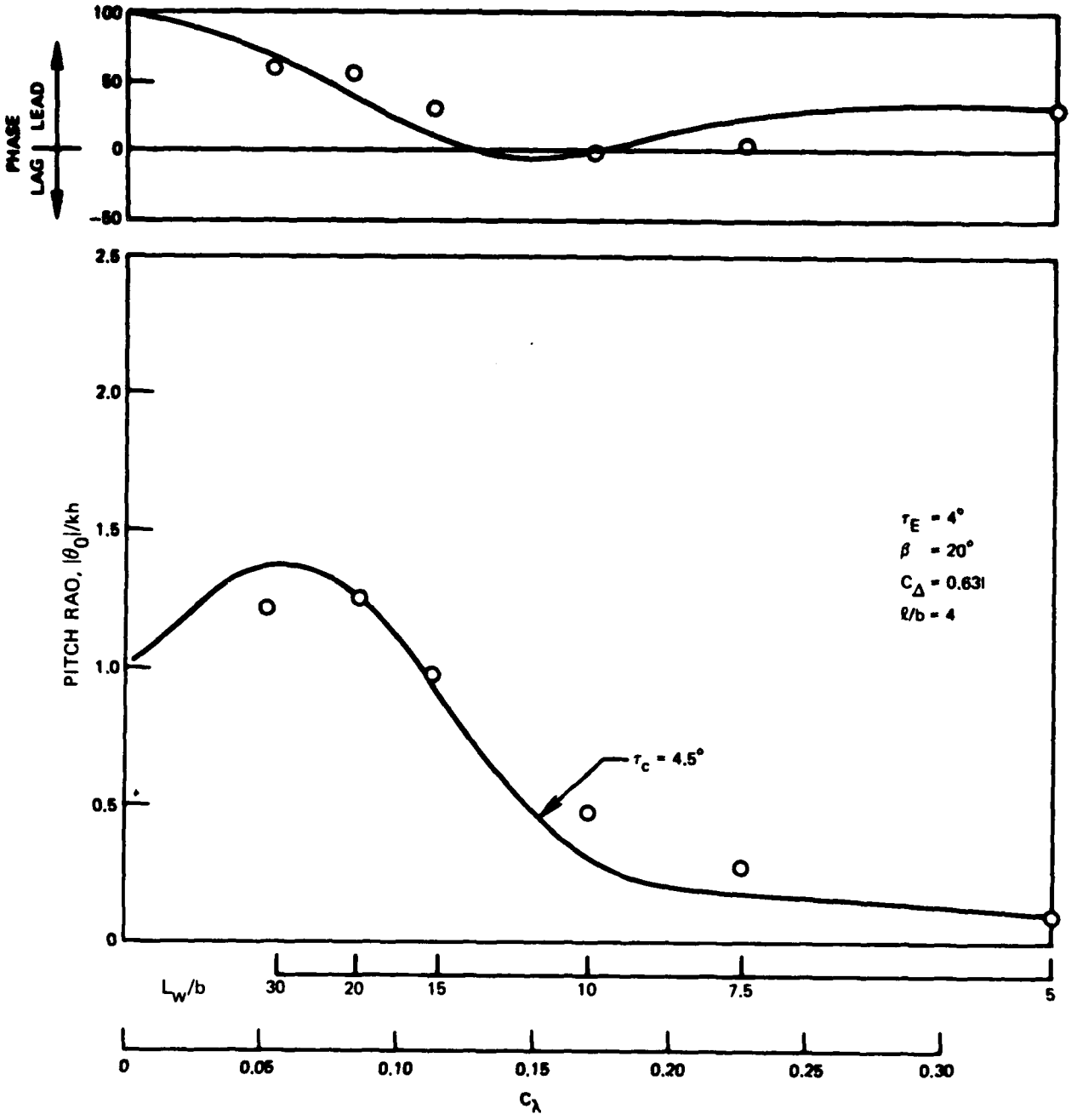

Figure 9b - Pitch Response, Speed-to-Length Ratio of 4

Figure 10 - Heave and Pitch Responses ($V/\sqrt{\ell} = 6$) Configuration B

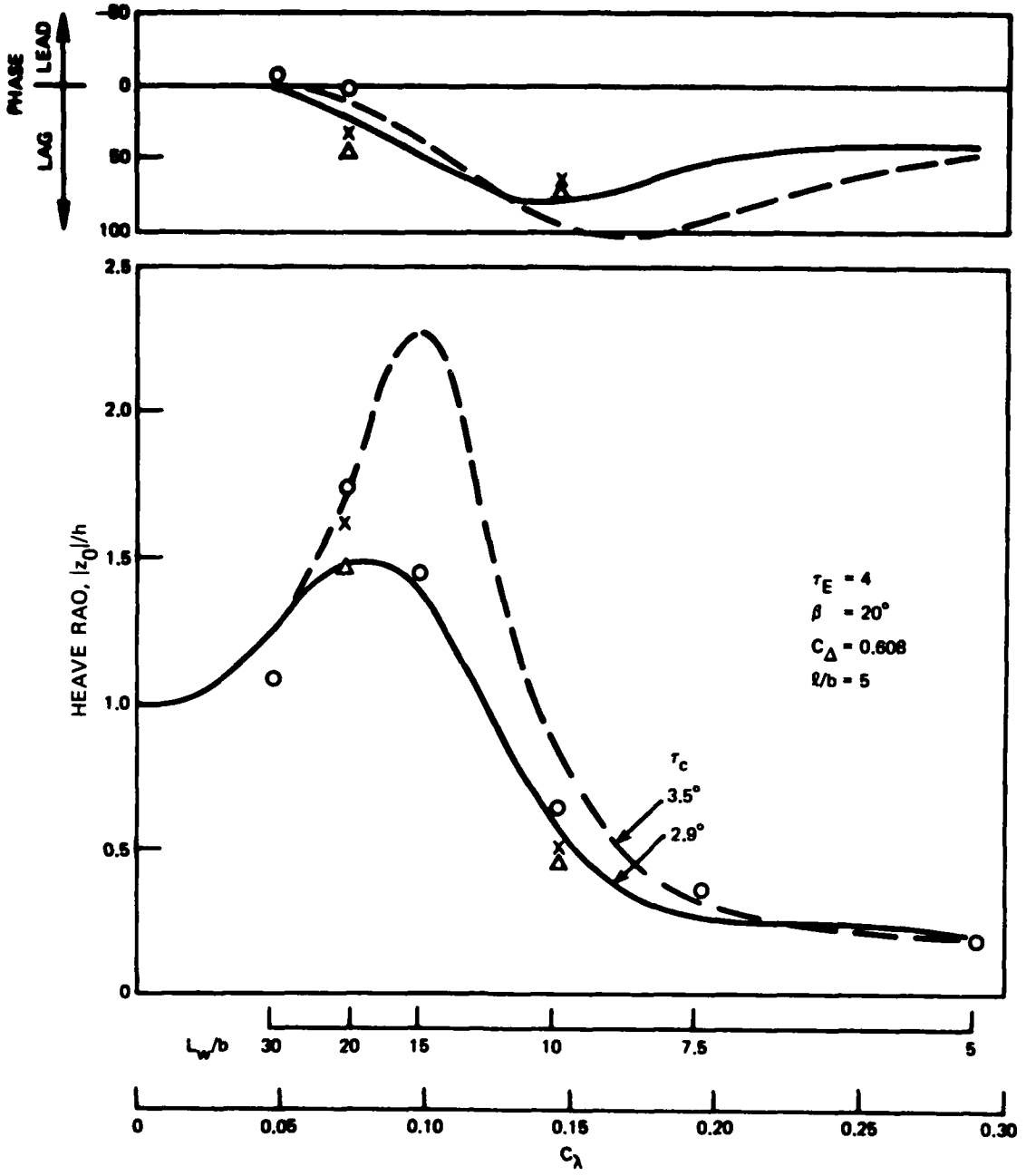

Figure 10a - Heave Response, Speed-to-Length Ratio of 6

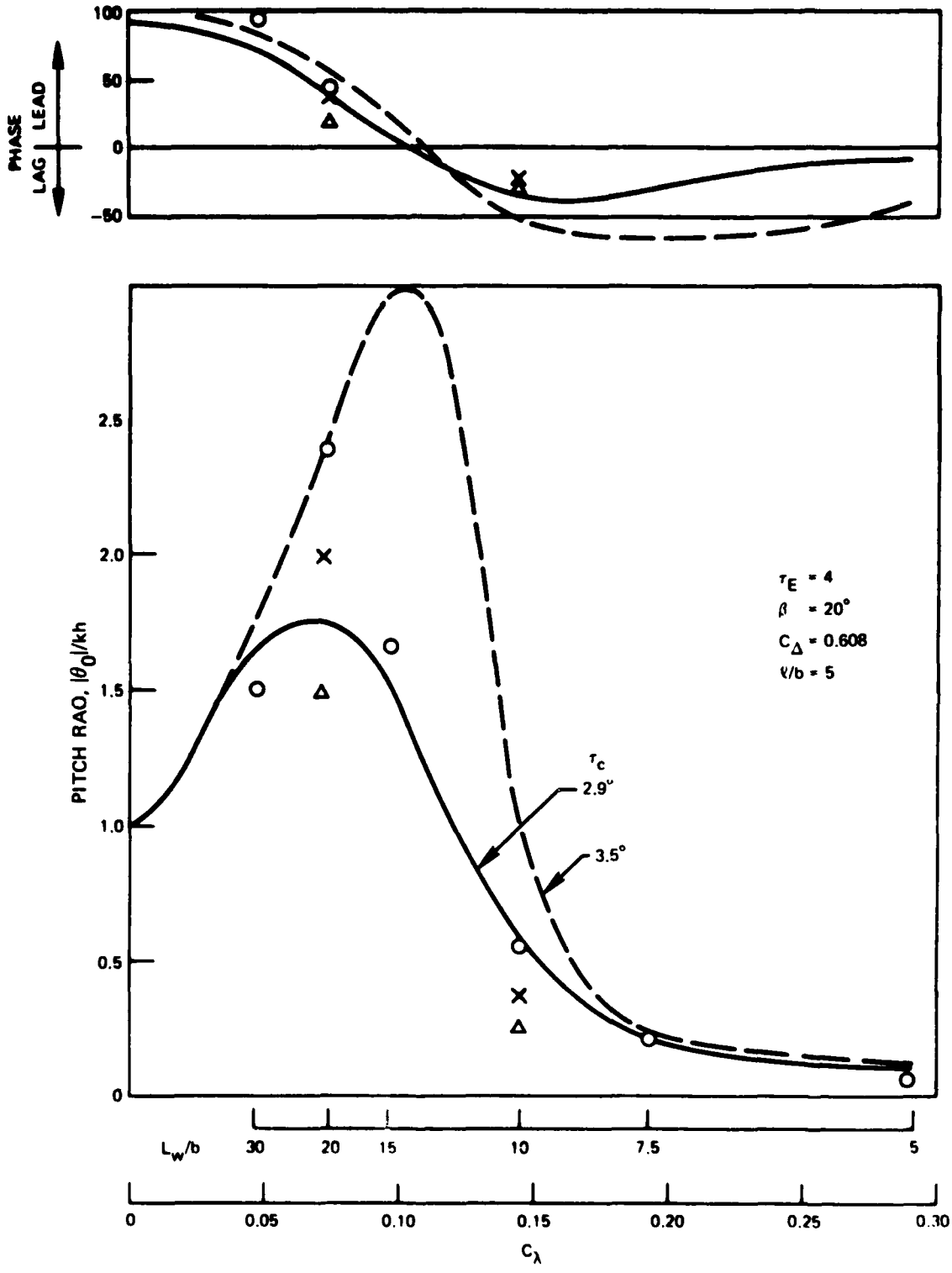

Figure 10b - Pitch Response, Speed-to-Length Ratio of 6

Figure 11 - Heave and Pitch Responses ($V/\sqrt{\ell} = 6$) Configuration G

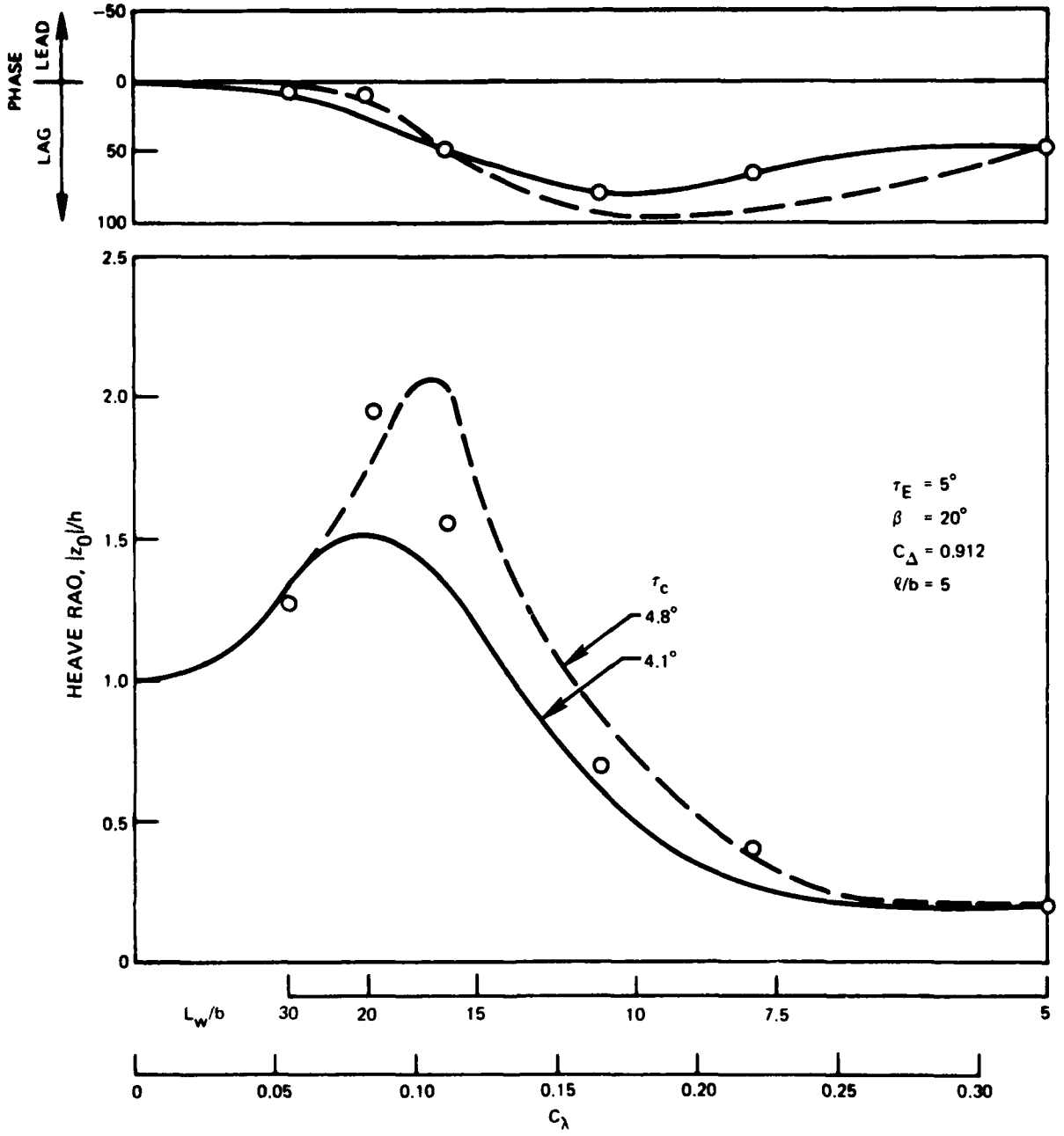

Figure 11a - Heave Response, Speed-to-Length Ratio of 6

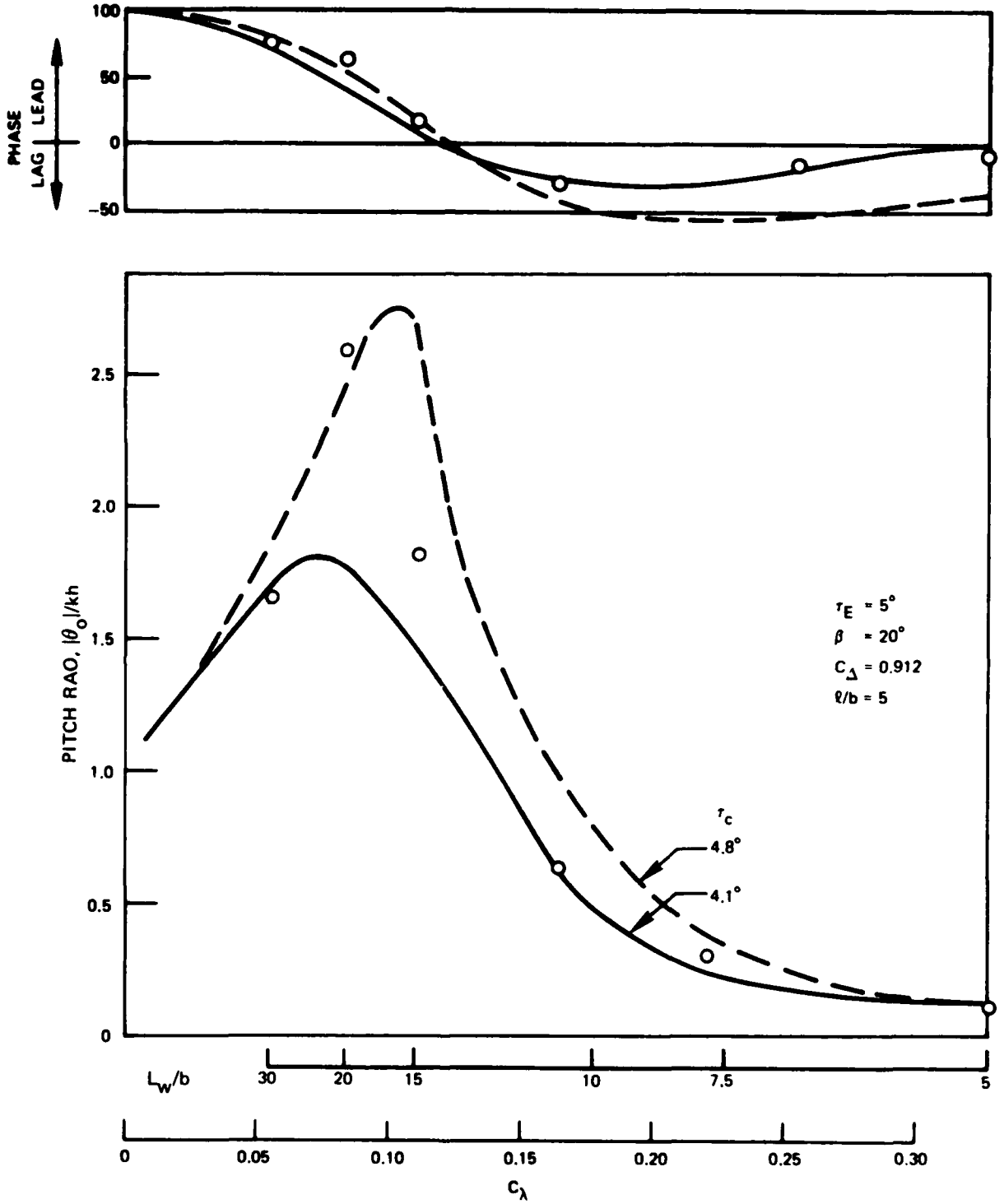

Figure 11b - Pitch Response, Speed-to-Length Ratio of 6

Figure 12 - Heave and Pitch Responses ($V/\sqrt{\ell} = 6$) Configuration M

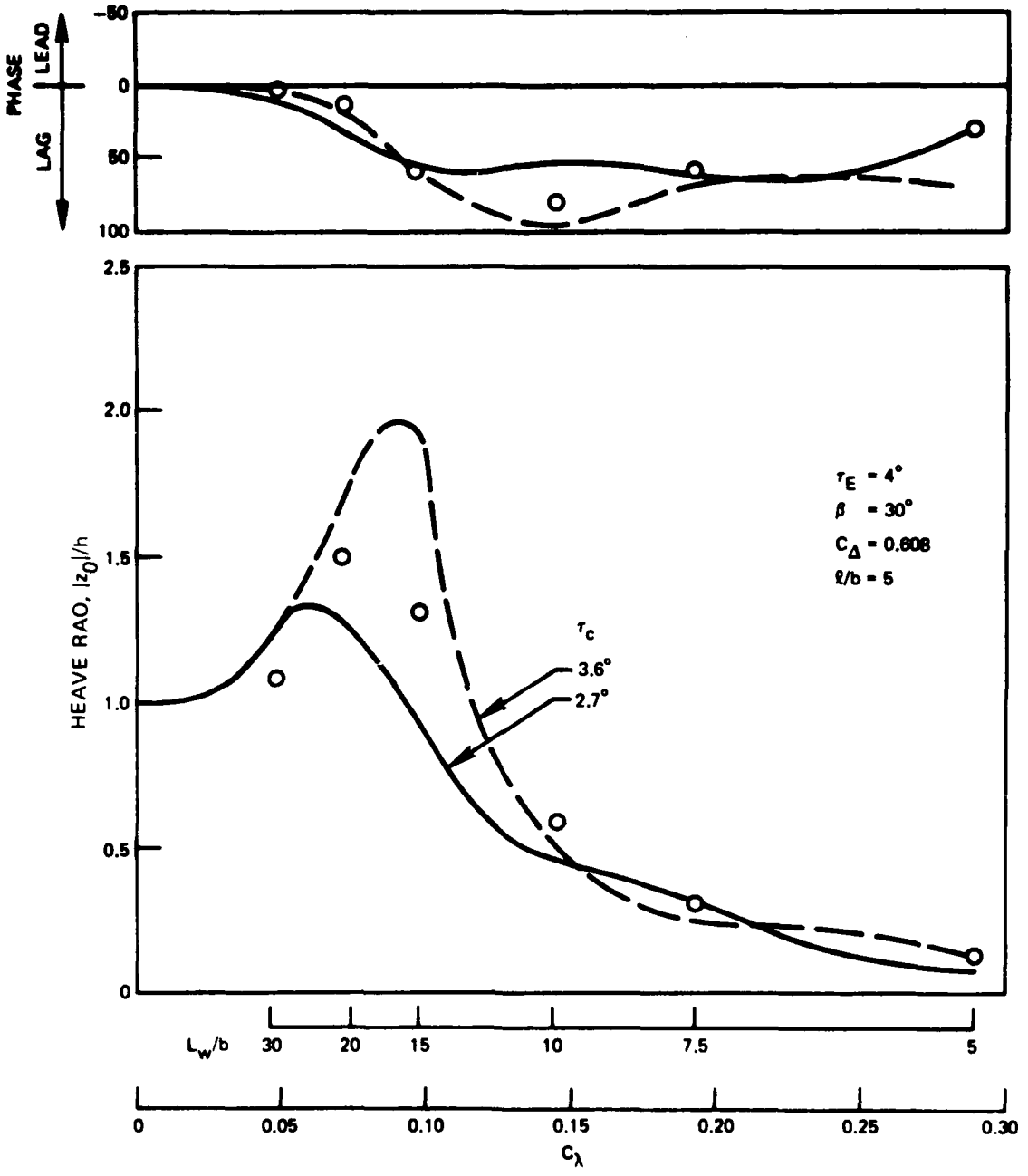

Figure 12a - Heave Response, Speed-to-Length Ratio of 6

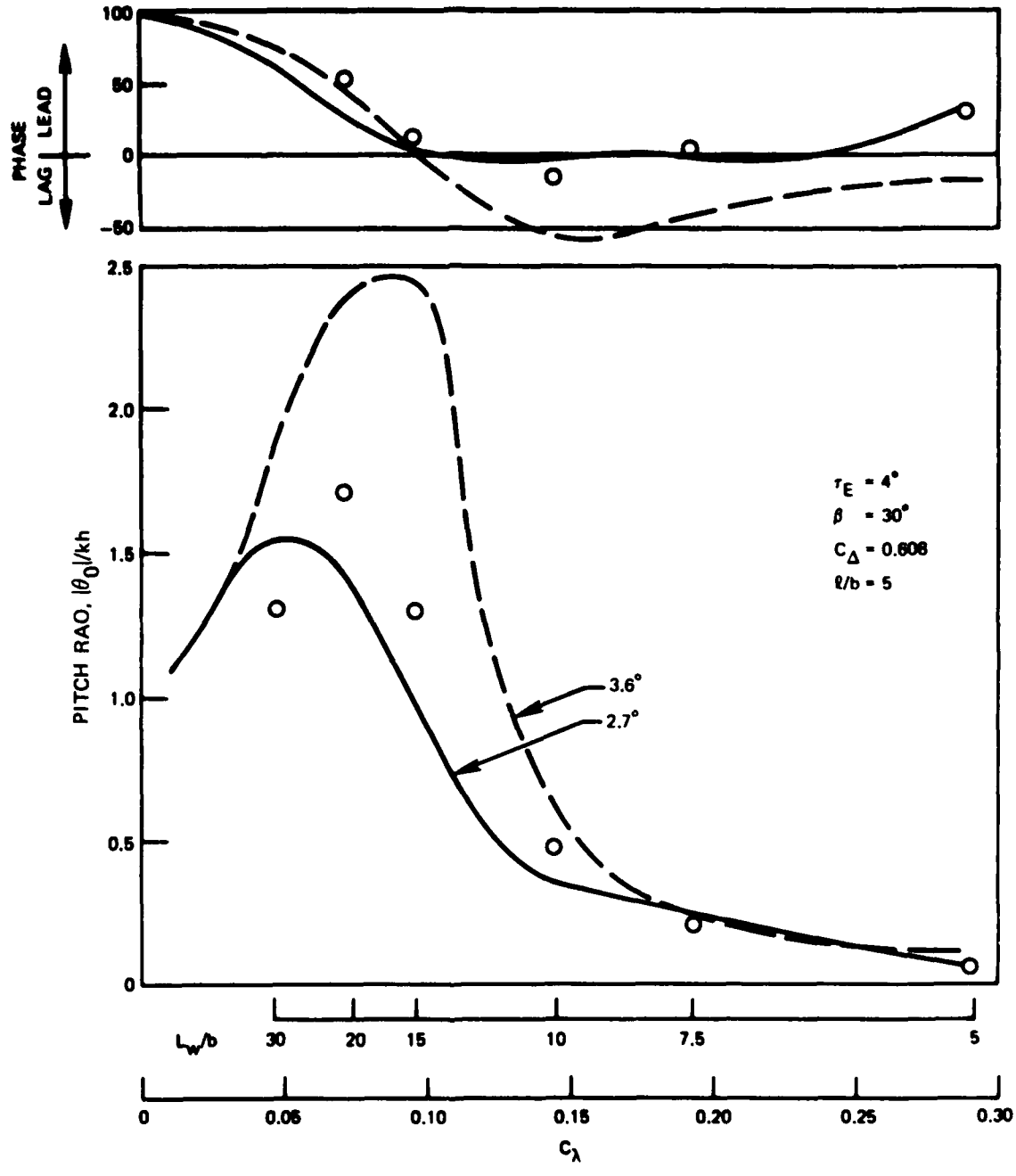

Figure 12b - Pitch Response, Speed-to-Length Ratio of 6

Figure 13 - Heave and Pitch Responses ($V/\sqrt{\ell} = 6$) Configuration J

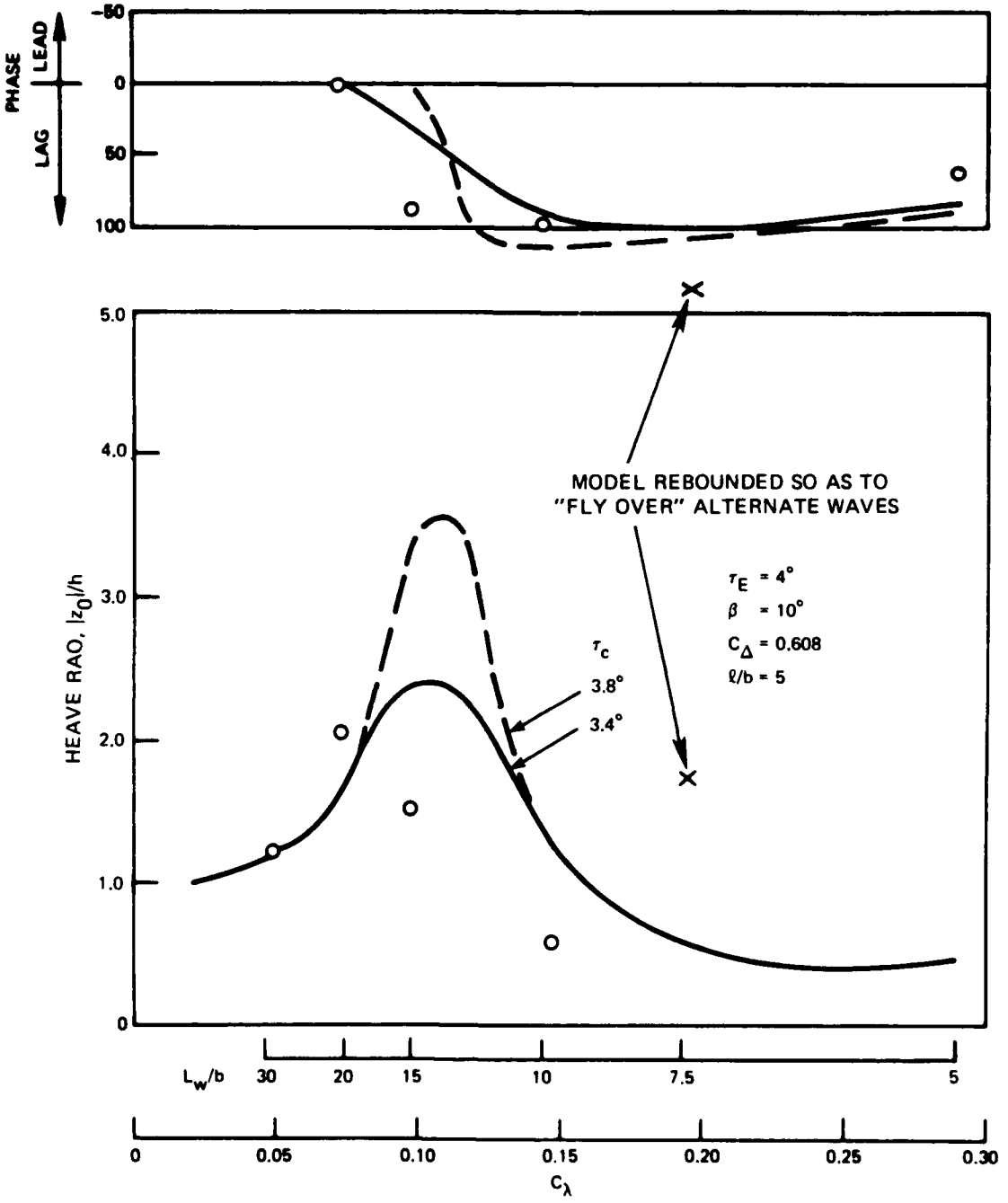

Figure 13a - Heave Response, Speed-to-Length Ratio of 6

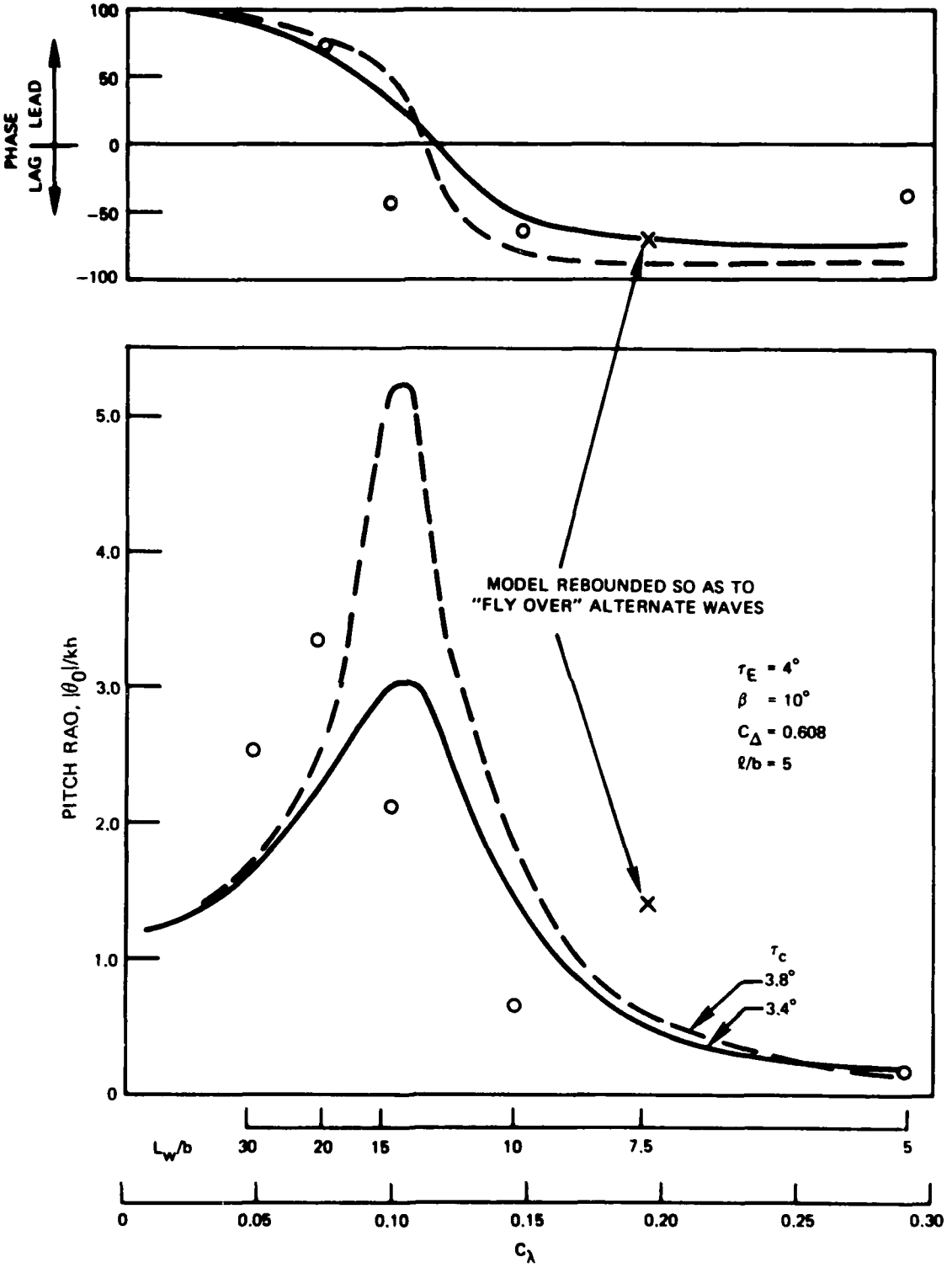

Figure 13b - Pitch Response, Speed-to-Length Ratio of 6

Figure 14 - Heave and Pitch Responses ($V/\sqrt{\ell} = 2$) Configuration C

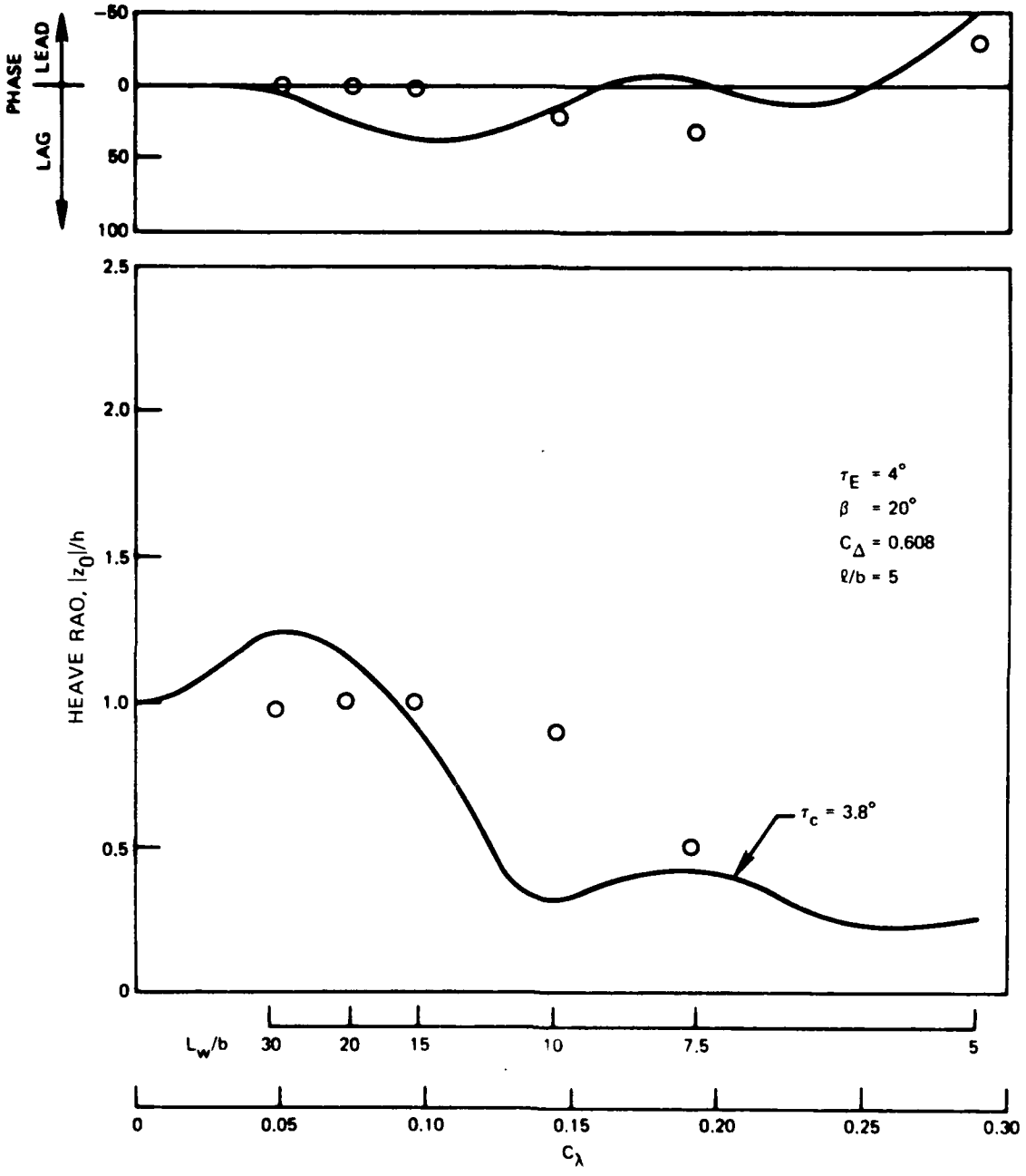

Figure 14a - Heave Response, Speed-to-Length Ratio of 2

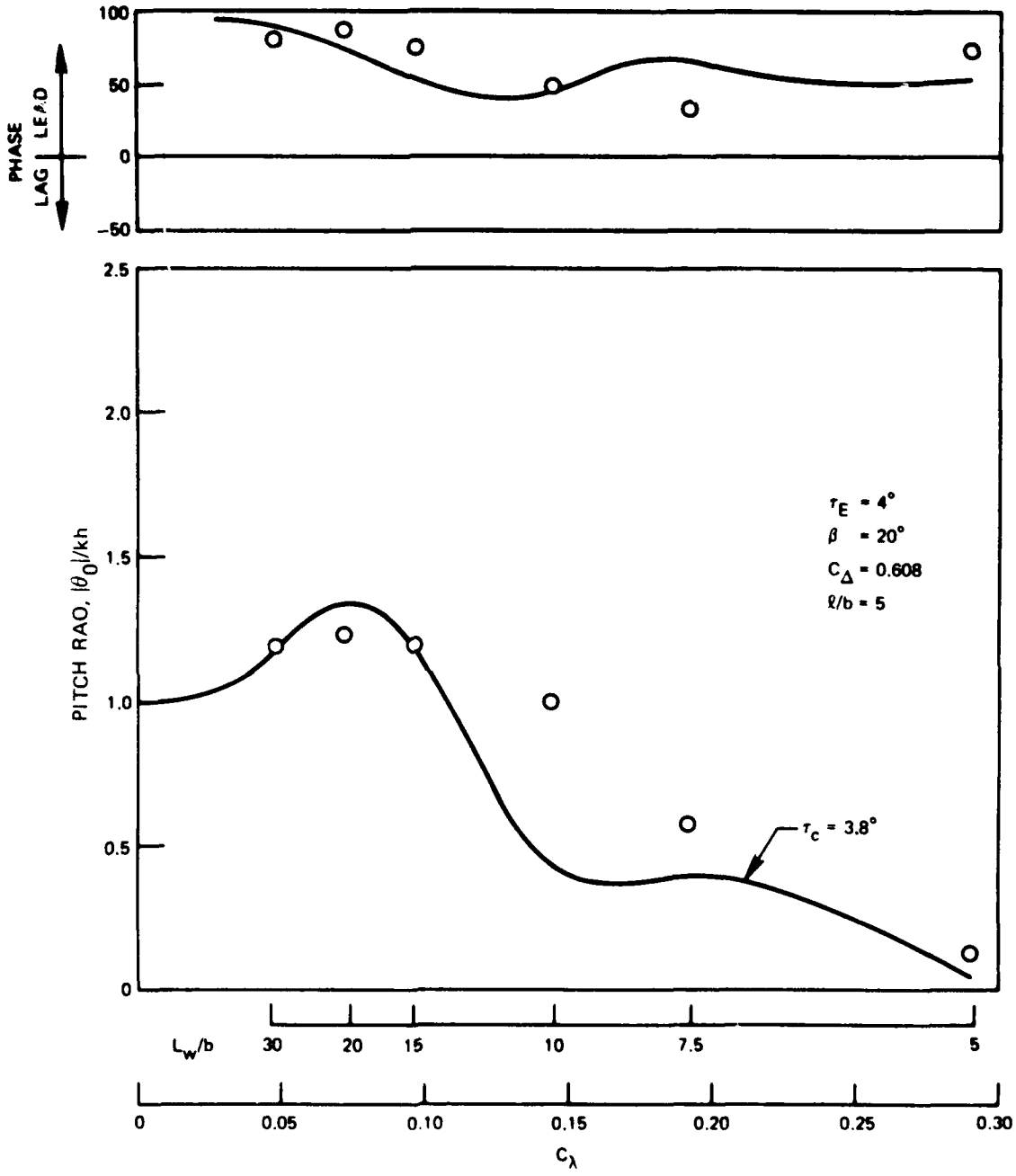

Figure 14b - Pitch Response, Speed-to-Length Ratio of 2

Figure 15 - Heave and Pitch Responses ($V/\sqrt{\ell} = 2$) Configuration D

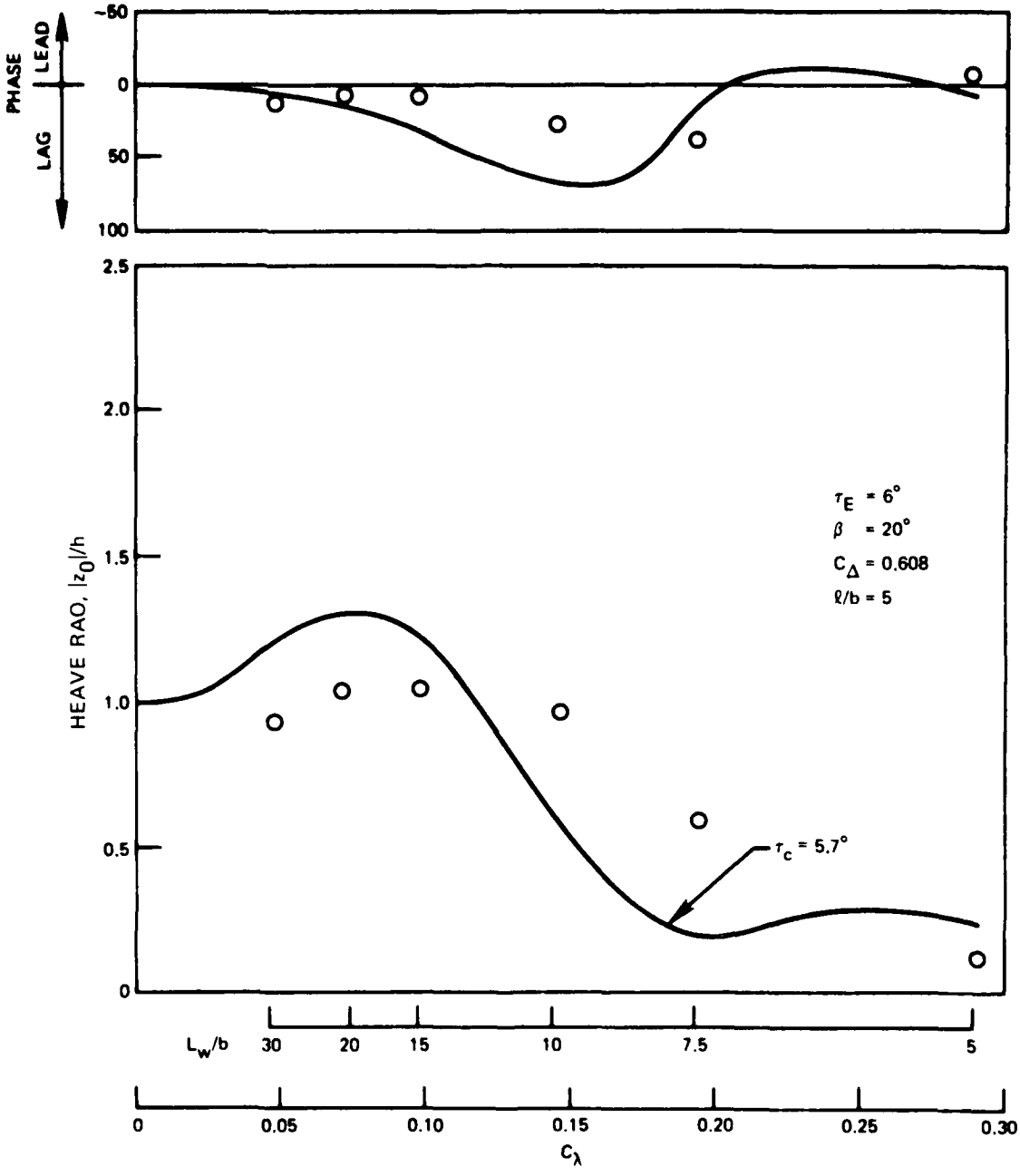

Figure 15a - Heave Response, Speed-to-Length Ratio of 2

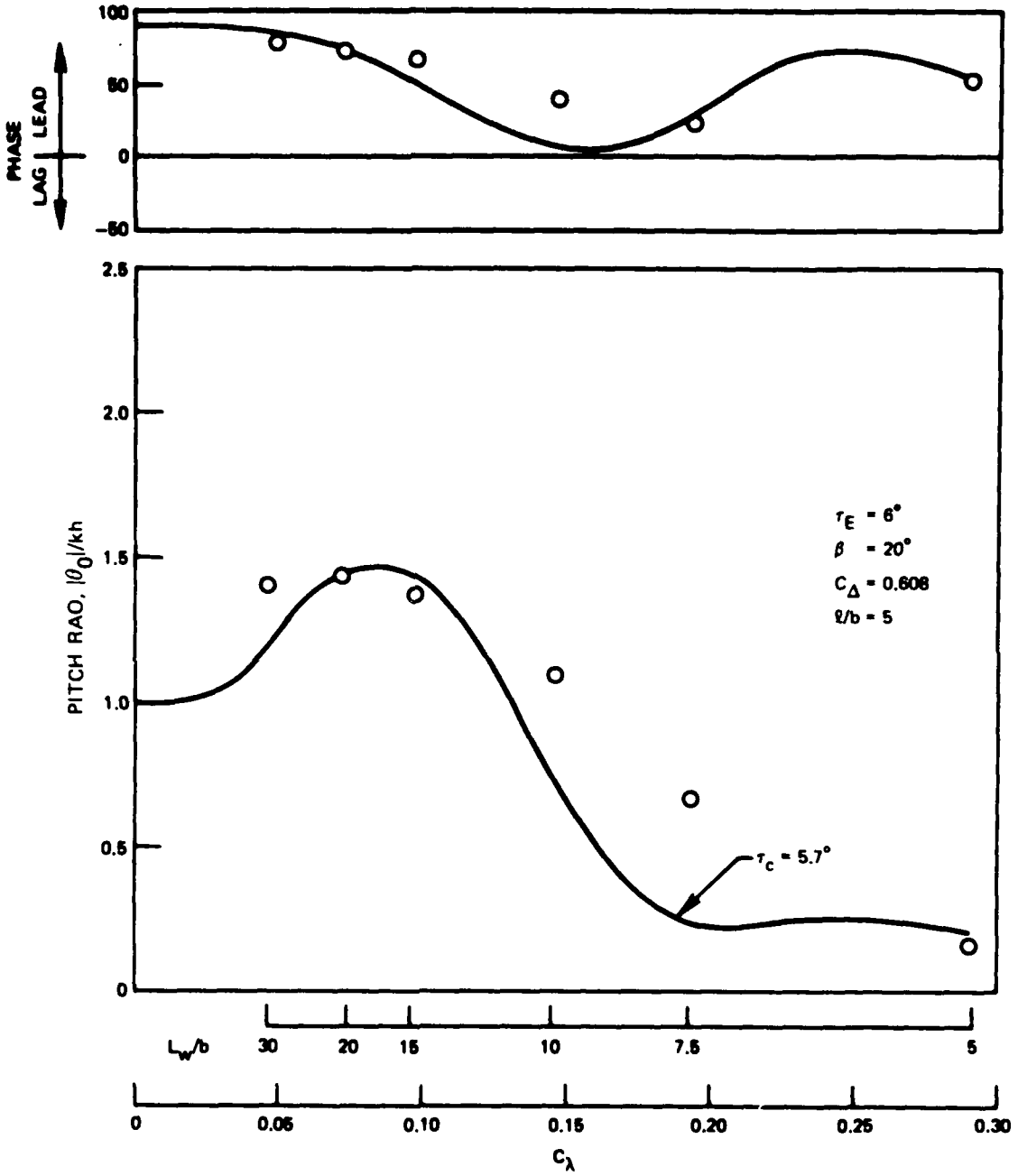

Figure 15b - Pitch Response, Speed-to-Length Ratio of 2

Figure 16 - Heave and Pitch Responses ($V/\sqrt{\ell} = 2$) Configuration H

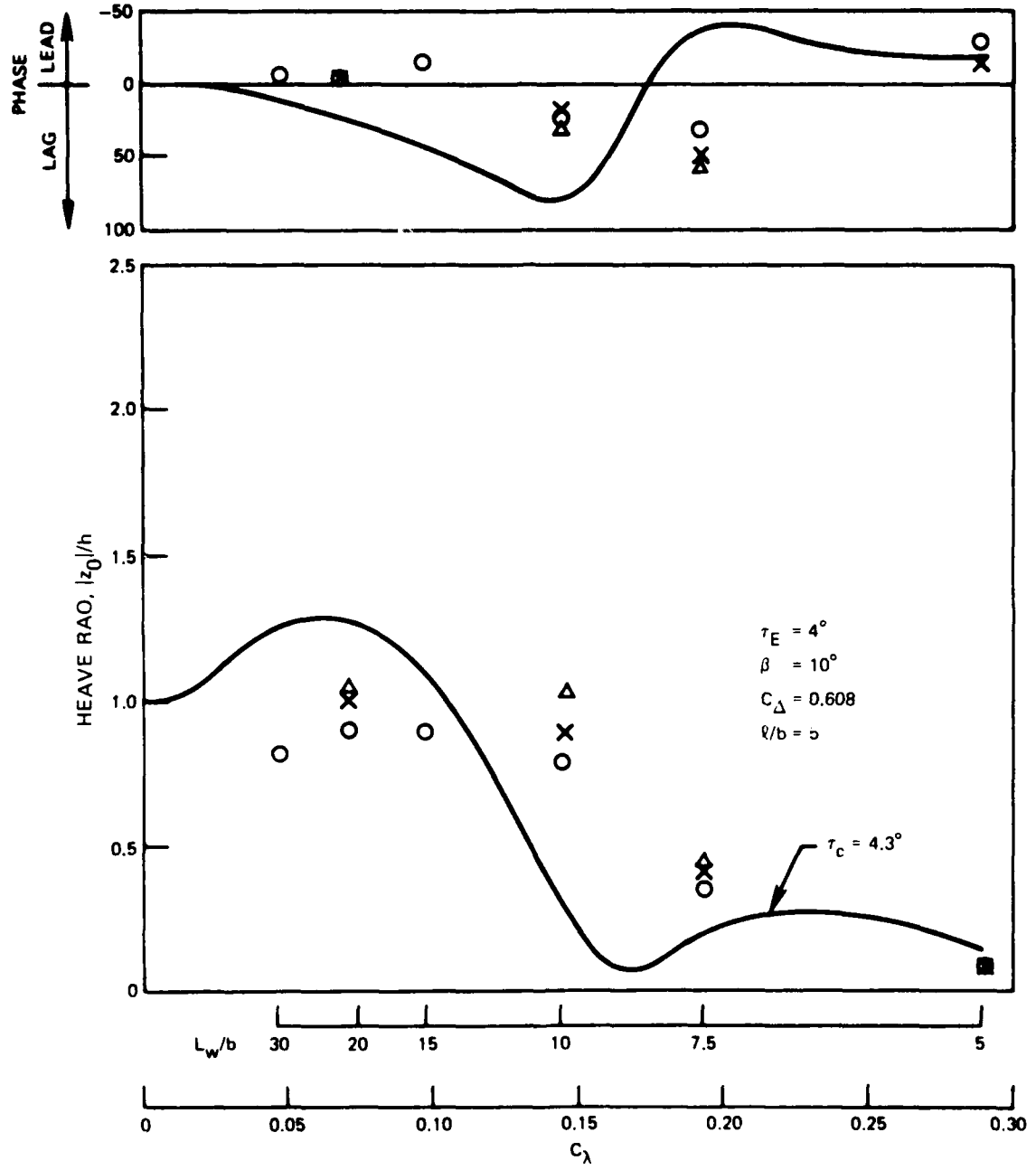

Figure 16a - Heave Response, Speed-to-Length Ratio of 2

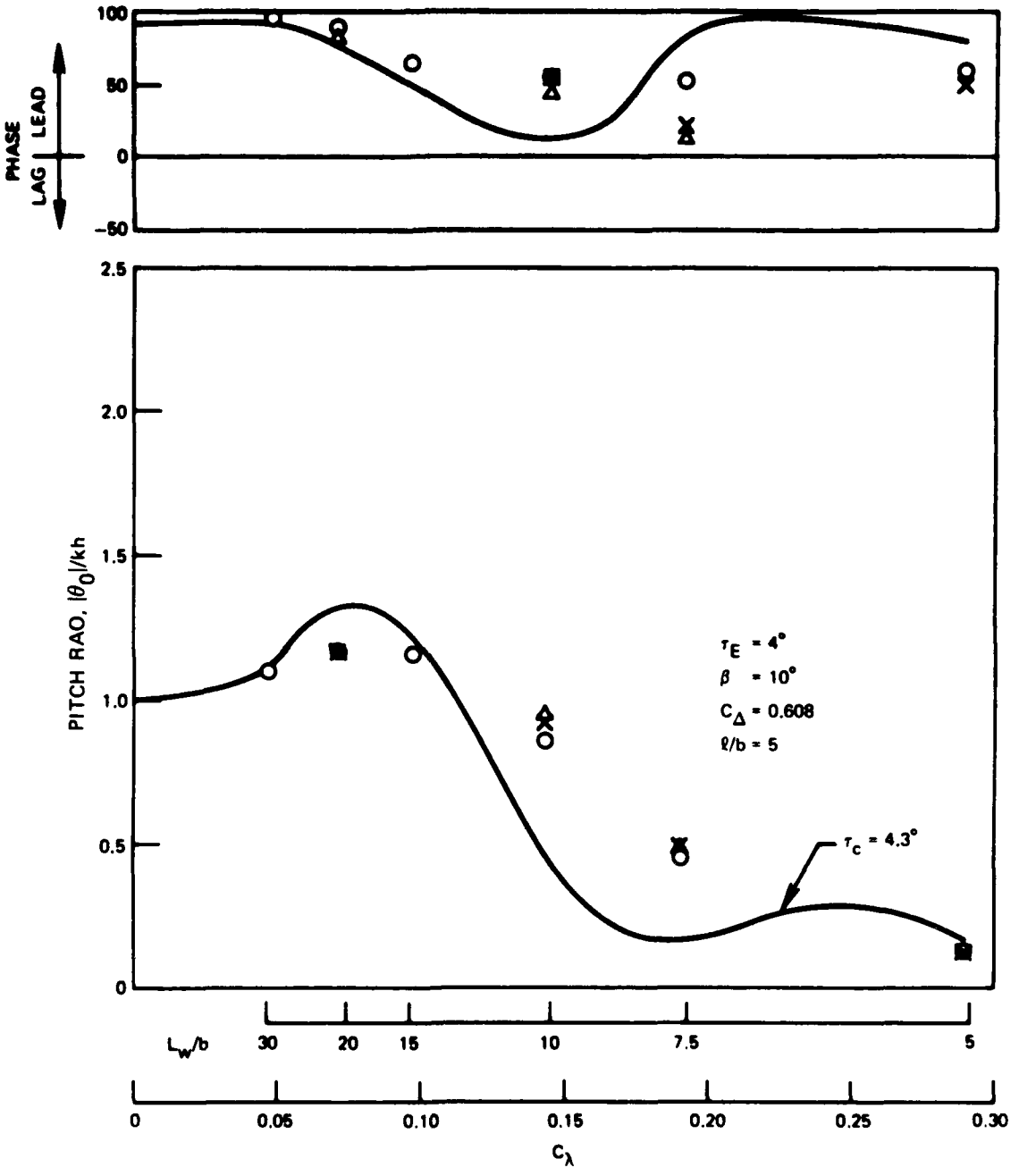

Figure 16b - Pitch Response, Speed-to-Length Ratio of 2

Figure 17 - Heave and Pitch Responses ($V/\sqrt{\ell} = 2$) Configuration L

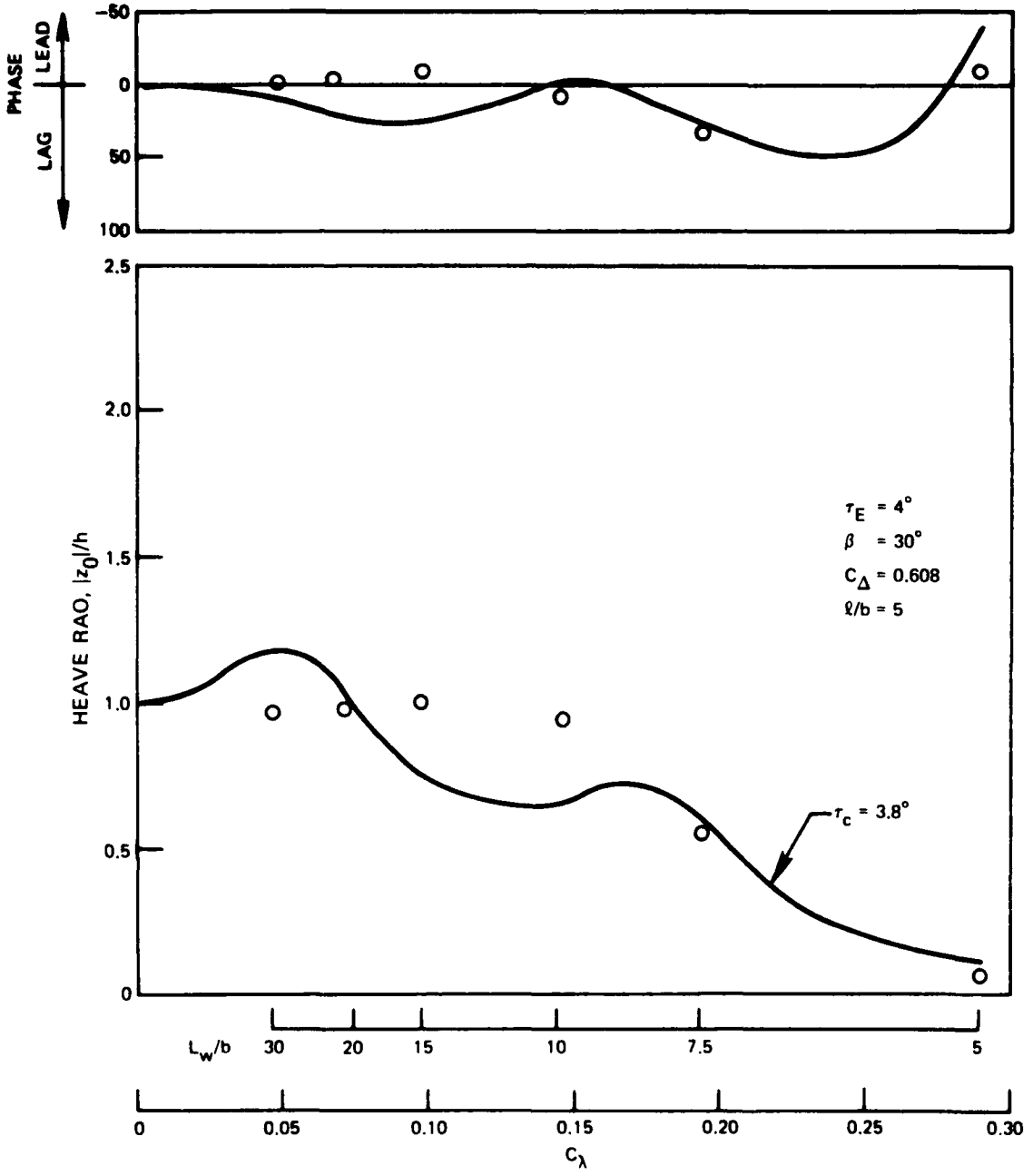

Figure 17a - Heave Response, Speed-to-Length Ratio of 2

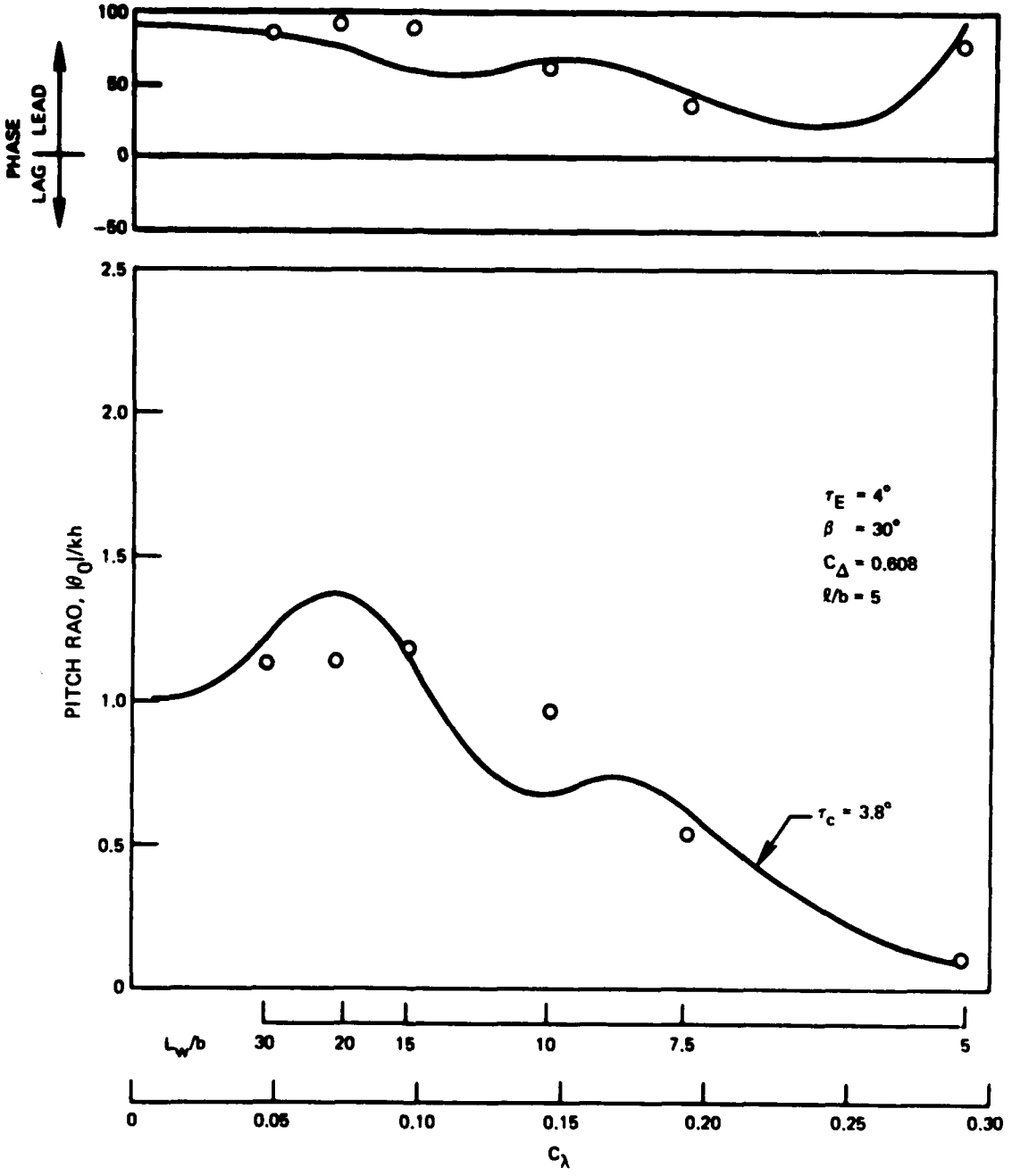

Figure 17b - Pitch Response, Speed-to-Length Ratio of 2

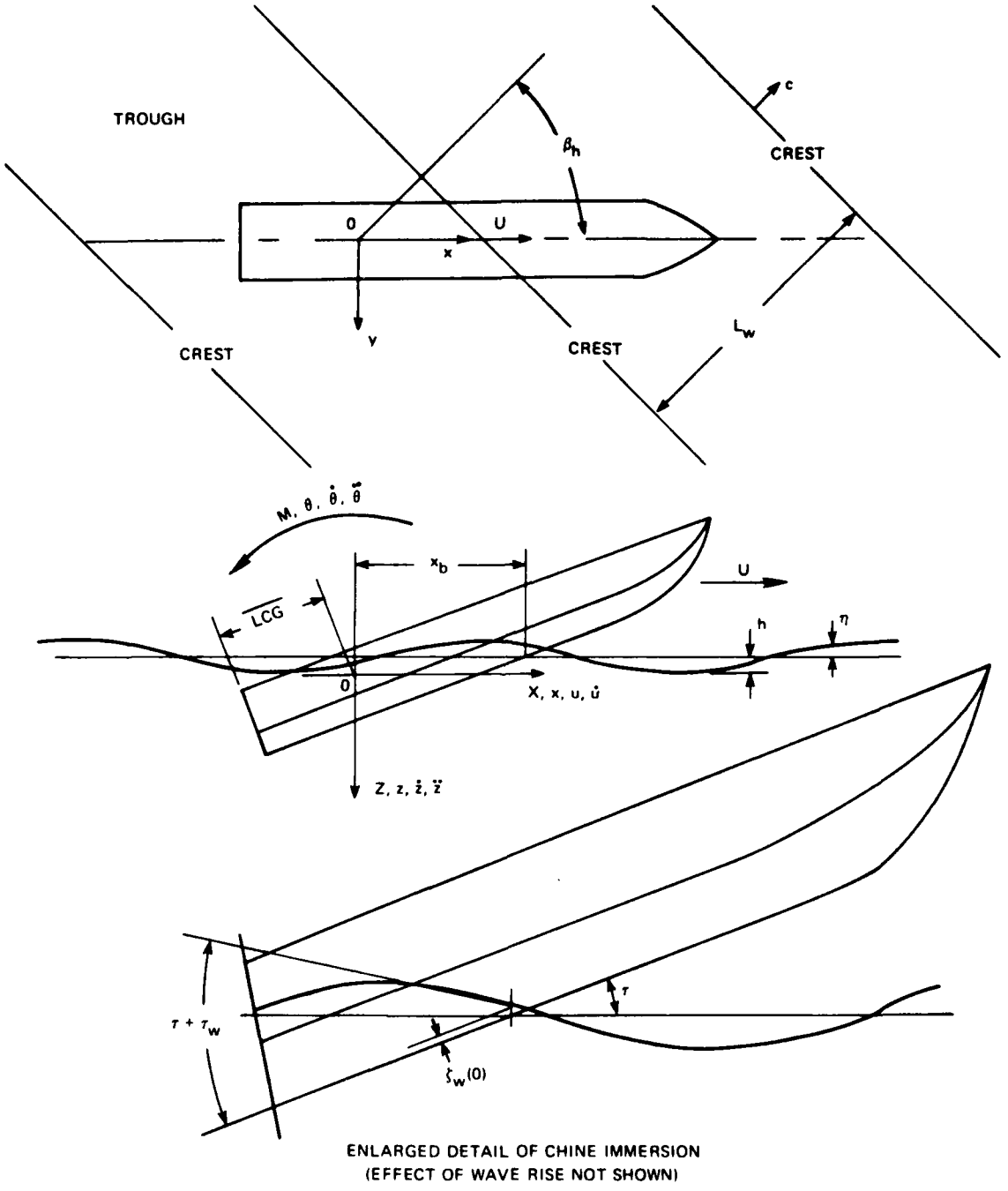

Figure 18 - Coordinate System and Symbol Illustrations

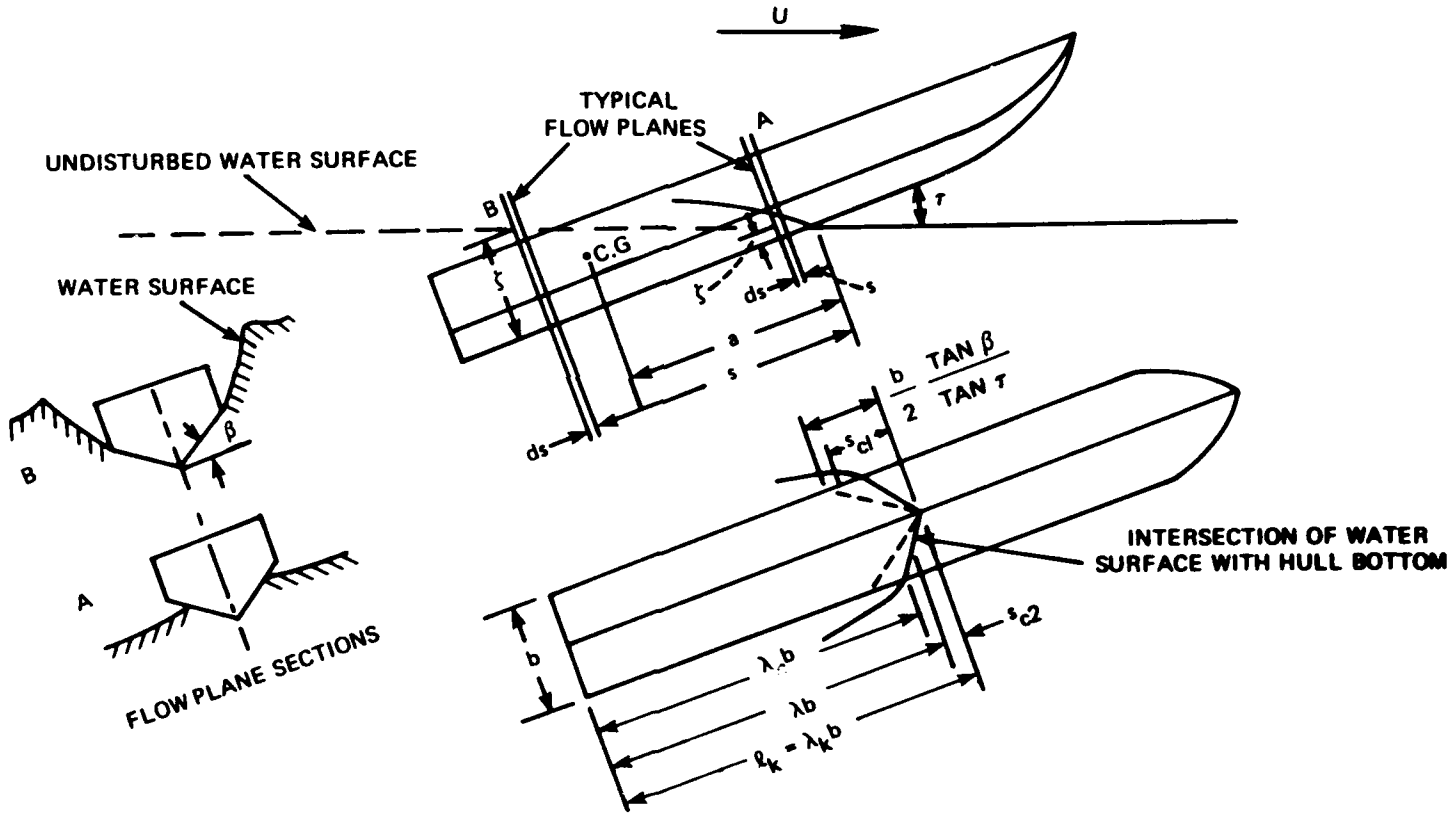

Figure 19 - Geometric Relationships in Steady State Planing

REFERENCES

1. Savitsky, D., "On the Seakeeping of Planing Hulls," Marine Technology (Apr 1968).

2. Fridsma, G., "A Systematic Study of the Rough-Water Performance of Planing Boats," Davidson Laboratory, Stevens Institute of Technology Report R-1275 (Nov 1969).

3. Fridsma, G., "A Systematic Study of the Rough-Water Performance of Planing Boats, Irregular Waves--Part 2," Davidson Laboratory, Stevens Institute of Technology Report R-1495 (Mar 1971).

4. Martin, M., "Theoretical Prediction of Porpoising Instability of High-Speed Planing Boats," DTNSRDC Report 76-0068 (Apr 1976).

5. Munk, M.M., "The Aerodynamic Forces on Airship Hulls," National Advisory Committee for Aeronautics Report 184 (1924).

6. Jones, R.T., "Properties of Low-Aspect-Ratio Wings at Speeds Below and Above the Speed of Sound," National Advisory Committee for Aeronautics Report 835 (1946).

7. Bryson, A.E., Jr., "Stability Derivatives for a Slender Missile with Application to Wing-Body-Vertical Tail Configuration," Journal of Aeronautical Sciences, Vol. 20, No. 5, pp. 297-308 (1953).

8. Mayo, W.L., "Analysis and Modification of Theory for Impact of Seaplanes on Water," National Advisory Committee for Aeronautics Report 810 (1945).

9. Milwitzky, B., "A Generalized Theoretical and Experimental Investigation of the Motions and Hydrodynamic Loads Experienced by V-Bottom Seaplanes During Step-Landing Impacts," National Advisory Committee for Aeronautics TN 1516 (1948).

10. Schnitzer, E., "Theory and Procedure for Determining Loads and Motions in Chine--Immersed Hydrodynamic Impacts of Prismatic Bodies," National Advisory Committee for Aeronautics Report 1152 (1953).

11. Wagner, H., "The Phenomena of Impact and Planing on Water," National Advisory Committee for Aeronautics Translation 1366, ZAMMBD 12, Heft 4, pp. 193-215 (Aug 1932).

12. Shuford, C.L., Jr., "A Theoretical and Experimental Study of Planing Surfaces Including Effects of Cross Section and Plan Form," National Advisory Committee for Aeronautics Report 1355 (1957).

13. Hsu, C.C., "On the Motions of High Speed Planing Craft," Hydronautics Report 603-1 (May 1967).

14. Brown, P.W., "An Experimental and Theoretical Study of Planing Surfaces with Trim Flaps," Davidson Laboratory, Stevens Institute of Technology Report 1463 (Apr 1971).

INITIAL DISTRIBUTION

Copies		Copies	
1	WES	1	NAVSHIPYD PHILA/Lib
1	CHONR/438 Cooper	1	NAVSHIPYD NORVA/Lib
2	NRL 1 Code 2027 1 Code 2629	1	NAVSHIPYD CHASN/Lib
1	ONR/Boston	1	NAVSHIPYD LBEACH/Lib
1	ONR/Chicago	2	NAVSHIPYD MARE 1 Library 1 Code 250
1	ONR/Pasadena	1	NAVSHIPYD BREM/Lib
1	NORDA	1	NAVSHIPYD PEARL/Code 202.32
4	USNA 1 Tech Lib 1 Nav Sys Eng Dept 1 B. Johnson 1 Bhattacheryye	8	NAVSEC 1 SEC 6034B 1 SEC 6110 1 SEC 6114H 1 SEC 6120 1 SEC 6136 1 SEC 6140B 1 SEC 6144G 1 SEC 6148
3	NAVPGSCOL 1 Library 1 T. Sarpkaya 1 J. Miller	1	NAVSEC, NORVA/6660.03 Blount
1	NADC	12	DDC
1	NELC/Lib	1	AFOSR/NAM
3	NUC, San Diego 1 Library 1 Fabula 1 Hoyt	1	AFFOL/FYS, J. Olsen
1	NCSL/712 D. Humphreys	1	NSF/Eng Lib
1	NCEL/Code L31	1	LC/Sci & Tech
1	NSWC, Dahlgren	1	DOT/Lib TAD-491.1
1	NUSC/Lib	2	MMA 1 Capt McCready 1 Library
7	NAVSEA 1 SEA 0322 1 SEA 033 1 SEA 03512/Peirce 1 SEA 037 3 SEA 09G32	1	U. Of BRIDGEPORT/E. Uram
1	NAVFAC/Code 032C	4	U. of CAL/Dept Naval Arch, Berkely 1 Library 1 Webster 1 Paulling 1 Wehausen
1	NAVSHIPYD PTSMH/Lib	2	U. of CAL, San Diego 1 A.T. Ellis 1 Scripps Inst Lib

Copies		Copies	
3	CIT 1 Aero Lib 1 T.Y. Wu 1 A. Acosta	3	U. of MICH/NAME 1 Library 1 Ogilivie 1 Hammitt
1	CITY COLLEGE, WAVE HILL/ Pierson	2	U. of NOTRE DAME 1 Eng Lib 1 Strandhagen
1	CATHOLIC U. of AMER./CIVIL & MECH ENG	2	NEW YORK U./COURANT INST 1 A. Peters 1 J. Stoker
1	COLORADO STATE U./ENG RES CEN	1	PENN STATE/ARL/B. Parkin
1	U. of CONNECTICUT/Scottron	1	PRINCETON U./Mellor
1	CORNELL U./Sears	5	SIT 1 Library 1 Breslin 1 Savitsky 1 P.W. Brown 1 Fridsma
2	FLORIDA ATLANTIC U. 1 Tech Lib 1 S. Dunne	1	U. of TEXAS/ARL Lib
2	HARVARD U. 1 G. Carrier 1 Gordon McKay Lib	1	UTAH STATE U./Jeppson
1	U. of HAWAII/ BRETSCHNEIDER	2	SOUTHWEST RES INST 1 Applied Mech Rev 1 Abramson
1	U. of ILLINOIS/J. Robertson	2	STANFORD U. 1 Eng Lib 1 R. Street
3	U. of IOWA 1 Library 1 Landweber 1 Kennedy	1	STANFORD RES INST/Lib
1	JOHN HOPKINS U./Phillips	1	U. of WASHINGTON/ARL Tech Lib
1	KANSAS STATE U./Nesmith	3	WEBB INST 1 Library 1 Lewis 1 Ward
1	U. of KANSAS/Civil Eng Lib	1	WOODS HOLE/Ocean Eng
1	LEHIGH U./Fritz Eng Lab Lib	1	WORCHESTER PI/Tech Lib
5	MIT 1 Library 1 Leehey 1 Mandel 1 Abkowitz 1 Newman	1	SNAME/Tech Lib
4	U. of MIN/ST. ANTHONY FALLS 1 Silberman 1 Schiebe 1 Wetzel 1 Song	1	BETHLEHEM STEEL/Sparrows Point
		1	BETHLEHEM STEEL/New York/Lib
		1	BOLT, BERANEK & NEWMAN/Lib

	Copies	Code	
DESIGN DIV,	1	1524	Y.T. Shen
T	1	1524	W.C. Lin
NAMICS, EB/	1	1532	G. Dobay
ht	1	1532	R. Roddy
X/Tech Info	1	1540	W.B. Morgan
CS	1	1552	J. McCarthy
y	1	1552	N. Salvesen
ler	1	1560	G. Hagen
dman	1	1560	N. Hubble
nson			
su	10	1562	M. Martin
Sunnyvale/Waid	1	1564	J. Feldman
DOUGLAS,	1	1568	G. Cox
ch	1	1572	M.D. Ochi
s	1	1572	E. Zarnick
eci	1	1572	C.M. Lee
WS SHIPBUILDING/	1	1576	W.E. Smith
G & RES	30	5211	Reports Distribution
	1	5221	Unclassified Library (C)
NTERNATIONAL/B.	1	5222	Unclassified Library (A)
D/Tech Lib			
ILDING/Chief			
ch			
GART			

TRIBUTION

Cummins

Monacella

Ochi

leslowski

Hadler

rmter

len

DTRSDOC ISSUES THREE TYPES OF REPORTS

(1) DTNSROC REPORTS, A FORMAL SERIES PUBLISHING INFORMATION OF PERMANENT TECHNICAL VALUE DESIGNATED BY A SERIAL REPORT NUMBER.

(2) DEPARTMENTAL REPORTS, A SEMIFORMAL SERIES, RECORDING INFORMATION OF A PRELIMINARY OR TEMPORARY NATURE, OR OF LIMITED INTEREST OR SIGNIFICANCE, CARRYING A DEPARTMENTAL ALPHANUMERIC IDENTIFICATION.

(3) TECHNICAL MEMORANDA, AN INFORMAL SERIES, USUALLY INTERNAL WORKING PAPERS OR DIRECT REPORTS TO SPONSORS, NUMBERED AS TM SERIES REPORTS, NOT FOR GENERAL DISTRIBUTION